Carbohydrate Nanotechnology, Edited by Keith Stine.
ISBN 0-471-XXXXX-X

Chapter 7

Glycoclusters and their applications as anti-infective agents, vaccines and targeted drug delivery systems

Juan Manuel Casas-Solvas and Antonio Vargas-Berenguel

Department of Chemistry and Physics, University of Almeria, Carretera de Sacramento s/n, 04120 Almeria, Spain

Corresponding/Contact Author Name : Antonio Vargas-Berenguel
Corresponding/Contact Author Phone: +34 950 015315
Corresponding/Contact Author Email: avargas@ual.es

Keywords: Glycoclusters, multivalent carbohydrates, bacterial inhibitors, viral inhibitors, carbohydrate-based vaccines, targeted drug delivery

Abstract:

This chapter reviews the most relevant and recent reports on the applications of glycoclusters as inhibitors and antiadhesive agents against bacteria and viruses, synthetic vaccines, and site-specific drug and gene delivery systems. A common strategy to achieve these goals is the targeting of carbohydrate-binding proteins (lectins) present on the surface of pathogens and tumour cells. Such target lectins are typically involved in cell recognition, signaling and adhesion, or are overexpressed in cell proliferation and tumor development. Multivalency is crucial for the enhancement of such carbohydrate-protein interactions, which are otherwise too weak in biological

terms for such applications. In addition, size and spatial arrangement matching between the glycocluster and the biological target is important to obtain a high binding affinity in many cases. A large number of different scaffolds have been used for building such multivalent structures, including cyclodextrins, calixarenes, oligo- and cyclooligopeptides, pentacyclen, pentaerythritol and saccharides, among others, giving rise to an enormous variety of modes of carbohydrate display with different topologies and valencies.

7.1. Introduction

The seminal contributions reporting on the enhanced affinity observed in the interaction of clustered carbohydrates with their protein receptors, also having clusters of binding sites, referred to such phenomenon as glycoside cluster effect.[1] Since then, glycoside clusters or glycoclusters became the topic of a very active research in the fields of glycochemistry and glycobiology.[2] Carbohydrate-protein interactions mediate a wide diversity of crucial biological events, but paradoxically interactions between saccharides and proteins are typically very weak.[3,4] Nature usually overcomes such low-affinity between glycans and their specific protein receptors (lectins) through glycoside cluster effects transforming such interactions into very high affinity bindings.[5,6] This phenomenon actually transcends the carbohydrate chemistry, referred as multivalent effect in its widespread version, is ubiquitous in biological systems where multivalent ligands of carbohydrate or non-carbohydrate nature bind to their respective multivalent receptors in a stronger and more selective fashion than their monovalent analogues.[7] In order to study and obtain a deeper understanding of these multivalent glycoside interactions, a great deal of research has been devoted to synthesize multivalent glycomimetics of various architectures. In this regard, an important challenge when designing multivalent architectures is the optimization of the several factors involved in the high affinity and selectivity of the multivalent systems.[2] Those factors include not only the ligand density but also the spatial arrangement of the ligands, the linker, the scaffold and the homo- and hetero-multivalency,[8] among others. Numerous excellent reviews dealing with multivalent neoglyconjugates have been published,[8-18] including the very comprehensive one by Chabre and Roy,[2]. A large number of different synthetic scaffolds have been used for building such multivalent structures, giving rise to a large variety of modes of carbohydrate display with different topologies

and valencies. Examples of scaffolds used are carbohydrates, dendrimers, cyclodextrins, calixarenes, oligopeptides, benzene derivatives, tetraphenylethylene, DNA, pentacyclen, azobenzene, triazine, corannulene, glycophanes, and porphyrins, to name but a few. This chapter will focus on the most relevant and recent reports on glycoclusters and their applications in the context of the study of carbohydrate-protein interactions and their uses for therapeutic purposes. For this review, we consider glycoclusters as multivalent glycoconjugates, regardless of the number of peripheral moieties, built on a well-defined central core to which saccharides are linked through tethers that in most of the cases do not contain repetitive units. Essentially, the potential biomedical applications of glycoclusters is based on the rational that the multivalency will allow for an enhanced avidity for a particular biological target. Glycoclusters with very high affinity for cell surface receptors of pathogens can favorably compete with them resulting in promising infection inhibitors. Such high affinity for a cell surface has been also used for the efficient targeting of drug delivery systems. Moreover, vaccines containing multiple copies of antigen glycosides can elicit immune response. This chapter will concentrate specifically on the uses of glycoclusters as pathogen infection inhibitors, vaccines and targeted drug delivery systems.

7.2. Inhibitors of bacterial and viral adhesion

High-affinity multivalent glycomimetics that inhibit the adhesion of pathogens to cell-surface receptors can be potential therapeutics. This approach is based on 1) the identification of pathogen-surface carbohydrates that are key for the cell-pathogen recognition process; and 2) the synthesis of a cluster glycoside consisting in a convenient scaffold displaying such carbohydrates. The resulting glycomimetics are expected to prevent the adhesion of the pathogen by interacting with their cell-surface lectin receptors.

The influenza virus infects mainly vertebrates by adhering to the cell-surface through the multivalent binding interaction between virus surface hemagglutinin (HA) and cell surface sialic acid.[19] Molecules that could inhibit the virus adhesion are potential antiinfective drugs. Pioneering work by Roy *et al.*[20] described the powerful inhibitor activity of dendritic sialosides based on hyperbranched L-lysine cores in experiments with influenza A. The results showed that even at the divalent level of clustering the glycomimetic is five times more potent that a monosialoside.

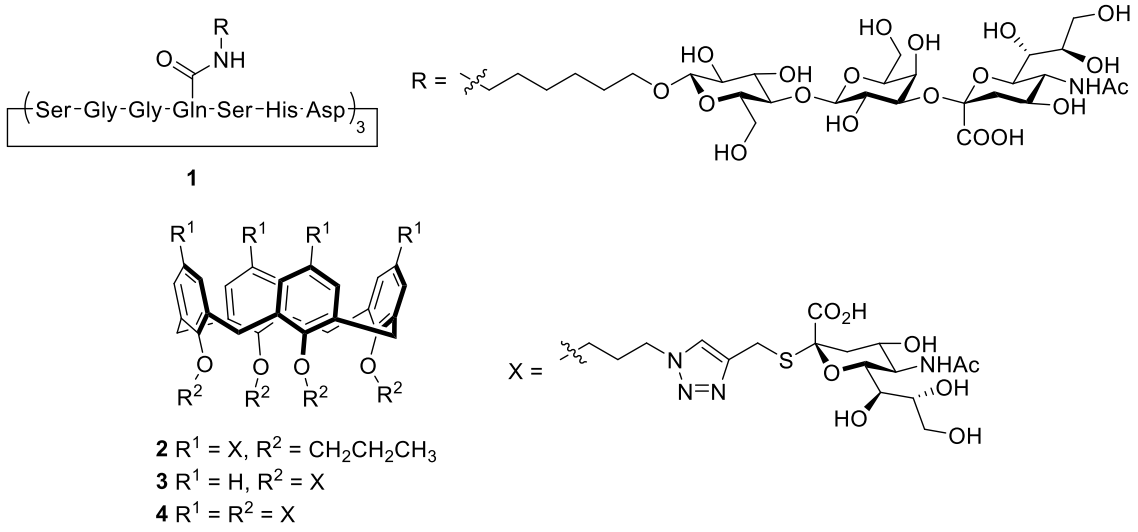

Figure 7-1. Influenza virus hemagglutinin (HA) inhibitors based on a cyclopeptide (**1**) and calix[4]arene (**2-4**) showing sialyl groups as vector moieties.

In the search for potential HA blockers, Nishimura and co-workers[21] designed glycoclusters by appending one, two or three sialotrisaccharide units to glutamine moieties on cyclopeptides of different sequences and sizes (for example **1**, in Fig. 7-1). For all cases, distances between sialic acid residues were estimated to be between 50 and 70 Å. These distances are slightly larger than that for the separation between HA binding sites (40-50 Å). Inhibition assays for hemagglutination on chicken erythrocytes induced by influenza virus A/PR/8/34 (H1N1) and SPR binding assays for the

interaction with the HA protein indicated that only bi- and trivalent conjugates based on the cyclic (Ser-Gly-Gly-Gln-Ser-His-Asp)$_3$ sequence were capable to bind HA protein.

Calixarenes are also very convenient macrocyclic scaffolds for building glycoclusters. Tetra- and octavalent sialoside clusters appended to a *cone*-blocked calix[4]arene through methyl- and propyl-based linkers were synthesized and evaluated as HA blockers.[22] Interestingly, when hemagglutination inhibition assays were performed against the influenza A virus, only those conjugates with propyl-based spacers (**2-4**) showed good inhibition properties, indicating that a minimum linker length is needed for the multivalent recognition. However, glycocluster effect operating in these compounds seemed to be moderate when relative inhibition properties per sialic acid moiety are considered, probably because the unsuitable length of the spacers. Nevertheless, the three conjugates **2-4** proved to be efficient anti-adhesive agents in MDCK cells.

Similarly to viral infection, bacterial adhesion occurs through specific interactions between proteins and glycoproteins or glycolipids at the surfaces of the bacteria and the target cell. Thus, a strategy to avoid the bacterial infection is the development of drugs that inhibit such interactions. In addition, many bacterial pathogens synthesize toxins that serve as primary virulence factor. Toxins can be single proteins or organized as oligomeric protein complexes with distinct AB structure-function properties.[23] The inhibition of the toxin attachment on the cell surface should be enough to avoid the infection.

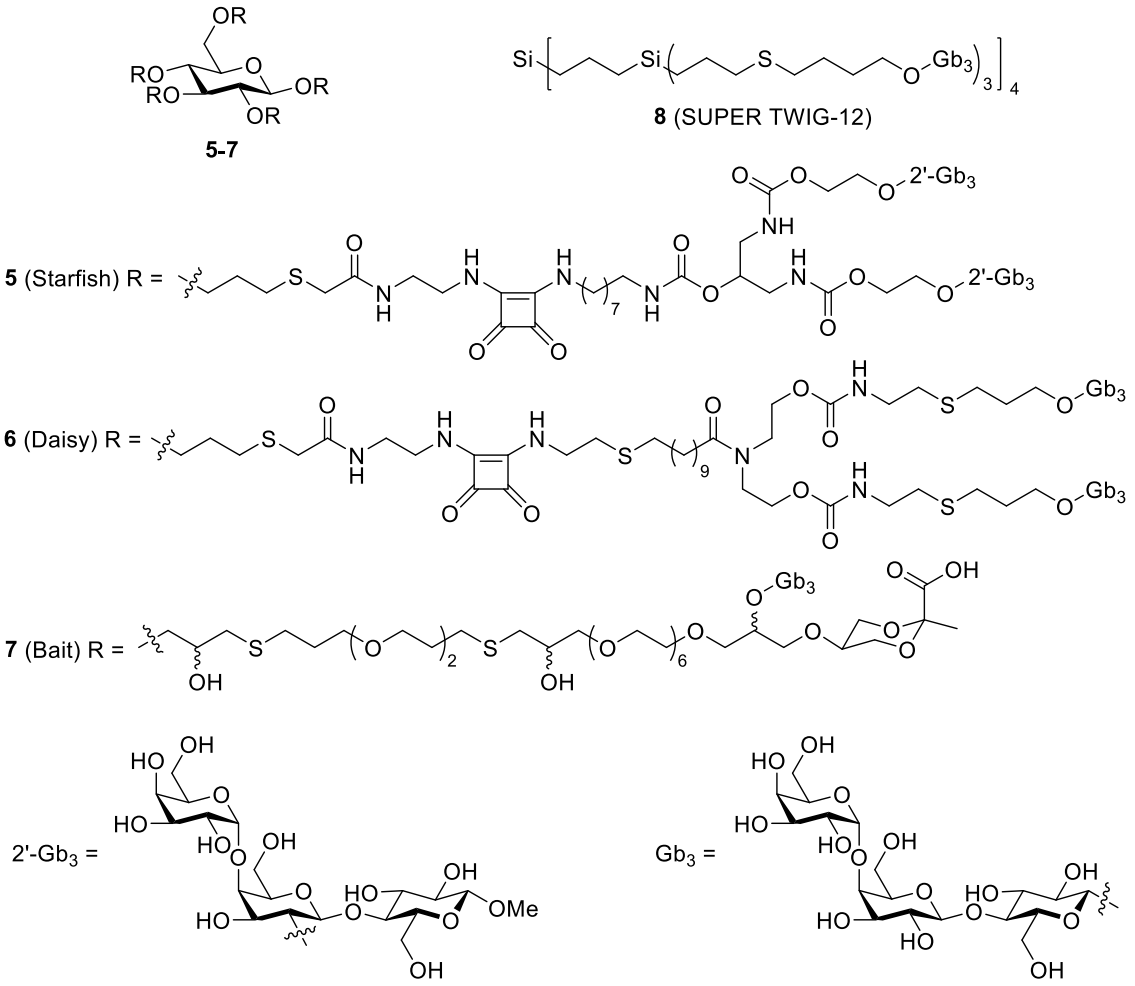

Figure 7-2. B_5 pentamer Shiga-like toxins (Stx-1/2) inhibitors centered on glucose (Starfish **5**, Daisy **6**, and Bait **7**) or carbosilane (SUPER TWIG-12 **8**) cores using globotriaosyl (Gb3) as binding residues.

In particular, Shiga-like toxins (SLT-1/2 or Stx-1/2), also called Verotoxins (VTs), are produced by some *Escherichia coli* strains called *shigatoxigenic*. They are named after Shiga toxin (Stx), which is produced by *Shigella dysenteriae* type 1, due to their high homology to the latter. These toxins present AB_5 structures and display selectivity towards the glycolipid globotriaosylceramide Gb3 [α-D-Gal(1→4)β-D-Gal(1→4)β-D-Glc(1→*O*-ceramide]. As an inhibitor for the B_5 pentamer, Bundle's group designed a decavalent glycocluster called Starfish **5** (Fig. 7-2),[24] composed of a glucose unit as central core to which ten Gb3 moieties are linked at position 2' through divalent linkers.

This design was intended to bind simultaneously recognition sites 1 and 2 present in each B monomer. However, crystallographic studies drew a different picture where each arm binds two B-subunit monomers from separate toxin molecules through their recognition sites 2, resulting in 2:1 AB_5:Starfish **5** sandwich-like structures. Inhibition abilities of Starfish were about 10^6 times more potent than monovalent Gb3 itself towards Stx-1. Thus, Starfish **5** was able to protect Vero cells against lethal doses of Stx-1 and Stx-2 over 2-days incubation periods. A modified version of Starfish, nicknamed Daisy (**6**), was later described by these authors.[25] Daisy displayed slightly longer arms, and Gb3 moieties were linked through the reducing terminus instead of position 2'. Interestingly, these changes induced somewhat weaker *in vitro* inhibitor abilities than Starfish (**5**), but *in vivo* administration protected mice against both Stx-1 and Stx-2 in a significant higher extension. A heterodifuctional analogue to Starfish (**5**) and Daisy (**6**), displaying five Gb3 moieties and five cyclic pyruvate ketal of glycerol residues was also synthesized and called Bait (**7**).[26] This derivative was able to bring together AB_5 Shiga-like toxins and similarly B_5 structured serum amyloid P component (SAP), one of the most abundant proteins in human serum, which would then act as a "trap" for the toxins in the so-called specific aggregation inhibition strategy. ELISA indicated that Bait (**7**) (IC_{50} = 140 μM) increased its inhibitory potency by 35 times in the presence of SAP (IC_{50} = 4 μM).

The use of diverse carbosilane scaffolds allowed for the synthesis of multivalent glycosides presenting different number (three, six and twelve) and spatial arrangements (fan-, dumbbell- and ball-shape) of trisaccharide globotriaose [α-D-Gal(1→4)β-D-Gal(1→4)β-D-Glc(1→] residues (SUPER TWIGs).[27] Hexa- and dodecavalent conjugates (Fig. 7-2), where distances from trisaccharide residues to central silicon carbon (~30 Å) matched predicted gap between Gb3-binding sites on the Shiga-Toxin B

subunit pentamer, showed 30-fold higher affinity than trivalent SUPER TWIGs. These two conjugates markedly inhibited the cytotoxic activity of Stx1 and Stx2 to Vero cells *in vitro* without affecting their viability. In mice, hexa- and dodecavalent SUPER TWIGs completely suppressed the lethal effect of Stx2. Interestingly, the dodecavalent conjugate showed higher activity *in vitro*, but the hexavalent analogue performed better *in vivo*. In a further study,[28] a SUPER TWIG presenting 18 trisaccharide residues also demonstrated to be another potent Stx neutralizer *in vivo*.

Cholera toxin is also an AB_5 protein that contains five galactoside binding sites and is able to recognize ganglioside GM1. The toxin is secreted by *Vibrio cholera* causing the disease of cholera.[29] The heat labile enterotoxin (LT-B_5), which is found in *Escherichia coli* is structurally similar to cholera toxin (CTB) and binds also to GM1. To prepare multivalent inhibitors of LT-B_5 and CTB, Fan and co-workers[30-33] have followed a modular approach employing aza crowns as scaffolds (Fig. 7-3). LT-B_5 and CTB are symmetrical proteins which contain five identical subunits presenting one binding site each. Distances between two nonadjacent binding sites are 45 Å. Using 4,7,10-trioxa-1,13-tridecanediamine as flexible modules,[30]**¡Error! Marcador no definido.** these authors synthesized a series of pentavalent galactoclusters (**9**-**12**) scaffolded on the 5-fold symmetric 15-azacrown-5 (pentacyclen), which present very well-defined effective length between nonadjacent galactoside units, varying from ~30 to ~45 Å. ELISA results of the LT-B5-GM1 binding inhibition of these compounds showed that IC_{50} values decreased with the increase of the spacer length, indicating a positive correlation between linker distance and affinity. The highest affinity (10^5-fold versus galactose) was achieved when the linker length was similar to the estimated distance in LT-B_5. Fan *et al.* also prepared an analogue containing *m*-nitrophenyl-α-D-galactoside (MNPG), a monomeric ligand 100-fold better than galactose.[31] Such

glycocluster **13** proved to be 18-fold more active than the equivalent compound **10**. In a further step, decavalent analogues of these pentavalent glycoclusters were designed to target two cholera toxin B-pentamers simultaneously.[32] Their IC_{50} values were one order of magnitude lower than those of their counterparts.

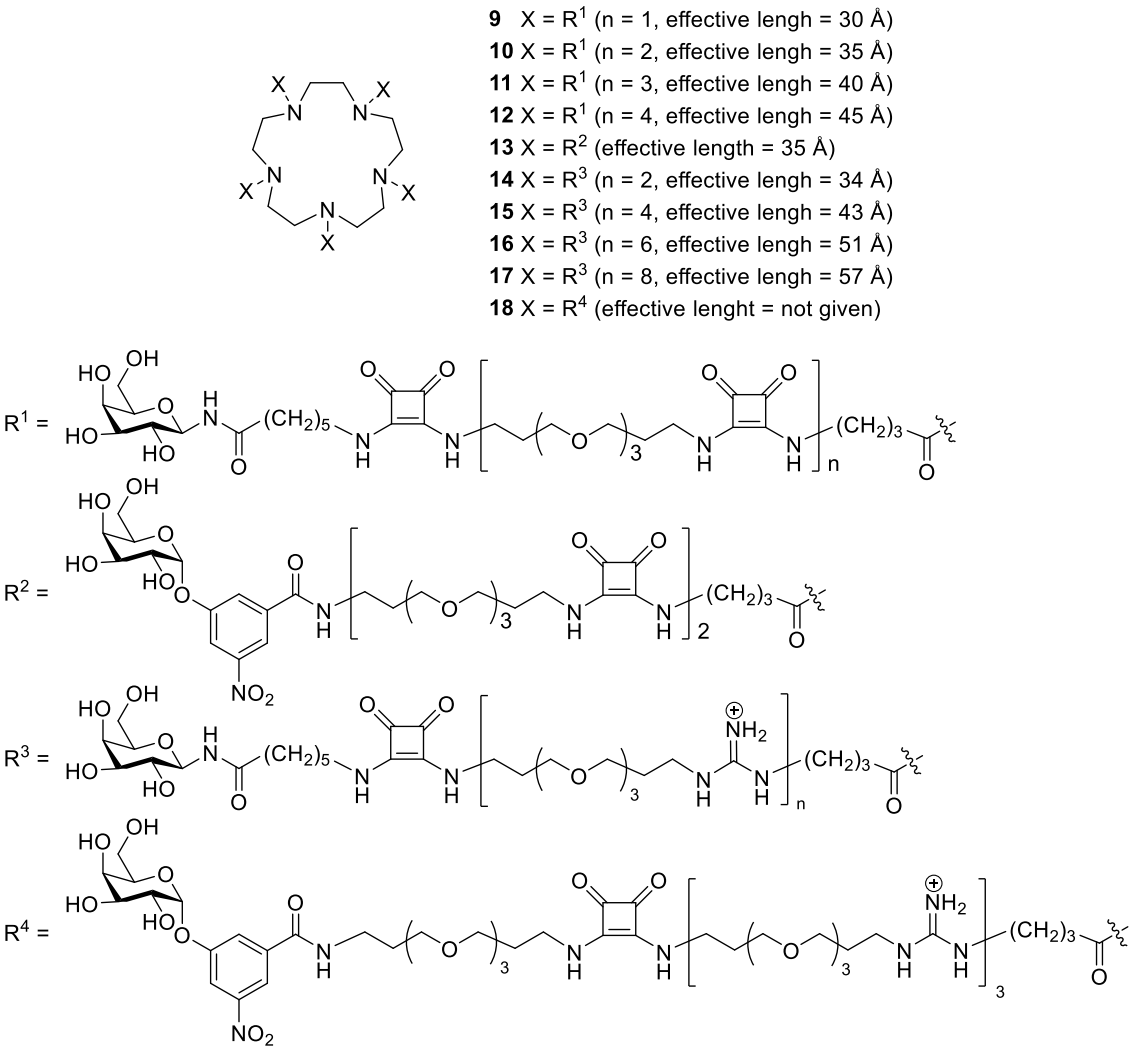

Figure 7-3. Cholera toxin B pentamer (CTB) inhibitors **9**-**18** designed on a pentacyclen core displaying five galactose residues.

Subsequent attempts to improve the inhibitory properties of pentacyclen-based galactoclusters following a rational design involved the synthesis of pentavalent

guanidinium-bridged derivatives **14**-**18** (Fig. 7-3).[33] MNPG-based ligand **18** was the first ligand displaying an IC_{50} lower than the natural receptor GM1.

Fan's group also grafted *N*-galactoside residues to Lys moieties of three different cyclic decapeptides through a series of four modular of the above mentioned linkers. These macrocycles contained five Lys moieties alternated with glycine (Gly), γ-aminobutyric acid (Abu) or ε-aminohexanoic acid (Ahx) in order to tune ring size and force the rings to adopt expanded conformations in solution.[34] The abilities to block the cholera toxin CTB pentamer from *E. coli* binding to GM1 were tested by ELISA and compared to those performed by analogous pentacyclen-based pentavalent ligands **14**-**17**. As the cyclic decapeptide core size increased, the number of modules needed in the linker for an optimal inhibition decreased, so effective distance between nonadjacent galactosamine moieties remained around 45 Å. Optimal distance yielded in all cases inhibitory powers around 100.000 times higher than that for monovalent galactose.

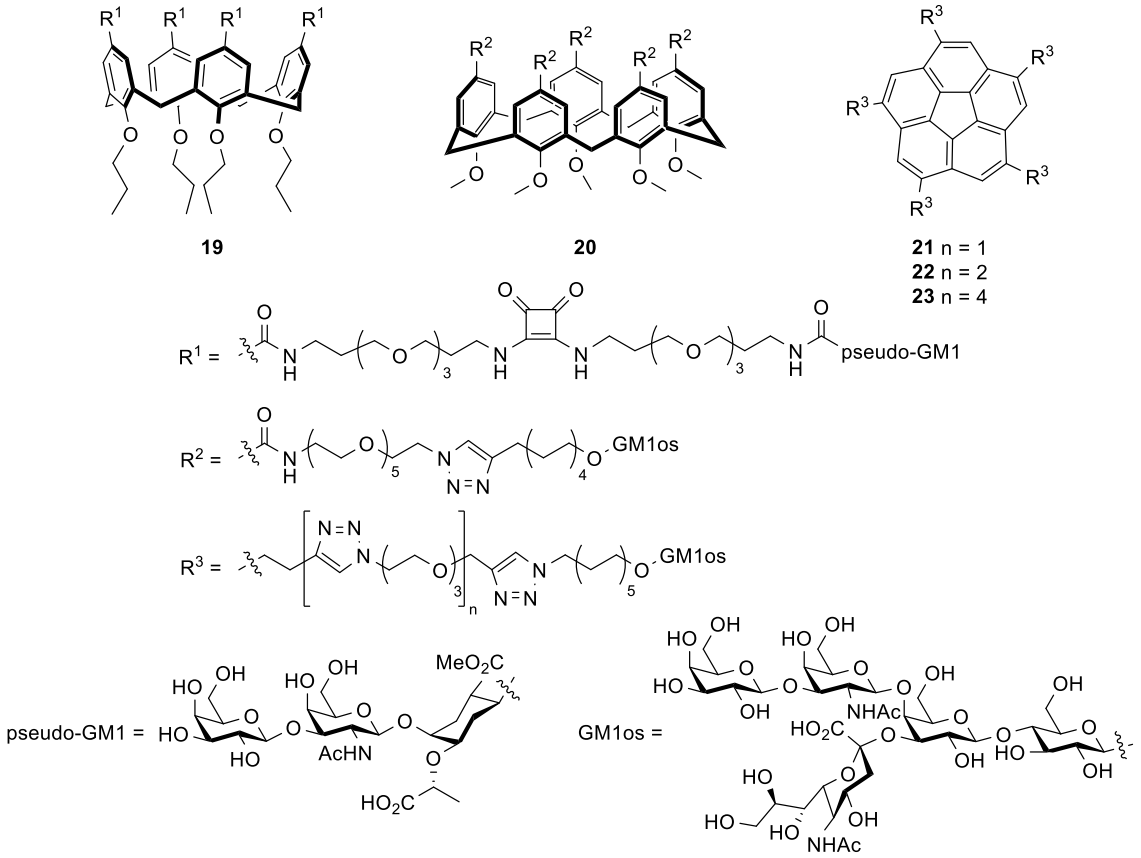

Figure 7-4. Cholera toxin B pentamer (CTB) inhibitors **19**-**23** presenting natural ganglioside GM1 and unnatural pseudo-GM2 mimic residues grafted on calix[4]arene, calix[5]arene and corannulene scaffolds.

Using a similar linker, Ariosio *et al.*[35] have conjugated two units of pseudo-GM1 at the upper-rim of a *cone*-locked calix[4]arene (Fig. 7-4**).** Such pseudo-trisaccaride is an unnatural mimic of the pentasaccharide GM1os of the natural ganglioside GM1, that is recognized by the cholera toxin CTB pentamer. The binding ability of this compound to CTB was studied by fluorescence spectroscopy titration and ELISA assays, and results indicated that the glycocluster displays only a slightly higher affinity for CT (K_d = 48 nM) than GM1os (K_d = 219 nM). However, when compared to the monovalent unnatural pseudo-GM1 (K_d = 190 μM), relative binding potency per branch enhanced in a factor of ~4000, probably due to the appropriate orientation and length of the sugar moieties provided by the calix[4]arene core and the spacer, respectively. In order to

match the CTB valency, a newer glycocluster (**20**) based on a *cone*-blocked calix[5]arene was subsequently prepared.[36] Five GM1os pentasaccharide units were grafted on the upper rim of the macrocycle but in this case through triazole-based linkers of an appropriate length (31 atoms). Such spatial arrangement allowes the simultaneous interaction of the five GM1os units with the five B-subunits of a single toxin. The inhibition potency of this conjugate towards the interaction of CTB with the natural ligand GM1 was measured by ELISA. Compound **20** showed a relative inhibitory potency 10^5 times (20000 times per residue) higher than that for a monovalent GM1os analogue. This result indicates that GM1os-calix[5]arene is one of the most potent known CTB inhibitors ever reported.

Pentasaccharide GM1os were also grafted through similar triazole-ethylenglycol linkers of different lengths, to *sym*-corannulene yielding heptavalent glycoclusters **21**-**23** (Fig. 7-4).[37] Although the interaction of these systems to the cholera toxin CTB pentamer was hampered by aggregation processes, high, nanomolar inhibitory potencies were obtained which were clearly affected by the linker length. In the case of GM1os family, conjugates **21**-**23** showed relative inhibitory potencies per sugar residue of 770, 3700 and 2600, respectively, when referred to monovalent GM1os.

As previously pointed out, a precise matching of the valency and spacing between the carbohydrate ligands and CTB is crucial in the design of an effective inhibitor for this toxin. Turnbull and co-workers postulated that the best scaffold for this aim would be the protein itself.[38] Thus, they modified an inactive mutant CTB protein unable to bind GM1os with five units of such oligosaccharide attached to its five *N*-terminal threonine residues, located on the protein surface toward the ligand-binding face and equally spaced around the protein between the GM1 binding sites. The synthesis of this conjugate was easy and relatively short, ensuring a potential large-scale application.

ELLA experiments toward CTB binding to GM1 reported the lowest IC_{50} value so far (104 pM), validating the proposed strategy. The formation of 1:1 CTB:neoglycoprotein heterodimers with an apparent K_d value of 30 nM was estimated by ITC, DLS and analytical ultracentrifugation (AUC).

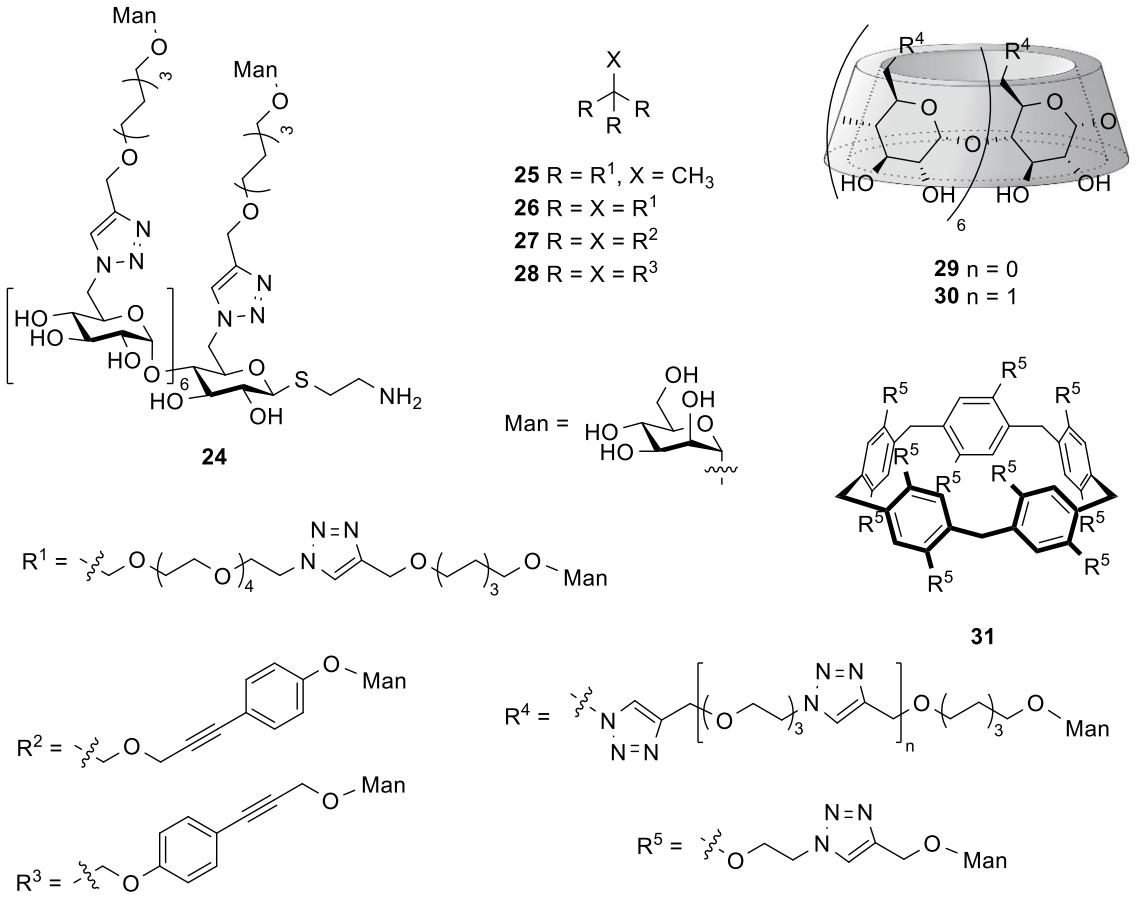

Figure 7-5. Antiadhesive cluster mannosiedes based on linear β-(1→4)-glucosides, pentaerythitol, β-cyclodextrin and pillar[5]arene cores **24**-**31** against FimH lectin, present in Type 1 piliated bacteria such as *E. coli.*

The surface of many bacteria is covered by the so-called Type 1 fimbriae, a sort of adhesive pilli presenting the mannose-binding lectin FimH which mediate the bacterial adhesion through the interaction with mannose residues of the host cell glycocalix. Lindhorst and co-workers[39] prepared a series of octa- and undecavalent mannosylated glycoclusters centered on mono-, di- and trisaccharides (trehalose, melibiose, raffinose

and glucose). However, such glycoconjugates displayed similar inhibitory properties for the adhesion of *Escherichia coli* bacteria to their host cells, regardless of the number of mannose residue or the spatial arrangement.

Also on saccharide cores such as di-, tri- and heptavalent linear β-(1→4)-glucosides, Almant *et al.* synthesized clusters of heptyl α-D-mannoside (HM) (one of the most potent FimH inhibitors reported to date).[40] Inhibition of haemagglutination (HAI) assay on guinea pig erythrocytes reported an inhibition potency enhancement with valency, the highest increase (64-fold, 9-fold per HM residue) corresponding to the heptavalent conjugate **24** (Fig. 7-5).

Gouin and co-workers prepared further tri- and tetra-(heptyl mannoside) clusters **25** and **26** based on a pentaerythritol scaffold.[41] These compounds were evaluated as antiadhesives towards type-1 piliated *E. coli* (covered by mannose-recognizing FimH lectins) by HIA and bladder binding assay (BBA). Results from HIA indicated that tri- and tetravalent conjugates were around 2-fold more potent inhibitors than heptyl mannoside (HM) for the hemagglutinantion of guinea pig erythrocytes promoted by *E. coli*. However, higher values were obtained when human bladder cells were used, indicating increases of 31- and 64-folds for the tri- and tetravalent conjugates, respectively.

Similarly, Touaibia *et al.* used pentaerythritol as a core for the preparation of a series of tetra- and hexavalent mannosylated glycoconjugates containing 1,2,3-triazolyl- or benzenethynyl-based linkers.[42] SPR experiments using soluble FimH lectin revealed that conjugate **27** was the best ligand, with a K_d = 0.45 nM (1277-fold better than that for mannose). Inversion of the spacer orientation (compound **28**) yielded K_d = 273 nM. Finally, inhibitory potencies against the haemagglutination of guinea pig or rabbit

erythrocytes by type-1 piliated clinical isolate of *E. coli* UTI89 were evaluated by HIA. Again, compound **27** showed the highest potency, with an inhibition titer of 3 μM (1000-fold better than mannose).

More recently, heptavalent HM clusters **29** and **30** based on β-cyclodextrin (β-CD) with two linkers of different length and flexibility were studied.[43] The study on the interaction *in vitro* with FimH revealed that the glycocluster with the longest spacer showed a higher effective valency, close to the structural valency, although both compounds were able to promote bacterial clustering through cross-linking interactions with cells in solution in a similar fashion. *In vivo* experiments for prevention of infection in mice bladder showed that both compounds caused a 10-fold reduction in the level of infection at 10 μM concentrations.

The inhibitory capability of a pillar[5]arene glycoconjugate **31** containing ten mannose residues (Fig. 7-5) against the adhesion of uropathogenic *E. coli* to guinea pig red blood cells has been tested by hemagglutination inhibition assay.[44] A relative potency per sugar moiety of 6.7 was found when compared to a monovalent analogue.

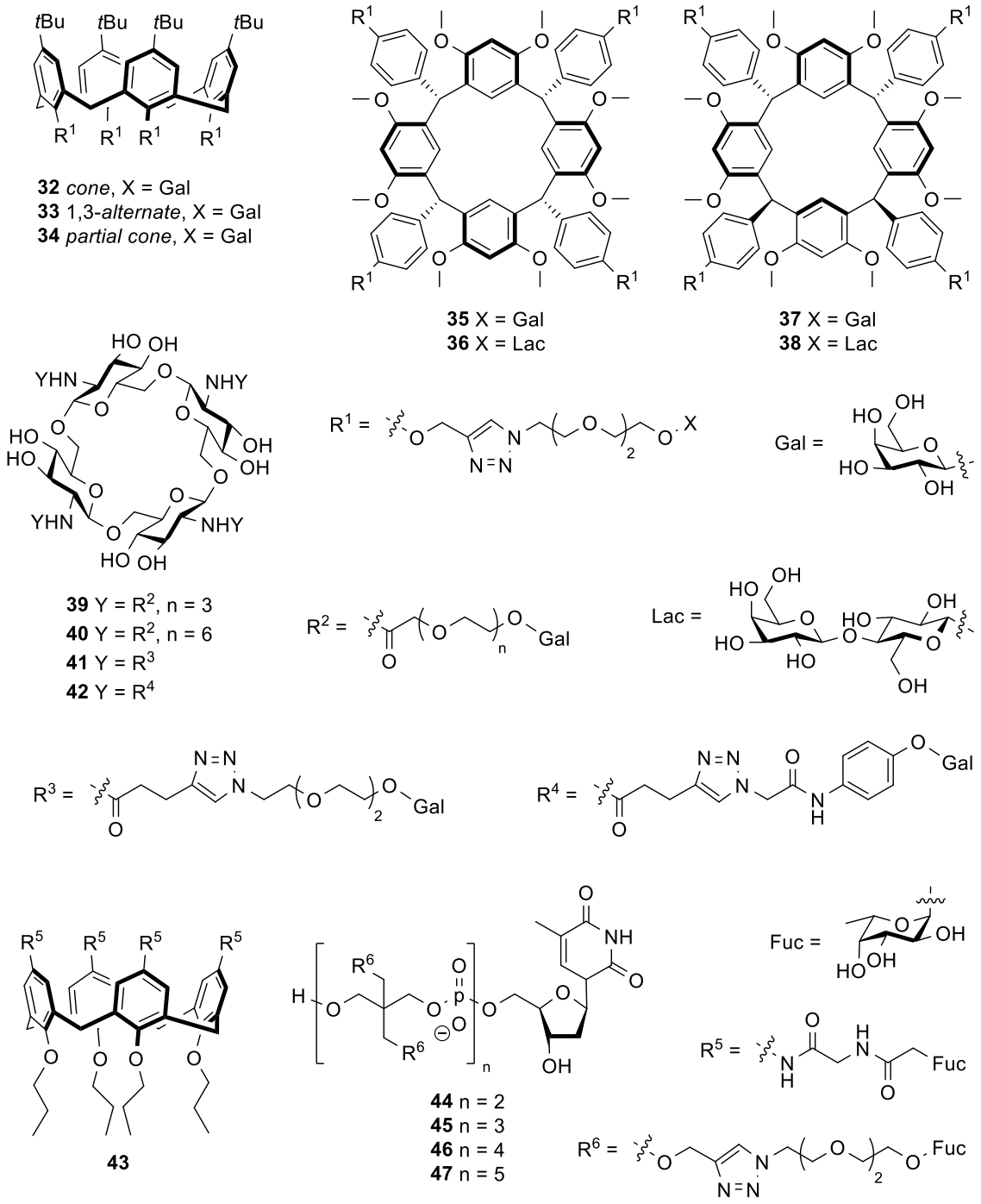

Figure 7-6. High affinity ligands for galactose-binding PA-IL (LecA) and fucose-binding PA-IIL (LecB) lectins from *Pseudomonas aeruginosa* (**32-42** and **43-47**, respectively) based on calix[4]arene, calix[4]resorcarene and pentaerythritol phosphodiester oligomer (PePOs) cores.

Another bacteria of interest is *Pseudomonas aeruginosa*, an opportunistic multidrug resistant (MDR) human pathogen and one of the leading causes of nosocomial infections worldwide.[45] Cell recognition is mediated by galactose-binding PA-IL (or LecA) and fucose-binding PA-IIL (or LecB) lectins, such lectins becoming biological targets of interest for the design of inhibitors and antiadhesives. For example, Vidal and co-workers prepared a series of seven lower-rim galactosyl calix[4]arene using a triethyleneglycol–triazolyl–methylene linker as ligands for PA-IL lectin.[46] Such series of glyconjugates included several valencies but also several topologycal arrangements of the galactoside residues. *Cone*-blocked calix[4]arene was grafted with one, two (1,2 and 1,3 positions), three and four saccharides. In addition, tetravalent 1,3-*alternate*-and *partial cone*-calix[4]arene conjugates were also prepared. Considering only the tetravalent conjugates, which display higher affinity than the rest, the 1,3-*alternate* conformation **33** showed the highest binding ability (K_d = 176 nM), followed by the *partial cone* **34** (K_d = 200 nM) and the *cone* **31** conjugates (K_d = 420 nM), yielding a 213-, 188- and 89-fold in affinity enhancement per carbohydrate residue, respectively. This trend is in agreement with the higher affinity found by other authors for the case of 1,3-*alternate* calix[4]arene derivatives (see below). These conjugates are thus more potent ligands than the best natural ligands of PA-IL (α-linked digalactoside).

These authors also carried out the synthesis of calix[4]resorcarene derivatives having four galactosil and lactosyl units on the lower rim of the macrocycle through the benzylic positions.[47] Calix[4]resorcarene conformation was fixed in two different topologies: the *rccc* boat (**35** and **36**) and the *rctt* chair (**37** and **38**) stereoisomers. Studies on the binding abilities of both galactosyl chair and boat conjugates towards PA-IL lectin showed a 314-fold and 244-fold improvement, respectively, when

compared to a monovalent analogue. However, the influence of the macrocyclic topology on the binding properties was barely observed.

Gening *et al.* prepared a family of cyclic oligo-(1→6)-β-D-glucosamines consisting of four monosaccharide units containing four attached galactoside ligands through spacer arms.[48] HIA, ELLA, and ITC were used to study their binding abilities toward PA-IL lectin from *P. aeruginosa*. Cluster **42**, having a rigid, short aromatic linker, in contrast with flexible and hydrophilic ethyleneglycol tethers of derivatives **39**-**41**, showed the lowest IC_{50} value (57 nM), with a relative potency per residue 1210-fold higher than the corresponding monovalent analogue. This glycocluster showed the highest reported affinity for PA-IL (K_d 80 nM).

In a similar fashion to that described above, fucosylated glycoclusters have been designed as potential biofilm inhibitors towards *P. aeruginosa* PA-IIL lectin. For example, a tetravalent α-L-fucosylated calix[4]arene **43** was prepared by Consoli *et al.* (Fig. 7-6).[49] The ability of this compound to inhibit the formation of the bacteria biofilm was evaluated by Minimum Biofilm Inhibitory Concentration (MBIC) assay. The activity was dose-dependent and the biofilm formation was inhibited in 73 % at 200 μM.

Tetra and deca α-L-fucosyl clusters **44**-**47** based on pentaerythrityl phosphodiester oligomeric cores (PePOs) were prepared by Morvan *et al.*[50] The structures also presented a thymidine moiety at the pseudo-3'-end in order to facilitate the determination of the conjugates concentration by UV spectroscopy. These compounds proved to inhibit the interaction of PA-IIL lectin with polymeric α-L-fucose. However, the increased binding found for these multivalent carbohydrate ligands was attributed to the *macromolecular* effect[39] rather than the cluster or multivalent effect.

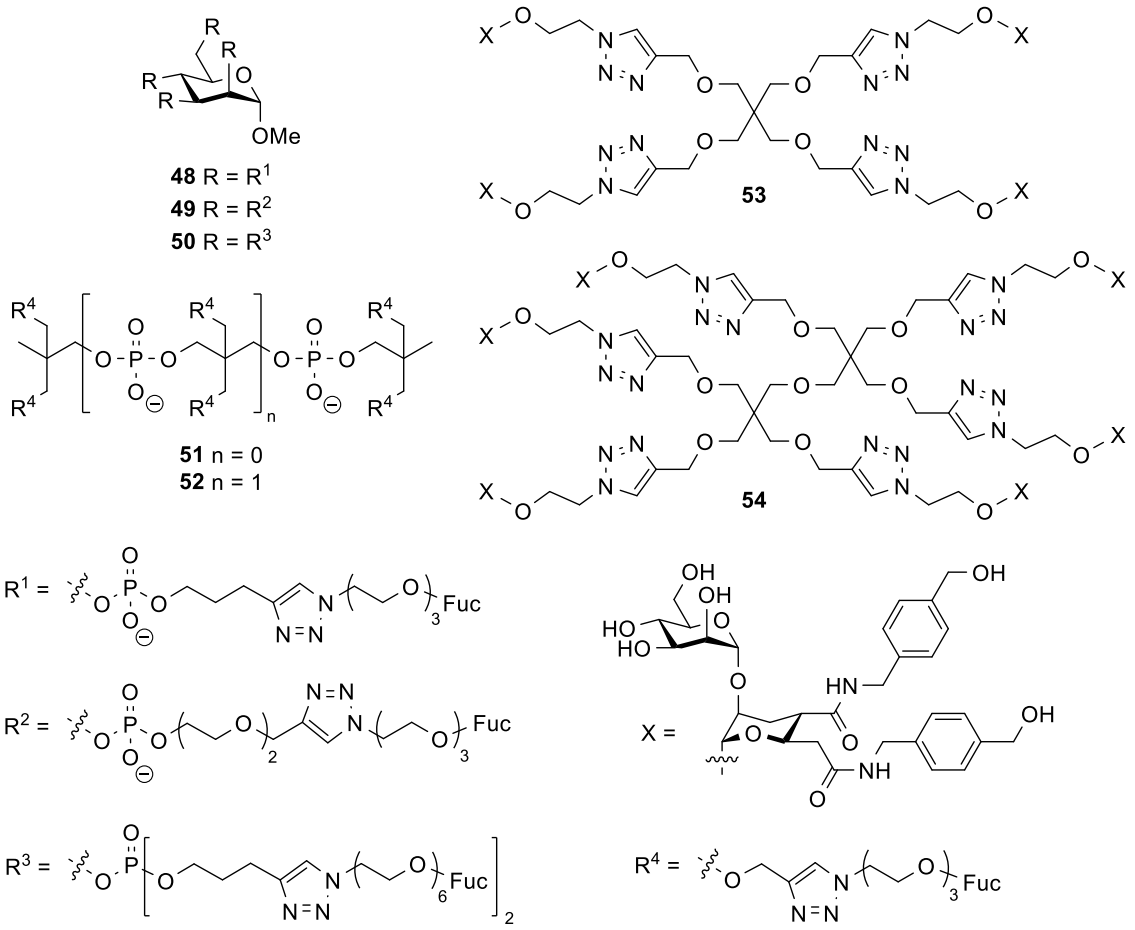

Figure 7-7. Fucosylated antiadhesive agents against BambL lectin from *Burkholderia ambifaria* bacteria (**48**-**52**) centered on mannose and pentaerythritol phosphodiester oligomers (PePOs), as well as HIV-1 and Dengue viruses inhibitors (**53** and **54**) bearing a non-natural pseudo-disaccharide DC-SIGN antagonist.

Fucosylated glycoclusters have also been reported as antiadhesives towards *Burkholderia ambifaria* bacteria, both using mannose (**48**-**50**) and a branched-phosphodiester (**51** and **52**) as scaffold and bearing four, six or eight sugar residues (Fig. 7-7).[51] The binding abilities of these conjugates towards this bacterial fucose-recognition lectin (BambL) were thus evaluated by means of HIA, SPR and ITC. As previously observed by other authors in similar studies,[52] these techniques yielded non-consistent values, although all conjugates demonstrated higher binding (between 9

and 22 folds) and inhibitory (between 16 and 256 folds) potencies than the monovalent methyl α-L-fucoside.

Apart from bacteria, viruses are also desirable targets for inhibitors. An interesting approach for the development of HIV-1 and Dengue virus (DV) inhibitors has been report by Varga *et al*.[53] A powerful synthetic pseudo-disaccharide DC-SIGN antagonist that mimics the natural trimannoside ligand was used to prepare a series of multivalent derivatives having from three to eighteen of valencies based on pentaerythritol cores (Fig. 7-7). Among the compounds tested as inhibitors *in vitro*, tetra- and hexavalent derivatives **53** and **54**, respectively, turned out to be the most active. While tetravalent **53** completely inhibited HIV *trans*-infection at 100 μM concentration, hexavalent **54** derivative only required 10 μM to perform the same result. The latter was also able to reduce DV serotype-2 infections to 85 %. This result is remarkable since no clinical treatments are available for DV infection.

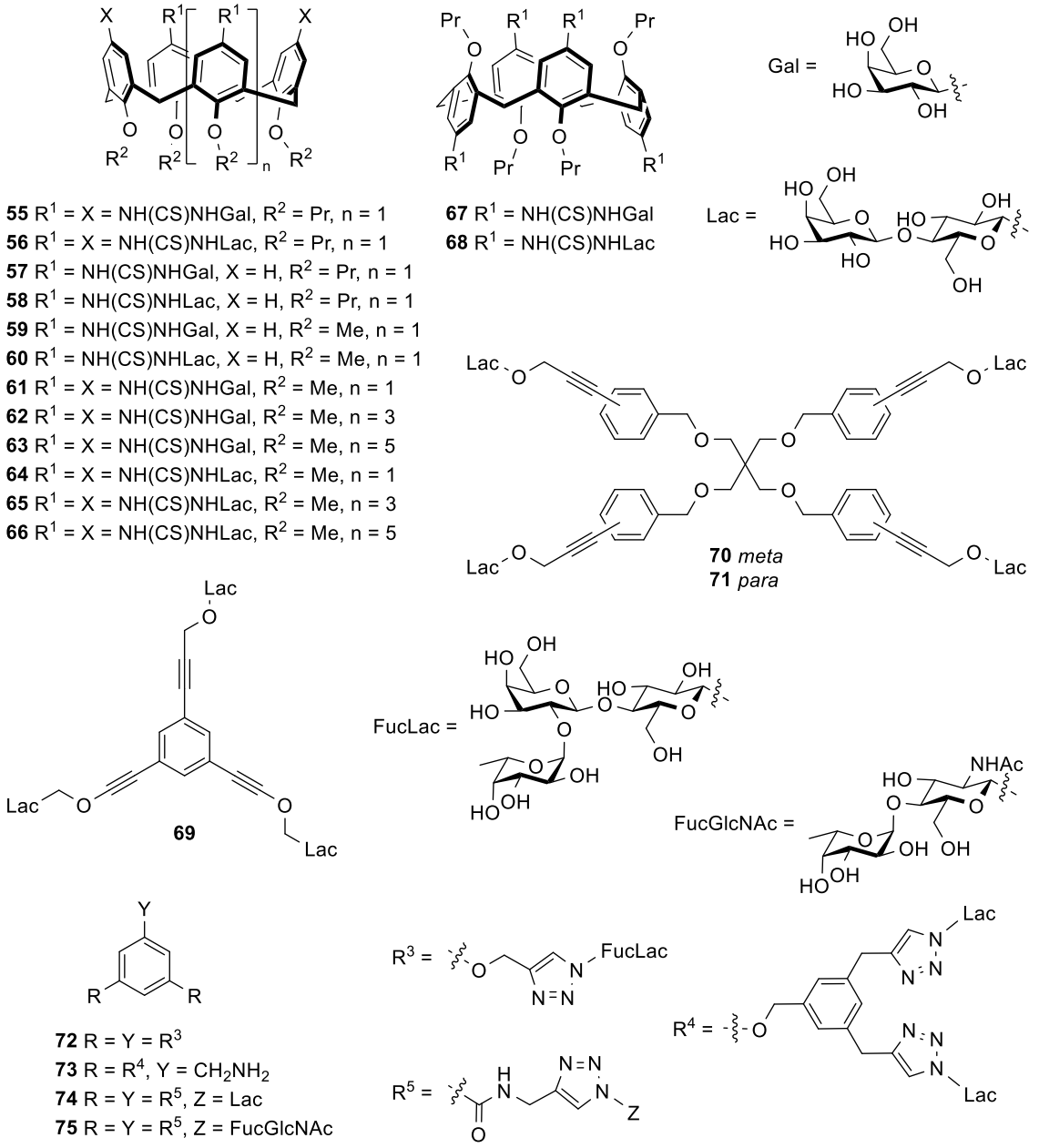

Figure 7-8. High affinity ligands for galactose-binding AB toxin *Viscum album* agglutinin (VVA) and tumor-overexpressed lectins Gal-1, -3, -7, -8 and -9, consisting on the attachment of galactose, lactose, 2'-fucosyllactose and 4-fucosylglucosamine residues on calix[n]arene (n = 4, 6 or 8), pentaerythritol or 1,3,5-benzene cores.

The inhibitory efficiency of glycocalixarenes **55-68** (Fig. 7-8) towards galactoside-binding AB toxin *Viscum album* agglutinin (VAA), but also lectins present in colon cancer such as galectins (Gal) 1, 3 and 4, was found to depend on the orientation of the

sugars, the size of the ring and the flexibility of the scaffold, apart from the valency.[54] This extensive study was developed from divalent to octavalent galactosyl- and lactosythioureido calix[n]arenes (n = 4, 6 and 8). Not only were decreases of IC_{50} values up to 300-fold relative to free sugar found, but also selectivity depending on the lectin employed was observed. In most cases, the highest inhibition potencies were found towards Gal-4, followed by VAA and Gal-3, whereas Gal-1 gave the poorest results. Interestingly, calix[6]- and calix[8]arenes being more flexible and dynamic gave the best inhibitory effects towards all the lectins tested, a result which contrasts with those reported by Consoli *et al.* on similar conjugates but using WGA as lectin.[55] In addition, tetravalent *cone*- and *alternated*-blocked calix[4]arene derivatives also showed sharp differences as inhibitors, despite of having the same valency. In general, *cone* conformation resulted in better inhibitory abilities except for the case of Gal-1, for which the *alternated* conjugate turned out to be the best ligand whereas the *cone* analogue was even worse than the monovalent carbohydrate. This behavior for Gal-1 is similar to those results collected by Vidal and co-workers for PA-IL lectin using longer, more flexible linkers.[46] These trends are more or less maintained when the conjugates were tested in inhibition assays involving human tumor cell lines. Thus, this series of glycocalixarenes allows the possibility of targeting galectins differently: Glycoconjugate **56** as blocker of Gal-3 binding to colon cancer cells; flexible **65** and **66** for Gal-4 binding to pancreatic carcinoma cells, and **68** as inhibitor of Gal-1 and -4. Selection between these three galectins could be further enhanced by replacing lactose residues with 3'-*O*-benzyl-LacNAc on *cone*-blocked calix[4]arene and calix[6]arene scaffolds. While the former showed a marked selectivity towards Gal-3, the latter displayed an improved efficiency towards Gal-4.[56]

Roy and *et al.* synthesized tri- and tetravalent lactosyl clusters based on 1,3,5-benzene and pentaerythritol cores (**69**-**71**), respectively, by Sonogashira reaction (Fig. 7-8).[57] Their inhibitor abilities were tested towards dimeric Gal-1 and -7, monomeric Gal-3, the β-trefoil mistletoe lectin *Viscum album* agglutinin (VAA), and a natural β-galactoside-specific immunoglobulin G fraction from human serum. Whereas Gal-1 and -7 were not affected by these glycoclusters, Gal-3 was effectively inhibited by the trivalent derivative **69** (IC_{50} = 30.8 μM, relative potency = 7.6 per residue; IC_{50}(lactose) = 700 μM). Weaker effect was shown by the two tetravalent analogues **70** and **71** (IC_{50} = 125 μM for *meta* and = 62.3 μM for *para*). In contrast, these tetravalent clusters exhibited the strongest inhibition in the case of VAA (IC_{50} = 40 μM, relative potency = 12.5 per residue for both compounds; IC_{50}(lactose) = 2000 μM). *meta*-Derivative **70** was also a good inhibitor for the natural immunoglobulin G fraction (IC_{50} = 199 μM, relative potency = 3.8 per residue; IC_{50}(lactose) = 3000 μM).

Murphy and co-workers reported a series of tri- and tetravalent lactosyl clusters based on 1,3,5-benzene and tris(3-aminopropyl)amine, as well as a trivalent 2′-fucosyllactosyl cluster based on 1,3,5-benzene.[58] Their binding and inhibition abilities were tested towards a series of different galactoside-binding proteins. Best results were obtained by trivalent fucosylated and tetravalent lactosylated compounds (**72** and **73**) towards chicken galectin CG-3 (63- and 42-fold enhancement per sugar residue when compared to lactose). Both derivatives also bound chicken galectin CG-8 with values between 10 and 19 times higher than lactose.

Trivalent lactosyl conjugates **74** and **75** demonstrated enhanced inhibitory ability towards human Gal-1 by hemagglutination assay on type O red blood cells, with a relative potency per lactose moiety around 13. However, no cluster effect was observed when monomeric Gal-3 was used, with a relative potency per lactose residue of

1.1.[59,60] Inhibition of adhesion of these and other lectins (VAA, Gal-8 and Gal-9) to human tumor cells (T-cell leukemia and a colon adenocarcinoma) assays, however, showed a remarkable activity of the lactosyl clusters towards Gal -3, -8 and -9, but not to Gal-1.[61]

7.3. Carbohydrate clusters as synthetic vaccines

An approach to develop synthetic vaccines involved the preparation of multivalent antigenic carbohydrates. Such multivalent display is crucial to cross-link with immunoglobulin receptors to generating anticarbohydrate antibodie responses.[62]

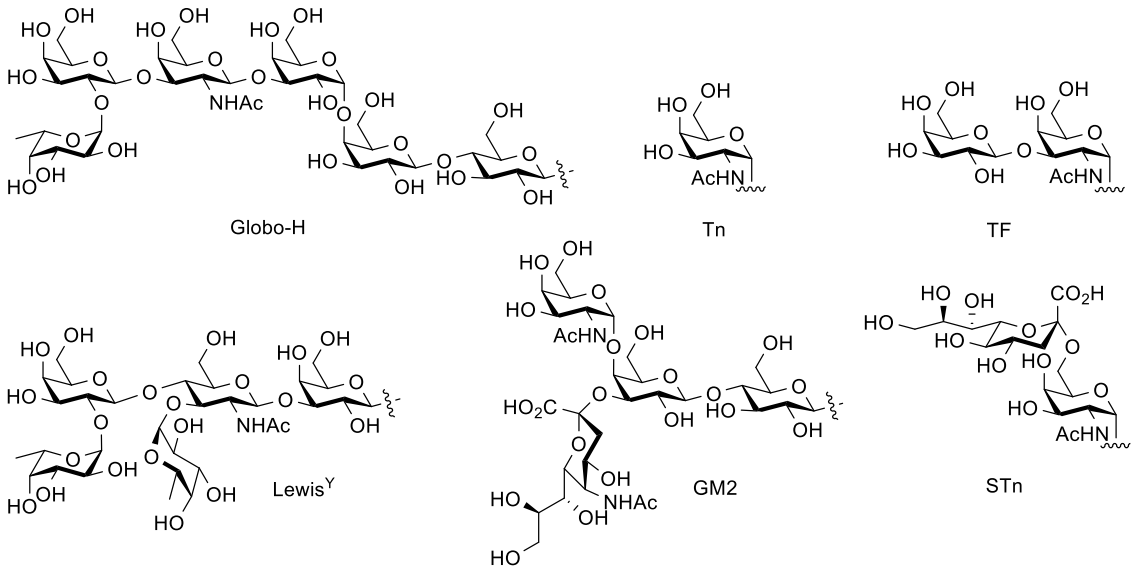

Figure 7-9. Tumour-Associated Carbohydrate Antigens (TACAs) commonly used in synthetic anti-cancer vaccines development.

A group of tumour-associated antigens of carbohydrate nature have been identified and characterized by virtue of their reactivity with antibodies and lectins and called tumour-associated carbohydrate antigens (TACAs), some of those are showed in Fig. 7-9.[63] It should be pointed that Tn, STn and TF antigens are in fact glycosides of serine (Ser) or threonine (Thr), although only their saccharide fractions are depicted for practical

purposes. In a pioneer work, Leclerc and co-workers designed tetrameric multiple antigen glycopeptide (MAG) **76** as a potential anticancer vaccine, consisting of a lysine tripeptide core with four arms linked to the PV oligopeptide from the poliovirus type 1 (Fig. 7-10).[64] Such MAG is bearing four tumour Tn epitope units (α-GalNAc-*O*-Ser/Thr) appended at the amino terminus (MAG:Tn-PV). ELISA experiments led to the conclusion that the Tn saccharidic epitope increased T-cell stimulation by 10,000-fold when compared to the Tn non-bearing analogue. Immunization of mice with MAG:Tn-PV in the presence of the mild and harmless adjuvant aluminum hydroxide induced the production of T-cell dependent IgG anti-Tn antibodies capable of recognizing native Tn antigen present on the human Jurkat T-lymphoma and LS180 adenocarcinoma cell lines. Dodecavalent analogue (MAG:Tn3-PV) **77** elicited a much more potent and persistent response than that described for MAG:Tn-PV and increased mice survival against TA3/Ha to 70-90 % depending on the dose.[65]

Danishefsky and co-workers developed a general strategy for the preparation of fully synthetic multiantigenic carbohydrate-based cancer vaccines consisting of oligopeptides presenting three (**78** and **79**)[66] or five (**80** and **81**)[67,68] different representative members of the four main classes of TACAs conjugated to the carrier protein KLH (Fig. 7-10). Using QS-21 as adjuvant, vaccines **78**, **79** and **81** induced the production of titers corresponding to all of the carbohydrate antigens showed in their structure, while derivative **80** was not successful in generating an immunoreponse against one of the antigens ($Lewis^Y$).[69] Moreover, Fluorescent Activated Cell Sorter (FACS) showed the induced antibodies to react strongly with cancer cell lines expressing those antigens. All four constructions **78**-**81** revealed notably superior responses that those given by the pooled combination of the corresponding monovalent vaccines, except for Tn mucin. Vaccine **81** is currently under phase I clinical trial in ovarian cancer patients.

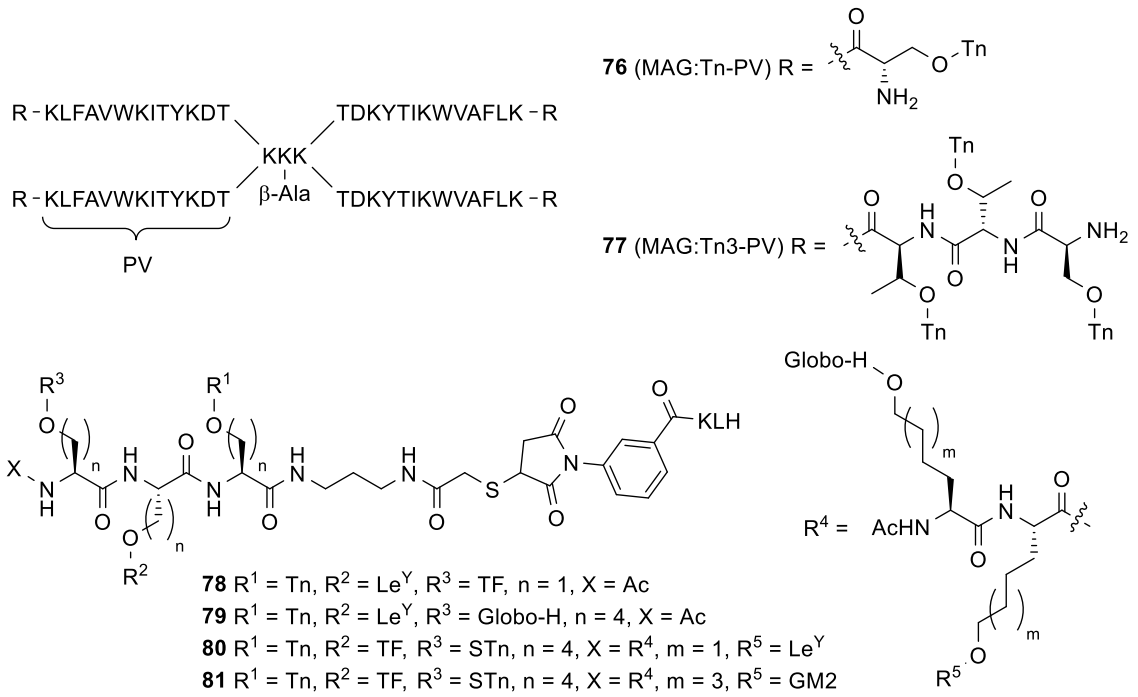

Figure 7-10. Anti-cancer vaccines based on the appendage of one or several TACAs on branched (**76** and **77**) or lineal (**78**-**81**) oligopeptides, using polivirus type 1 PV oligopeptide or keyhole limpet hemocyanin (KLH) carrier protein, respectively.

Leclerc's and Bay's groups[70] have developed an enzymatic method for the *in vitro* glycosylation of human mucin MUC6 from the MCF7 breast cancer cell line with different densities of the tumour epitope Tn. MUC6 protein is naturally expressed in gastric tissues, but it has been detected aberrantly glycosylated in several types of tumors such as intestinal, pulmonary, colorectal, and breast carcinomas. Although this method afforded different densities of glycosylation varying from 14 to 54 α-GalNAc units per protein molecule depending on the enzyme source and the protein acceptor (a major drawback of this vaccine preparation strategy), all protein glycoconjugates were recognized by two anti-Tn monoclonal antibodies specific to human cancer cells. Sera

from mice immunized with these glycoclusters showed IgG antibodies that recognized the Jurkat human tumor cell line.

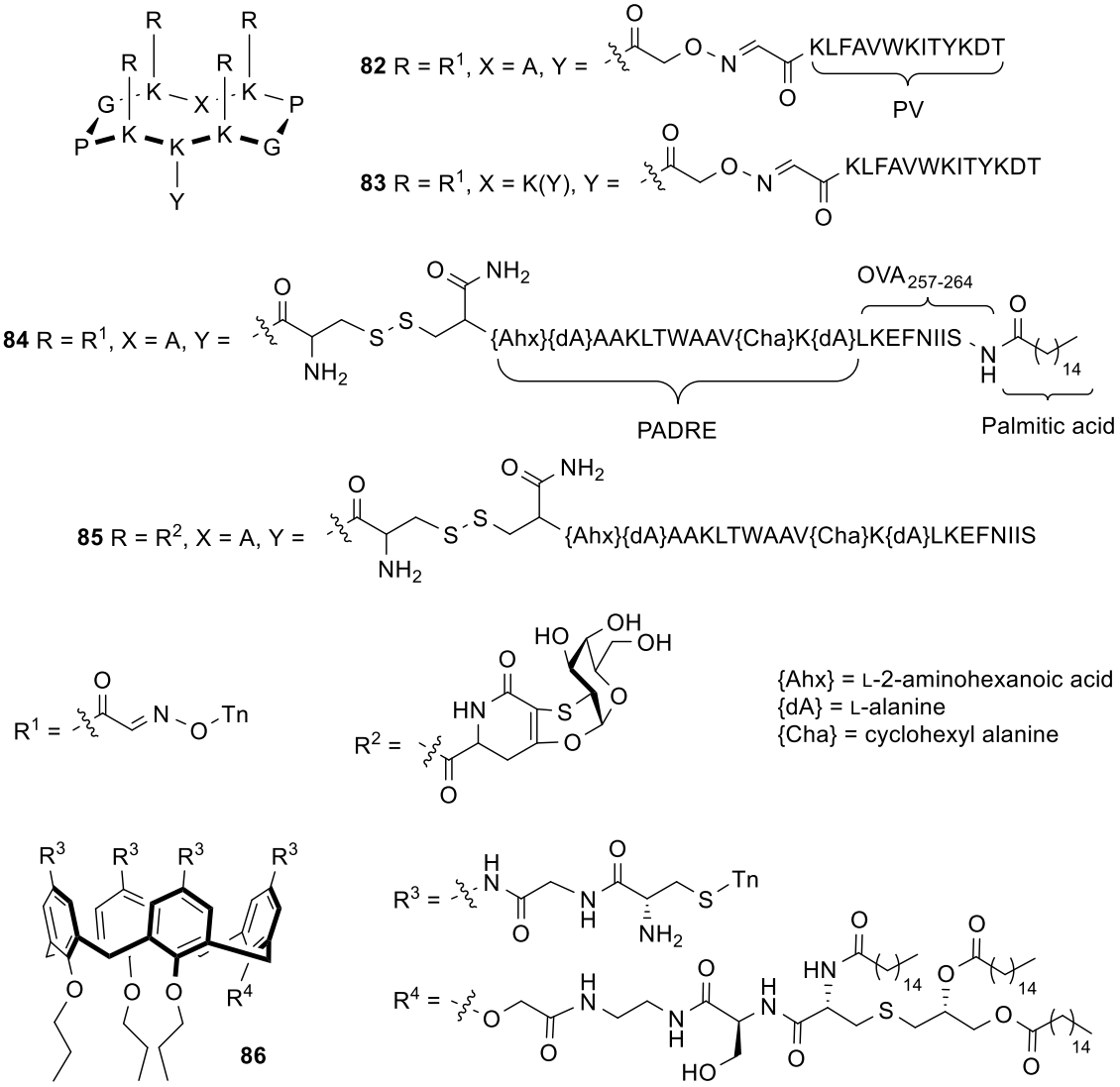

Figure 7-11. Anti cancer vaccines containing Tn and Tn-antigen mimetic MIM_Tn clusters grafted on 10-Residues Addressable Functionalized Template (RAFT) (**82**-**85**) and calix[4]arene (**86**) as scaffolds.

Dumy and co-workers have developed an anticancer vaccine designed as a Tn antigen cluster regioselectively appended on two different 10-residues addressable functionalized templates (RAFTs), backbone-cyclized decapeptides that present a stable β-sheet conformation in solution.[71] These templates served as scaffolds for the

attachment of four Tn epitopes, as well as one (**82**) or two (**83**) polivirus PV peptides (Fig. 7-11). Resulting glycoclusters were recognizable by two anti-Tn monoclonal antibodies. Sera from mice immunized with these two glycoclusters showed similar levels of Tn-specific IgG antibodies, indicating that the second PV epitope does not induce any immune response enhancement. Flow cytometry studies confirmed that elicited IgG antibodies were able to bind to the human Jurkat tumor cell line expressing the Tn antigen. As a further extension of this strategy, a four Tn epitopes containing RAFT was appended with a linear CD8+ T-cell peptide from ovalbumin ($OVA_{257–264}$), a CD4+ T-cell peptide (PADRE), and a palmitic acid moiety (PAM) as built-in lipid adjuvant that induces DC maturation. Resulting ovalbumin glyco-lipopeptide **84** (OVA-GLP) elicited significant levels of RAFT-specific antibodies in sera from mice even in the absence of any external adjuvant. Furthermore, 90% OVA-GLP immunized mice rejected mouse melanoma cells (B16) expressing ovalbumin, and 90 % non-immunized, B16 inoculated mice evidenced tumor growth delay when treated with OVA-GLP.[72,73] Very recently, two saccharide epitopes, Tn and TF were simultaneously combined on the RAFT platform in five different ratios (from 4:0 to 0:4), however the immunological ability of these glycoclusters have not evaluated yet.[74]

Given the sensitivity of TACAs to the action of glycosidases, the use of modified TACAs (such as *C*- or *S*-glycosides) or glycosidase-resistant mimics was suggested. In this context, BenMohammed and co-workers prepared the new RAFT-based tetravalent glycocluster **85** presenting four Tn-antigen mimetic MIM_Tn residues and the immunostimulant peptide epitope OvaPADRE.[75] Sera from immunized mice with this conjugate using CpG_{1826} as adjuvant showed significant levels of mucin-specific IgG/IgM antibodies that bound Tn-expressing cancer cell lines both from mouse (NT2

and TA3HA) and human (MCF7). Furthermore, immunized mice showed a survival of 70 % upon tumor implantation after 2 months through a B cells-mediated mechanism.

Spadaro and co-workers[76] synthesized *cone*-blocked calix[4]arene glycoconjugate **86** bearing four *S*-Tn (α-GalNAc-*S*-Ser) antigen residues and an immunoadjuvant moiety, tripalmitoyl-*S*-glycerylcysteinylserine (P_3CS) at the opposite rim of the macrocycle (Fig. 7-11). Sera from mice immunized with this structure showed the presence of an increased concentration of Tn-specific IgG antibodies, 4 times higher than non-immunized mice.

The use of carbohydrate clusters as vaccines against HIV has also been investigated. As the major carbohydrate present on the surface of the HIV envelope spike protein gp120, glycan $Man_9GlcNAc_2$ is expected to stimulate the production of 2G12 antibody, rarely excreted in human HIV immunological response and capable of neutralizing a broad range of HIV strains. Danishefsky and coworkers synthetized a fully synthetic HIV antigen **87** consisting of two copies of high-mannose glycan $Man_9GlcNAc_2$ assembled on a *β*-sheet shaped 14-residues cyclopeptide (Fig. 7-12).[77] Glycan-cyclopeptide conjugate was covalently coupled onto the outer membrane protein complex (OMPC) from *Neisseria meningitides*, a highly effective immunostimulatory carrier protein. This conjugation was estimated to give ~2000 copies of the glycopeptide per OMPC unit. The mimetic-OMPC conjugate showed a clear response, although it was not as robust as that of the positive control, gp160. Further studies presented evidence, from both direct and competitive binding assays, that there was no significant recognition of the glycopeptides, although certain sera did contain antibodies that could compete with 2G12 for binding to recombinant gp120. [78] Similar derivatives were prepared by Wang and co-workers but with substantial differences in the structure and valency of the oligosaccharide[79] that included the fluorination at 6-position of the terminal

mannose residue of gp120 glycan D1 tetramannoside arm in order to enhance the immunogenicity of the saccharide **89**. But the estimation of the binding abilities of this GCP to human 2G12 human antibody led to higher values for a non-fluorinated analogue **88** used as control.

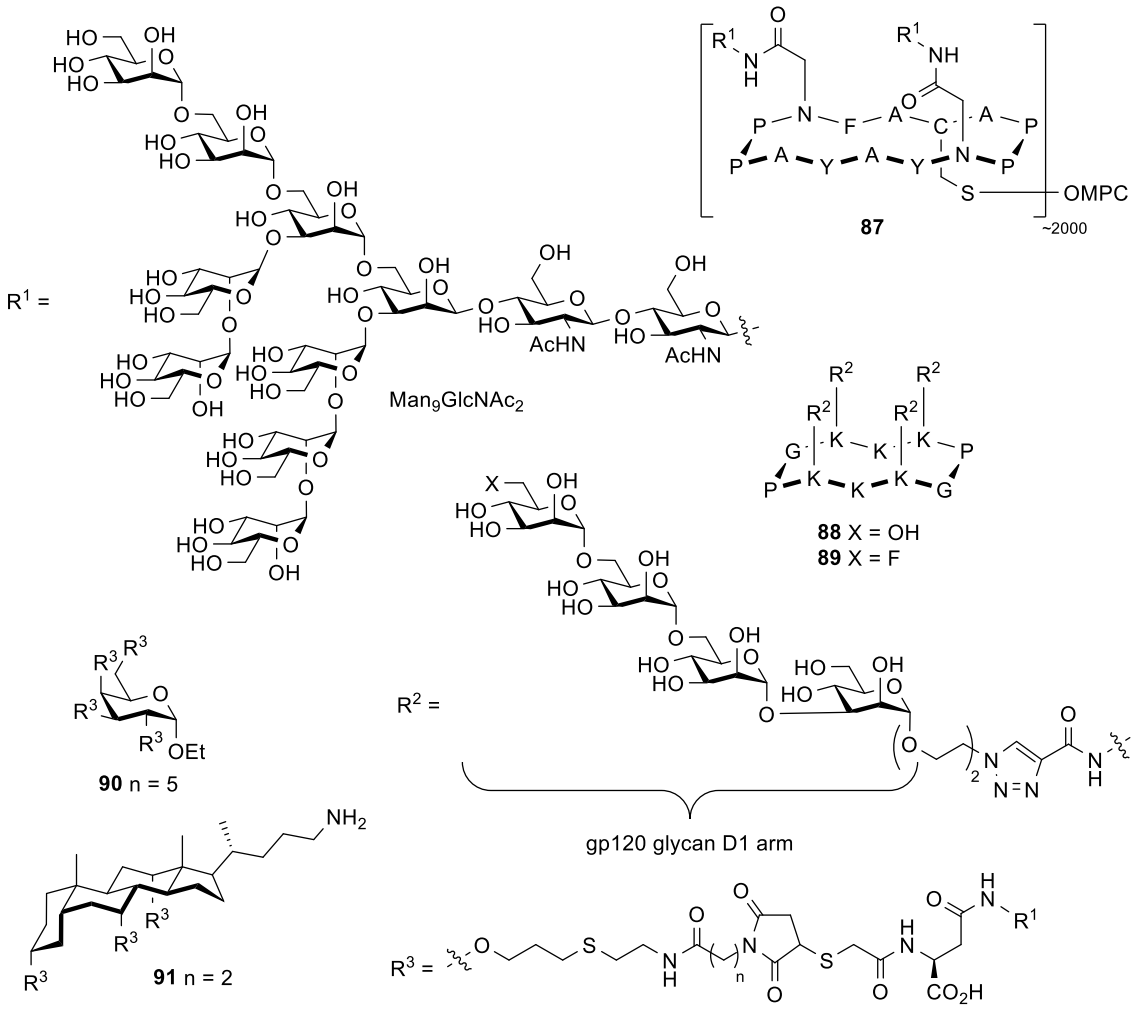

Figure 7-12. Carbohydrate-based vaccines against HIV designed as clusters of gp120 glypan ($Man_9GlcNAc_2$) or its structurally simpler D1 tetramannoside arm grafted on different scaffolds such as 14- (**87**) and 10-RAFTs (**88** and **89**), galactose (**90**) and cholic acid (**91**).

Wang's group had already explored the use of galactose-centered and cholic acid-scaffolded analogues containing the whole $Man_9GlcNAc_2$ glycan (Fig. 7-12).[80,81]

They prepared a compound with four $Man_9GlcNAc_2$ moieties appended on positions 2, 3, 4 and 6 of the galactose core (**90**), as well as a cholate derivative having three glycan moieties at the cholate positions 3α, 7α and 12α (**91**). The inhibition studies for these tetravalent and trivalent glycoclusters of 2G12 binding to gp120 showed IC_{50} values 73-fold and 46-fold higher than the monomeric $Man_9GlcNAc_2Asn$, respectively, but the relative affinity of this cluster, in the μM level, was much lower than the affinity of 2G12 for gp120 in the nM level. When the galactose-centered glycocluster **90** was grafted with a T-helper epitope from tetanus toxoid or the carrier protein KLH it was found that sera from immunized rabbits with such glycoclusters showed higher IgG type antibody titers than those immunized with a monovalent analogue. However, the majority of antibody responses were directed to the linkers.[82]

As a further step in developing an anti-HIV vaccine, a number of multivalent 33-mer glycopeptides containing 3-4 copies of Man_9 epitope ($Man_9GlcNAc$) for 2G12 anti-HIV antibody were prepared by a directed evolution-based strategy (SELMA), in which a DNA backbone evolves to optimally cluster the epitope glycans.[83] Multiples mRNA oligopeptides directly linked to their encoding mRNA strands and showing a random distribution of 1 to 6 homopropargylglycine moieties where prepared by ribosomal translation from a DNA library. Propargylated glycine units were then grafted with the 2G12 Man_9 epitope and tested as 2G12 ligands. Those showing highest binding abilities were reverse transcribed to cDNA, from which a second generation DNA library was generated. Iterative repetition of this process led to the identification of the 10 highest-affinity conjugates for the target 2G12 antibody, which were finally prepared without the mRNA tags. These glycopeptides showed tight binding abilities towards 2G12 antibody (K_D = 0.5-5 nM) and inhibitory properties towards the interaction of 2G12

with gp120 protein. These results represent an enhancement of up to 360000-fold as compared to monovalent Man_9 glycan.

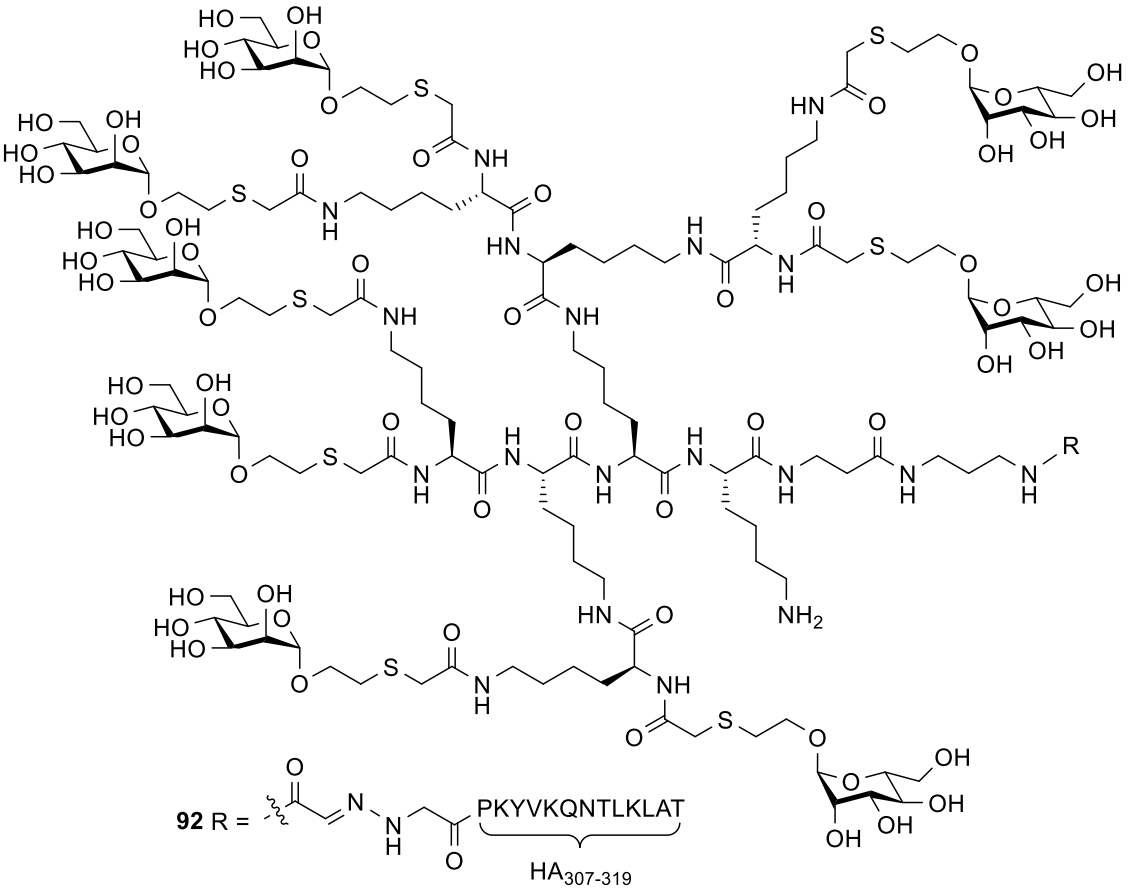

Figure 7-13. Mannosylated $HA_{307-319}$ peptidic epitope from Influenza virus hemagglutinin.

Dendritic cells (DCs), well-known T-lymphocyte stimulators, accomplish antigen uptake through a mechanism, among others, that involves the association with a surface mannose-binding C-lectin named DC-SIGN. As a consequence, mannosylation of antigens has been proposed as a strategy to improve the efficacy of vaccines as it would promote their internalization and recognition by the immune system. Following this concept, Melnyk *et al.* decorated the $HA_{307-319}$ peptidic epitope from Influenza hemagglutinin with an octavalent mannose cluster based on a branched Lys-Ala oligopeptide as scaffold (Fig. 7-13).[84] Human dendritic cells from peripheral blood

proved to specifically uptake fluorescent-labeled analogues of this mannocluster. The influence of the glycocluster valence was also studied by varying the number of epitopes from 2 to 8. Interestingly, highest uptake was achieved by the tetravalent glycomimetics (quinic and shikimic acids, as mannose mimetics) and the octavalent mannocluster **92**.[85]

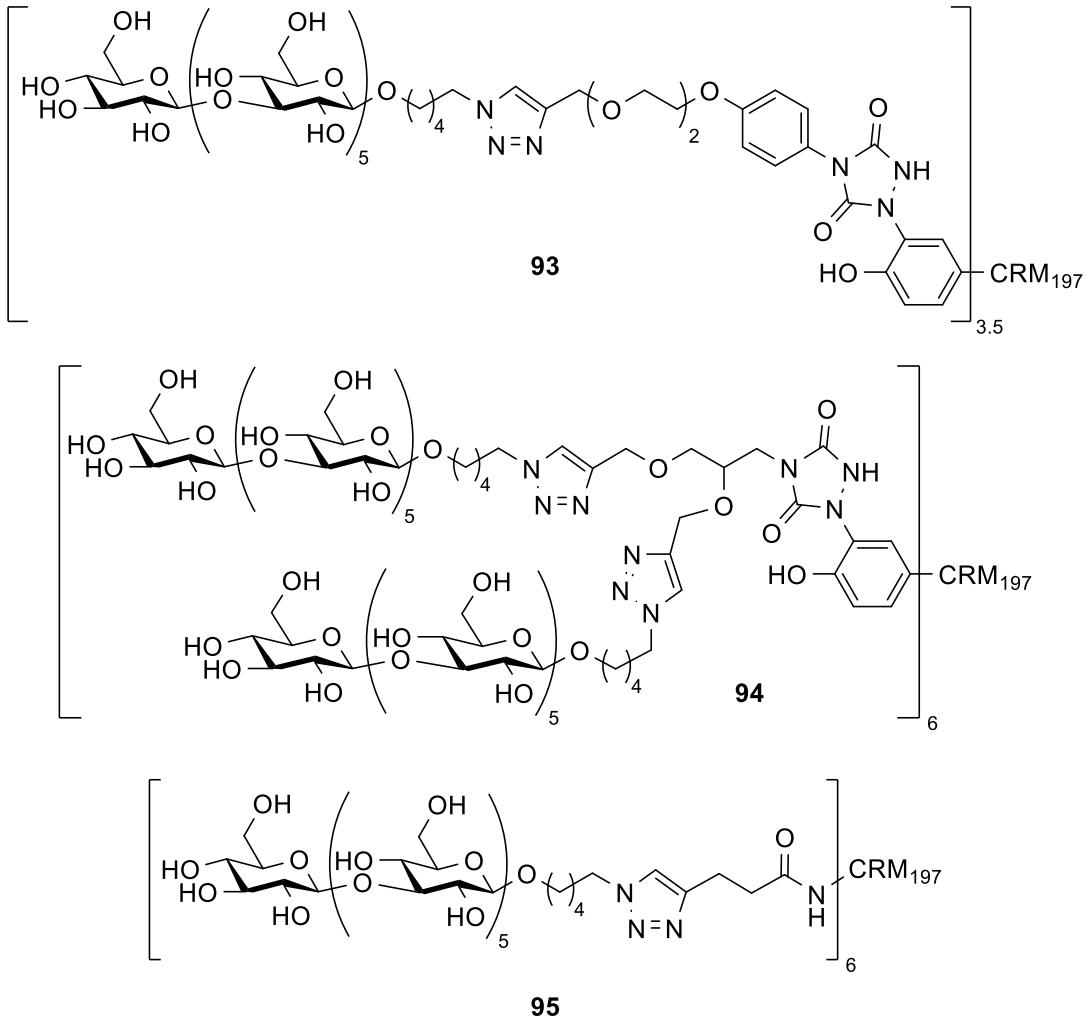

Figure 7-14. Synthetic vaccines **93-95** against *Candida albicans* based on the attachment of a controlled number of β-(1→3) glucan hexasaccharide moieties to tyrosine or lysine residues of CRM_{197} carrier protein from diphtheria toxin.

Berti and co-workers have recently reported multivalent synthetic vaccines against *Candida albicans* fungi based on a carrier protein from diphtheria toxin (CRM_{197}). Such

conjugate presents a controlled number of β-(1→3) glucan hexasaccharide moieties linked through some of its tyrosine or lysine residues (Fig. 7-14).[86] Modification of tyrosine residues was achieved in an average of 4 out of the 18 available linking points when a monovalent linker was used (**93**), whereas 6 of them were modified when a double spacer was employed (**94**). Attachment to lysine residues yielded a hexavalent glycoprotein (**95**). These glycoconjugates were expected to induce the production of anti-laminarin antibodies. Laminarin is a natural β-(1→3)-β-(1→6) glucan present on the *Candida albicans* surface which mediates fungal adhesion to human epithelial cells. Sera from immunized CD1 mice using MF59 as coadjuvant showed high levels of IgG anti-laminarin antibodies by ELISA. Neoglycoproteins **93** and **94** having carbohydrate derivatives linked to the tyrosine residues induced higher IgG levels, indicating that the attachment site of the glycan moiety was important. Sera were positively tested as inhibitors for the adhesion of *C. albicans* to human epithelial (HEP-2) cells. Interestingly, lysine-modified conjugate **95** (62% inhibition) proved to be as effective as the highly protective, anti β-glucan murine monoclonal antibody mAb 2G831, used as positive control.

7.4. Carbohydrate clusters as drug delivery systems

Targeted drug delivery systems are engineered technologies for delivering therapeutic agents in a manner that increases their relative concentration in specific biological sites while reducing it in the remaining tissues. Synthetic glycoclusters that are able to carry therapeutics in a covalent and/or non-covalent fashion can be used as delivery systems directed to the specific carbohydrate moieties receptors. Thus, endogenous lectins are attractive targets for drug delivery and multivalency can favorably increase the avidity of their interaction with the targeting ligand.

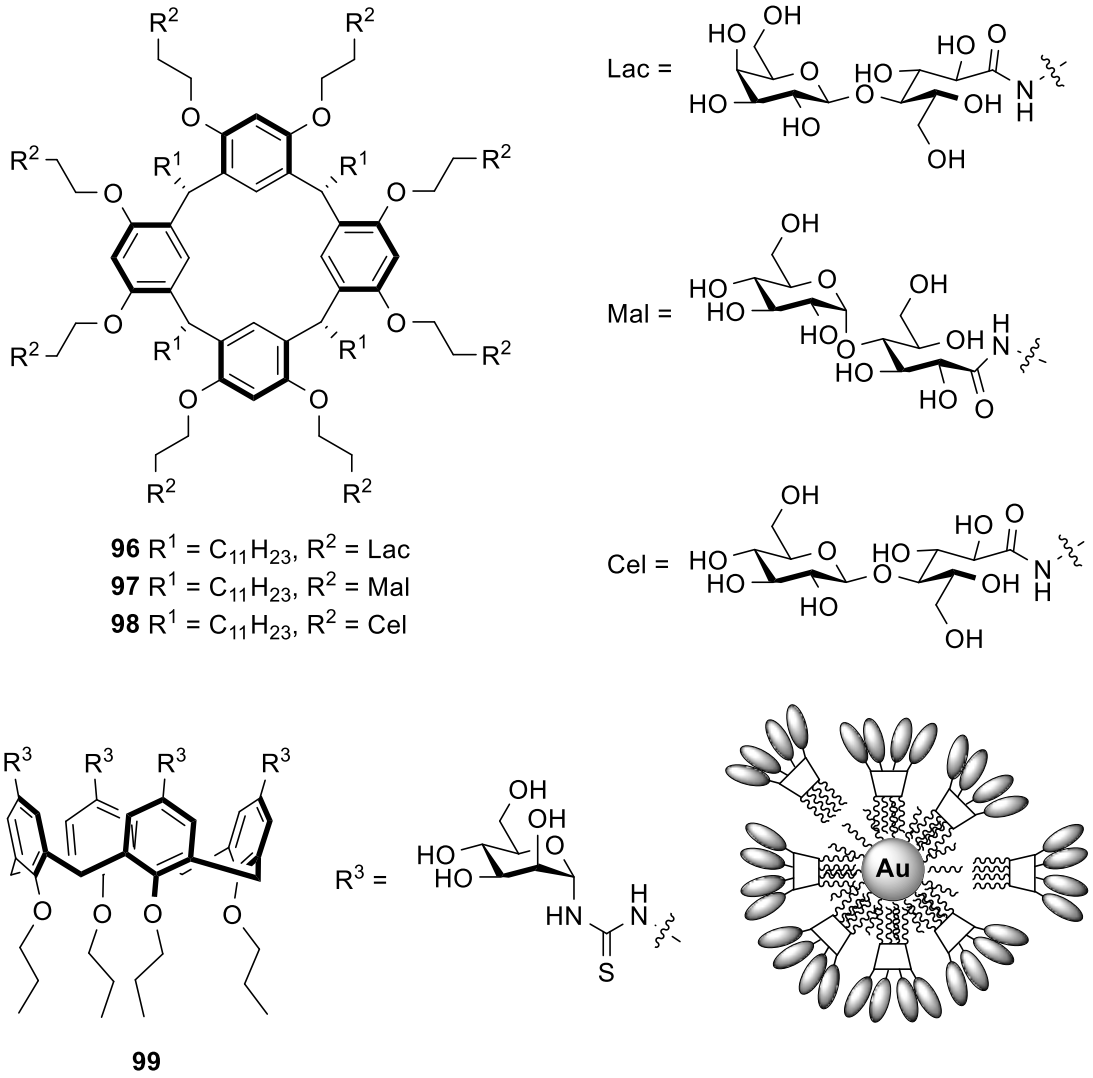

Figure 7-15. Artificial glycoviruses based on the supramolecular aggregation of calix[4]resorcarene-scaffolded glycoclusters **96**-**98** as DNA delivery systems. Amphiphilic glycocalix[4]arene **99** and its non-covalently self-assembly on *n*-dodecanyl AuNPs as a potential drug delivery system.

Several types of glycoclusters have been explored for targeted delivery of genes to the specific cells and/or for augmenting gene transfer efficiency. Aoyama and co-workers[87] proposed the use of octavalent lactose, maltose and cellobiose calix[4]resorcarene-scaffoled glycoclusters **96**-**98** (Fig. 7-15) to create “artificial viruses” called “glycoviruses”. These glycoconjugates self-aggregate to form spherical

and neutral nanoparticles (NPs) which are strongly adhesive on DNA aligning 2 glycoNPs along the major groove in every successive pitch, located at north and south or east and west pitch by pitch, resulting in a neutral glycoviral particle (GP). Such particle containing a single molecule of DNA highly efficiently packed in a viral size ($d \approx 50$ nm). GPs derived from **98** are nonadhesive with each other and keep monomolecularity, whereas those derived from **96** and **97** undergo reversible saccharide-dependent self-aggregation resulting in GPs aggregates of big size ($d \approx 200$ nm for **96** and ≈300 nm for **97**). Only monomeric GPs **98** possess substantial transfection ability in HeLa cells, where the activities are size-regulated. However, when hepatic HepG2 cells, which possess specific receptors for β-galactose residues, were used, the activity of the GPs from **96** increased to reach a similar value than that for **98** due to size/receptor compensation, while activities of GPs from **97** and **98** kept unchanged.

The ability of amphiphilic glycoclusters to aggregate in water has also been exploited for the preparation of supramolecular gold glyconanoparticles (glycoAuNPs). Avvakumova *et al.* have recently reported the non-covalent self-assembly of the amphiphilic *cone*-glycocalixarene **99** bearing four mannose residues on the surface of *n*-dodecanyl-decorated AuNPs.[88]. The resulting glycocalixarene-AuNP was three-fold more efficiently uptake by HeLa cells than the glycoAuNP that resulted from the assembly of a mannose-benzene conjugate on the *n*-dodecanyl-decorated AuNPs. This result indicated the relevance of using clustered multivalent glycosides on the AuNPs.

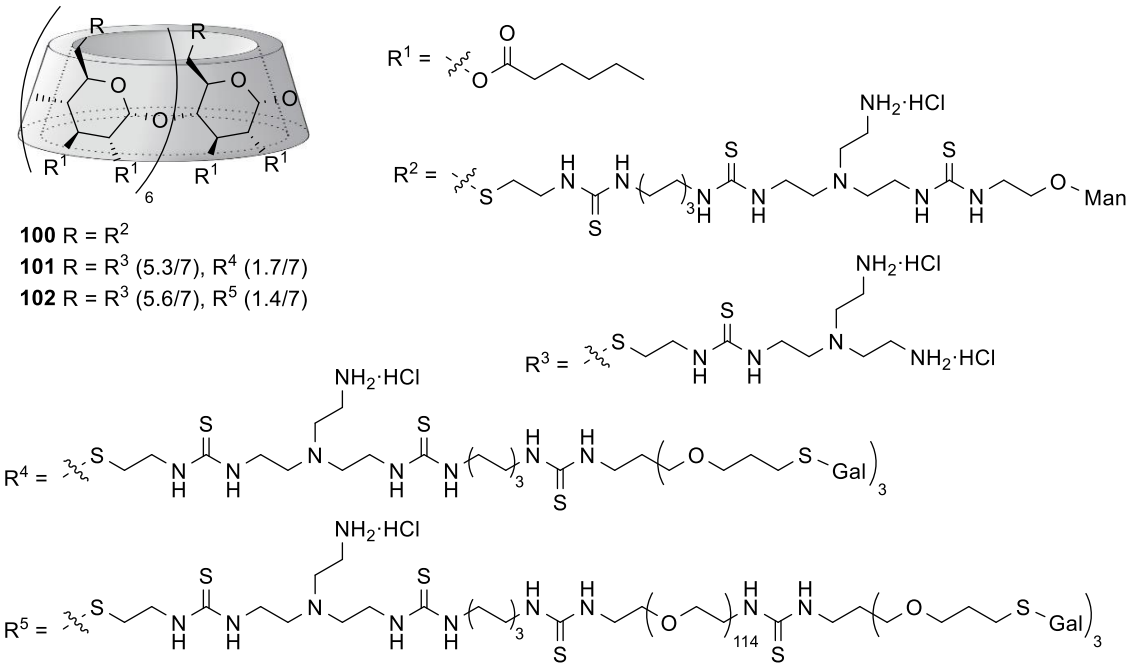

Figure 7-16. Polycationic amphiphilic β-CD-based mannosyl clusters **100**-**102** as pDNA and mRNA nanocarriers targeting macrophage mannose (MMR) and asyaloglycoprotein (ASGPr) receptors.

A polycationic amphiphilic β-cyclodextrin (β-CD)-based mannosylcluster **100** bearing seven protonable amino groups on the primary face was tested as a site-specific gene delivery system (Fig. 7-16).[89] This new glycocluster was expected to combine the enhancing, although non-specific, effect on the cellular uptake and transfection efficiency promoted by the overall positive surface electrostatic potential with the specific and selective recognition by cell membrane lectin receptors provided by the attached carbohydrates. Such conjugate forms stable cationic snake-like glyco-β-CD complexes (glyco-β-CDplexes) in the presence of pDNA. These glyco-β-CDplexes were recognizable by ConA and human macrophage mannose receptor (MMR) lectins. Interaction studies on resident peritoneal macrophages from mice indicated that adhesion of the glyco-β-CDplexes can operate in a non-specific, electrostatic-mediated fashion or in a specific, lectin conducted mode. MMR-mediated transfection of mouse

leukaemic monocyte macrophage cells using a luciferase gene was achieved more efficiently than the reference commercial compound JetPEI^{TM}-Hepatocyte. In a further step, triantennary galactose dendrons were randomly attached on such amphiphilic β-CD (**101**).[90] A PEG_{5000}-glycodendron was also used for the functionalization of the β-CD derivative leading to **102** in order to provide stabilization against serum proteins. Interestingly, these conjugates were able to form complexes with pDNA, but their transfecting abilities towards HepG2 cells were quite modest probably due to the difficulties in translocation of the pDNA into the nucleus. In contrast, very efficient asialoglycoprotein receptor (ASGPr) mediated transfection was found when mRNA (which is translated in the cytoplasm) was used. Small changes in the arrangement of the cationic elements of such amphiphilic β-CDs-based have a strong influence on their gene transfer capabilities.[91]

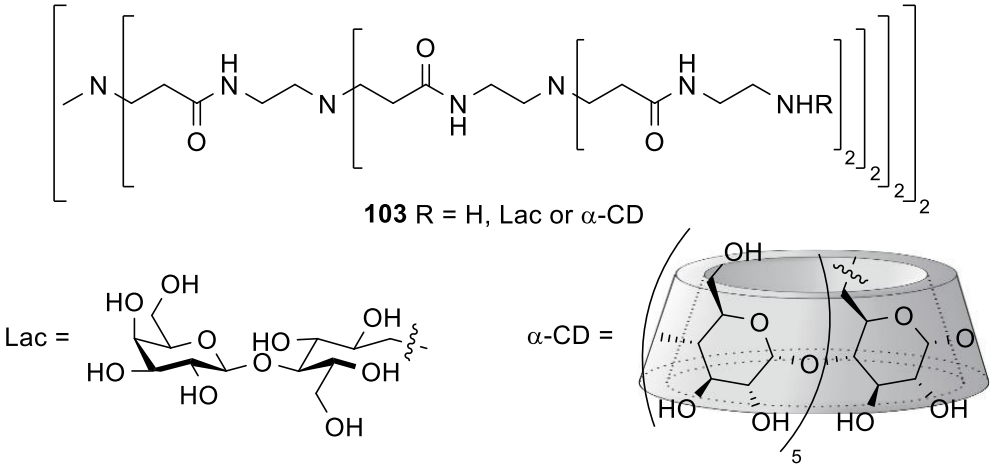

Figure 7-17. ASGPr-mediated gene delivery system in HepG2 cells using G2-PAMAM dendrimer as core.

A second generation (G2) PAMAM dendrimer functionalized with a random number of lactose and primary-rim-grafted α-CD residues (Fig. 7-17) was tested as hepatocyte-selective non-viral vector for gene delivery in HepG2 cells and mice by measuring

Renilla luciferase activity after transfection of pDNA.[92] Different degrees of substitution of the lactose moiety (1.2, 2.6, 4.6, 6.2 and 10.2) were tested. *In vitro* experiments pointed an optimal degree of substitution of 2.6 for the transfection, with low cytotoxicity and excellent hepatocyte selectivity through the interaction with ASGP-r. In contrast, A549 and KB cells did not show any activity. The role played by the cyclooligosaccharide in the transfection process is assumed to enhance endosomal escape of the pDNA complex through the membrane-disrupting. In mice, luciferase activity mainly cumulated in the liver. Better results were found when a G3 analogue with a degree of substitution of the lactose moiety of 1.2 was used, although only *in vitro* experiments were performed with this multivalent system.[93]

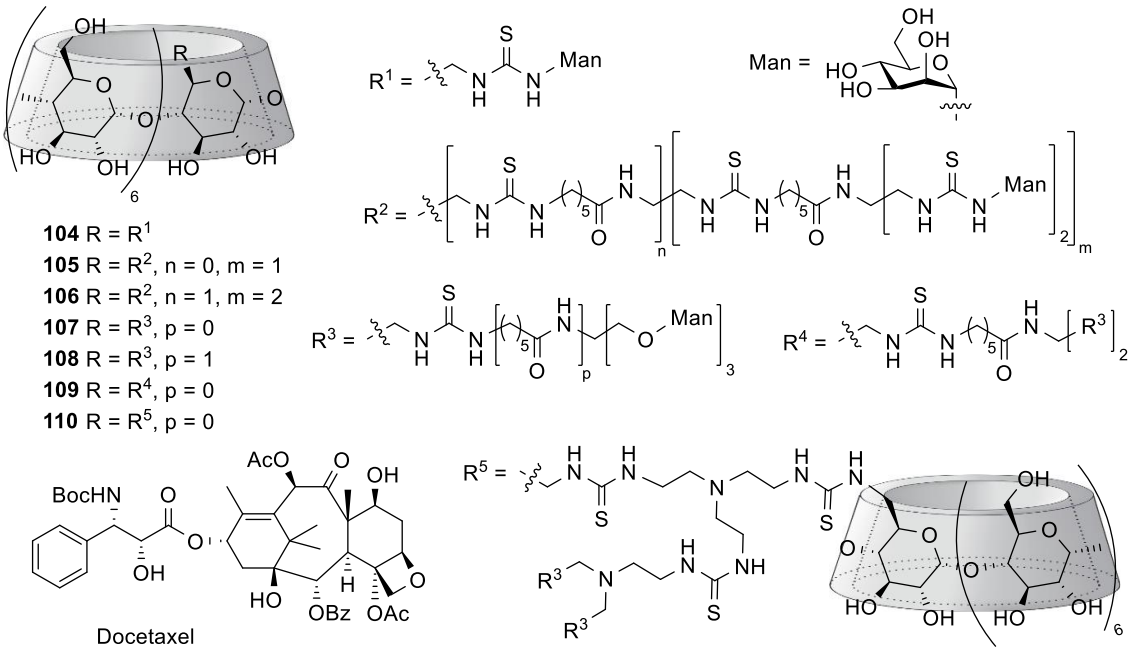

Figure 7-18. Primary face monosubstituted β-CD derivatives **104-109** and β-CD dimer **110** as mammalian mannose/fucose specific cell surface receptor targeted delivery systems for water insoluble anti-cancer drug docetaxel.

The use of a CD as scaffold of cluster glycosides offers the advantages of providing to the glycocluster the ability to form inclusion complexes with a large variety of drugs in aqueous solution. Thus, the combination of the ability to encapsulate drugs and being biorecognizable has converted such glycoclusters in the focus of attention of an extensive research.[11,18] The group of García-Fernández synthesized β-CD-based cluster mannosides **104**-**109** (Fig. 7-18) in which only one of the seven α-D-glucose moieties of the macrocycle was modified.[94,95] The solubilization experiments in water with anticancer drug docetaxel showed similar values to those obtained previously for monovalent β-CDs and higher than those for heptavalent per-6-substituted β-CD analogues. The IC_{50} values obtained by ELLA assays for Con A affinity showed the expected enhancement of lectin-binding strength for the higher-valent β-CD (up to 22-fold for hexavalent to monovalent derivatives), due to the cluster effect. In addition, results showed that the Con A affinity for **109**-docetaxel complex is 2-fold higher than that for the free host **109**. Such increase in Con A affinity was attributed to the interaction of a hexavalent 2:1 **109**-docetaxel complex with the lectin. In a further step, the authors synthesized the *bis*-β-CD-glycocluster **110**. While the binding affinity of **109** and **110** towards Con A had similar IC_{50} values (ca. 10 mM for both), estimated association constant (K_c) values from solubility diagrams for glycocluster **109** and *bis*-β-CD-glycocluster **110** were 4000 and 1.5 x 10^5 M^{-1}, respectively. The drug targeting potential of glycoclusters-β-CD **105** and **110** was then evaluated with a mammalian mannose/fucose specific cell surface receptor from macrophages obtaining similar results to those obtained for the affinity of the docetaxel complexes to Con A.

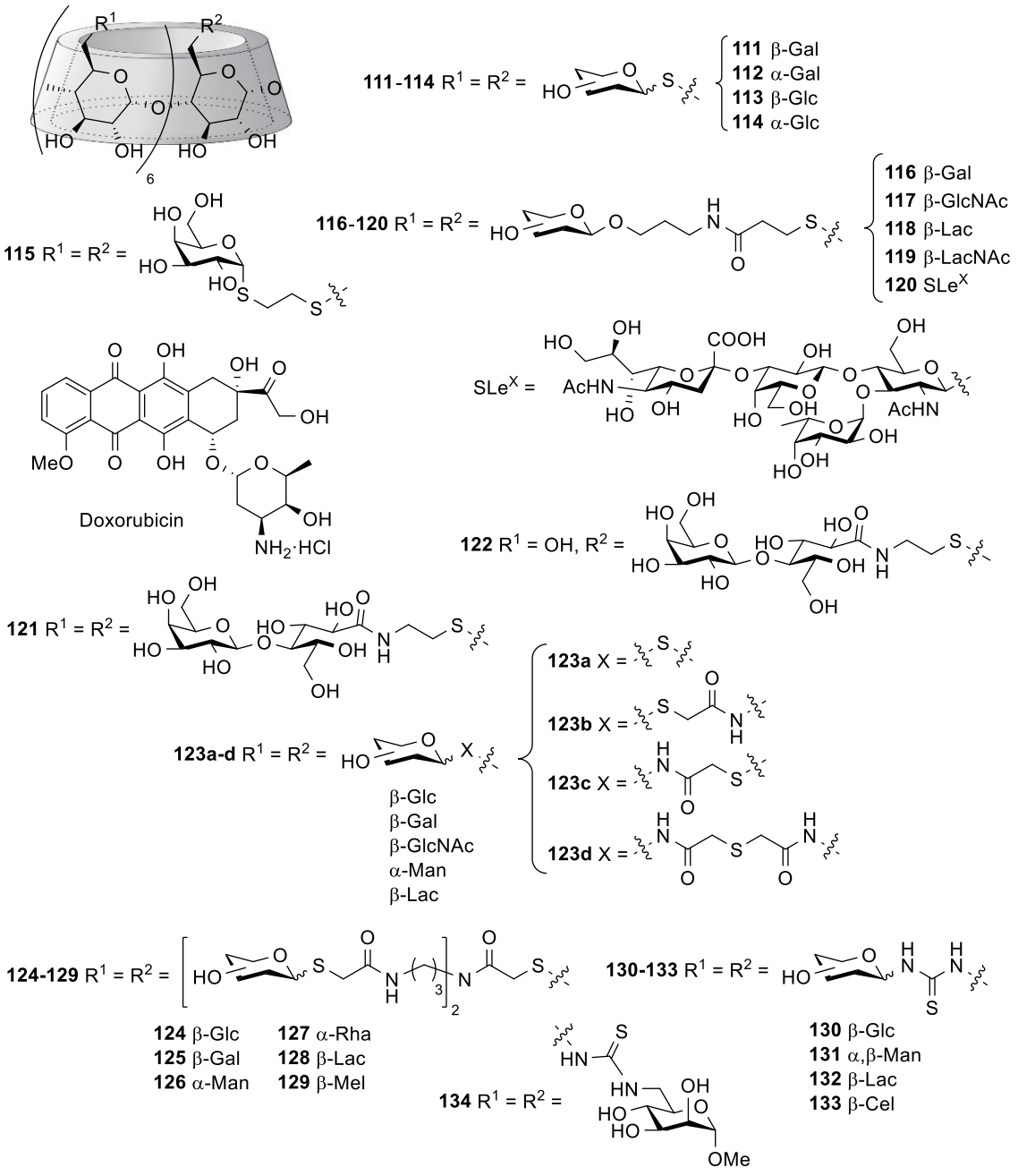

Figure 7-19. β-CD Glycoclusters persubstituted on primary face (**111-121** and **123-133**).

Per-substitution of the β-CD at C-6 has been used as a very convenient way to synthesize glycoclusters (Fig. 7-19). Pioneer reports[96,97] described the synthesis of several per-6-glycosyl-thio-β-CDs having α/β Glc and Gal (**111-115**). The biorecognizable properties of such per-glyco-β-CDs were studied by testing their inhibitory power towards specific lectins (*Kluyveromyces bulgaricus*). Results showed

that the heptavalent glycoclusters displayed better inhibitory properties than the monovalent analogues. Per-glucosyl-β-CD **113** formed stable complexes with *p*-nitrophenol and prednisolone (K_a 2×10^3 and 0.2×10^3 $M^{-1,}$ respectively), but less stable than those formed with the native β-CD.

A similar synthetic strategy was applied for the synthesis of a heptavalent persubstituted β-CDs in which the carbohydrate ligands are bound to C-6 through spacer arms of different length and nature. Furuike *et al.* [98] prepared glycoclusters **116**-**119** with Gal, *N*-GlcNAc, lactose and *N*-acetyllactosamine. Lectin binding studies with these glyco-β-CDs were performed by haemagglutination inhibition test of the wheat germ agglutinin (WGA) and *Erythrina corallodendron* lectin (ECorL), GlcNAc and *N*-acetyllactosamine specific lectins, respectively. The inhibitory ability for glycoCDs **119** and **117** were 4 and 40-fold higher, respectively, than the monovalent structures. Factors on the lectin binding abilities such as the carbohydrate epitope density and topology were also studied by measurements of the inhibition activities of glyco-β-CDs **116**-**119** against galactoside-specific agglutinin from *Viscum album* L lectin, Gal-1, -3 and -7 and lactoside-binding immunoglobulin G.[99] Authors found for heptavalent glyco-β-CDs notable inhibitory potencies per galactosyl residue relative to free lactose, as well as galectin binding selectivity.

A chemoenzimatic approach was carried out by Furuike *et al.* for an efficient synthesis of glyco-β-CDs having seven sialyl Lewis X units.[100] Surface plasmon resonance (SPR) inhibitory experiments performed using immobilized SLeX-containing neoglycoprotein (SLeXn-BSA) and E-selectin showed that glycocluster **120** exhibited a highly enhanced inhibitory ability (IC_{50} of 1.5 mM), relative to SLeX.

Yasuda *et al.* [101] have reported the synthesis of both per-6-galactosyl-glucono-amide-CD **121** and its monovalent analogue **122** (Fig. 7-19). The authors carried out SPR measurements that showed that both compounds form ternary complexes with PNA and the anticancer drug doxorubicin (DXR). The K_a value for the binding of **121** to PNA was two orders of magnitude higher than that for **122**. Interestingly, the per-substituted β-CD showed a K_a value for the binding to DXR of an order of magnitude higher than the monovalent β-CD that was attributed to the formation of an inclusion complex in the cavity formed by the carbohydrate appendages.

A series of heptavalent and tetradecavalent β-CD-based *S*- and *N*-glycoclusters **123a-d** and **124-129**, having spacers of different length and nature, was synthesized (Fig. 7-19).[102-105] ITC experiments gave the K_a values and the thermodynamic parameters for the inclusion complexation of such glycoclusters with sodium 8-anilino-1-naphthalensulfonate (ANS) and 2-naphthalensulfonate (NS) as guest models. While persubstitution of the β-CD at C-6 with the appended carbohydrates led to a slight increase of the K_a values for ANS relative to β-CD, a higher steric congestion on the primary face resulted in to lower K_a values for NS. These ITC studies also showed that the spacer arms that link the appended saccharide units and the β-CD core had an influence on the complex stability according to their chemical nature. In addition, an increase of the valency of the glyco-β-CDs from 7 to 14 ligands gave rise to low stable complexes. The binding properties of glyco-β-CDs **123a-d** and **124-129** towards several plants lectins were evaluated using inhibition experiments (ELLA) and ITC, among other techniques. *S*-Glycoβ-CDs, but no *N*-monosaccharide-β-CDs, showed good to excellent inhibition properties with the corresponding specific pea, PNA and Con A lectins. PNA formed stable cross-linked complexes with Gal_7-β-CD **123b**, Lac_7-β-CD **123a-d** and Lac_{14}-β-CD **128** but not with the galactosylamine Gal_7-β-CD **123c** and

123d. The strength of the Gal_7-β-CDs·PNA complexes was attributed to the cluster effect. ITC results also showed that the use of 14-valent Glyco- β-CDs did not contribute to the improvement of the complex stability relative to the heptavalent clusters.

García-Fernández, Ortiz Mellet and co-workers developed another successful strategy for the efficient attachment of carbohydrates on β-CD, based on the formation of thiourea bridges (Fig. 7-19).[106,107] Following this strategy, the synthesis of per-glycosyl-thioureido-β-CDs **130-134** has been performed in high yields. Docetaxel solubilization experiments in water showed solubility values higher than those obtained for the native β-CD but lower than those for the monovalent glyco-β-CD analogues. ELLA assays showed that heptavalent persubstituted glyco-β-CDs **131** and **134** exhibited a much lower inhibitory ability than the monovalent β-CD analogues (IC_{50} 3200 and 2900 μM, respectively) for the binding towards Con A.

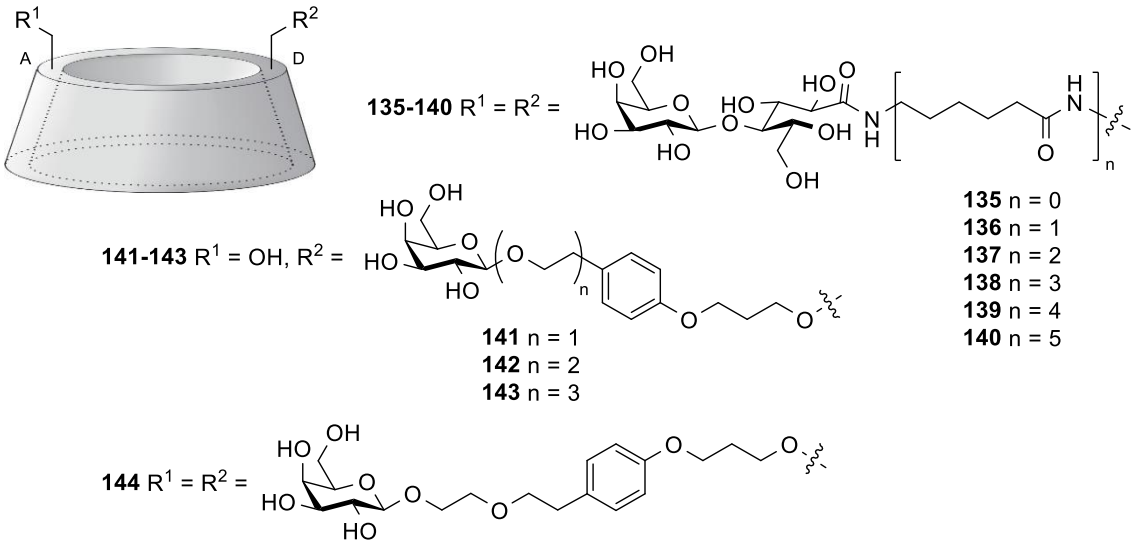

Figure 7-20. Mono- (**141**-**143**) and divalent (**135**-**140** and **144**) galactosylated β-CD derivatives as DXR delivery systems.

As an alternative to the persubstituted glyco-β-CDs having seven or more carbohydrate units, divalent 6A,6D-galactose-β-CD derivatives having different spacer arm lengths

were synthesized (Fig. 7-20).[108] The formation of complexes with PNA lectin and the anticancer drug DXR was quantitatively evaluated by SPR and atomic force microscopy (AFM). Such *bis*-Lac-β-CDs **135-140** were found to have the optimum length for association with PNA lectin [K_a value for **139** (n = 4) 4.6 x 10^6 M^{-1}] and their complex stability with the drug gradually increases along with the spacer lengths [K_a value for **140** (n = 5) 5.1 x 10^4 M^{-1}]. Similarly, Yamanoi and co-workers[109] prepared galactosylated *mono*- and *bis*-branched-β-CD conjugates (**141-143** and **144**, respectively) displaying *p*-phenyl ethylene glycol based arms of different lengths between the carbohydrate moiety and the sugar residue. Both the drug encapsulation and the lectin specific recognition abilities were evaluated by SPR experiments, using immobilized DXR and PNA lectin, respectively. PNA binding K_a values were estimated to be 5.4-9.2 × 10^4 M^{-1} for **141-143** and 1.3 × 10^5 M^{-1} for **144**, evidencing no significant influence of the spacer length or the number of branches over the recognition of the lectin. The inclusion of the DXR into the cavity yielded K_i values between 1.1 × 10^5 M^{-1} and 1.5 × 10^5 M^{-1} for conjugates **141-143**, while derivative **144** showed 100-fold higher inclusion constant (1.5 × 10^7 M^{-1}) due to the presence of two aromatic rings in the structure which likely enhances π-π interactions with the drug.

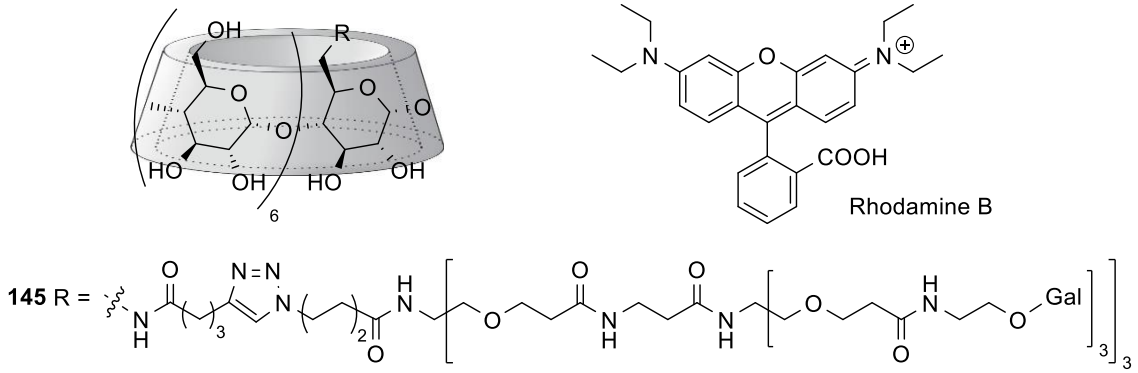

Figure 7-21. Nonavalent galactosylated β-CD conjugate **145** as a HepG2 hepatocyte-targeted delivery system for Rhodamine B and anti-cancer drug DXR.

Seeberger and co-workers[110] designed a galactosylated dendrimer attached to the primary face of a β-CD macrocycle (**145**) as potential targeted drug delivery system towards ASGP-r, which is exclusively expressed on parenchymal hepatocytes (Fig. 7-21). Evaluation of its delivery ability was performed by its uptake into hepatocellular carcinoma HepG2 cells using fluorescent dye rhodamine B as drug model. A mannosylated analogue was used as a negative control. Flow cytometry confirmed that galactosylated conjugate was efficiently uptaken by HepG2 cells indicating receptor-mediated endocytosis. The inclusion complex of this conjugate with anti-cancer drug DXR proved to induce apoptosis when incubated with HepG2, whereas the conjugate itself did not.

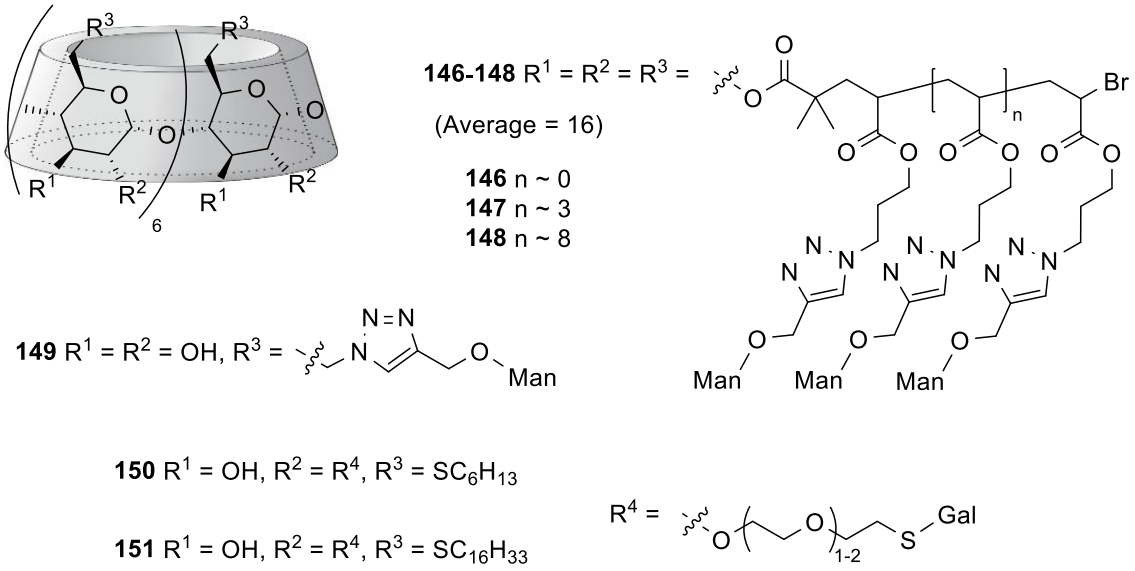

Figure 7-22. β-CD-based star mannosylated glycopolymers **146**-**148** as DC-SIGN-mediated delivery systems for anti-cancer agent docosahexaenoic acid and anti-HIV drug Saquinavir, as well as amphiphilic β-CD derivatives **150** and **151** grafted in their secondary faces with galactose residues as nanoparticles- and vesicles-forming nanocarriers.

Haddleton, Bercer and co-workers[111] prepared a series of β-CD-based star glycopolymers (Fig. 7-22) containing an average degree of substituted hydroxyl groups at the periphery of β-CD approximately equal to 16, and three different degree of polymerization equal to 2, 5 and 10 (**146**-**148**). SPR technique was used to test binding abilities of these glycopolymers to DC-SIGN lectin. Affinity of these conjugates was much higher than the heptavalent β-CD analogue **149**. The conjugate showing a DP of 10 yielded a dissociation constant of 0.22 nM, only 2-fold higher than that described for the natural DC-SIGN ligand gp120. In addition, these glycopolymers were able to encapsulate docosahexaenoic acid, a potential anticancer chemotherapeutic agent, as well as the anti-HIV drug Saquinavir as judged from UV-Vis and ^{1}H NMR spectroscopy, respectively.

Mazzaglia *et al.* [112] synthesised amphiphilic β-CDs **150** and **151** having alkythio chains at the primary face and galactosylthio-oligo-(ethyleneglycol) at the secondary rim (Fig. 7-22). These amphiphilic β-CDs formed nanoparticles and vesicles, respectively, showing multivalent effect in their binding to a lectin. The binding of the amphiphilic β-CD colloids to galactose specific lectins from *Pseudomonas aeruginosa* and to PNA was investigated by MALDI-MS, fluorescence spectroscopy and by SPR, respectively. β-CD **151**-based vesicle showed better binding abilities than β-CD **150**-based nanoparticle. It was suggested that a binding optimization effect based on a dynamic and reversible self-assembly process might occur upon the binding interaction between the aggregates and the lectin. Further studies confirmed that balance between hydrophilic ethylene glycol groups and hydrophobic alkyl chains controls the self-organization that the conjugates adopt in water. Usually, a polydisperse mixture of small micelles (~4 nm) or nanospheres (20-30 nm) is obtain, which eventually aggregates into larger structures (500-600 nm), or vesicles (100-200 nm). Both micellar

aggregates and vesicles present compartments (up to 20 % v/v) able to encapsulate small molecules such as the fluorescent dye Rhodamine 6G.[113]

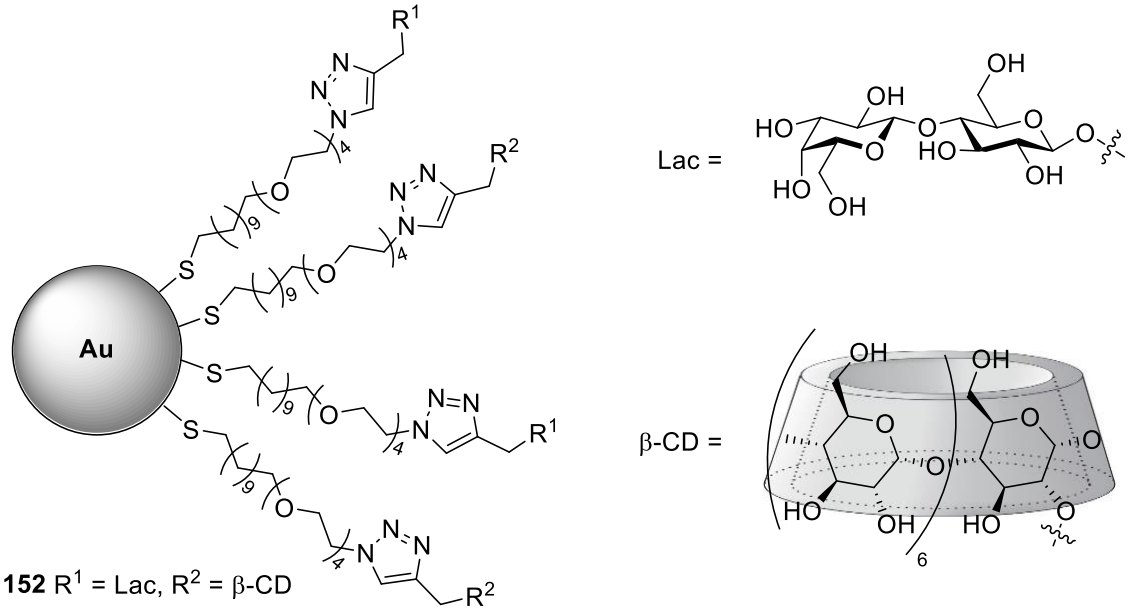

Figure 7-23. Dually functionalized gold nanoparticle **152** bearing simultenously lactose residues as targeting ligands for Gal-3 lectin and β-CD macrocycles as encapsulating moieties for anti-cancer drug methotrexate (MTX).

The concept based on the combination of the β-CD ability for drug complexation and the targeting properties of multivalent carbohydrates evolved to the preparation of gold nanoparticles (AuNP) containing multiple copies of lactose and β-CD (Fig. 7-23).[114] Gal 3 demonstrated interaction with the lactose-containing AuNPs as they induced evident changes in their optical properties. The estimated loading capability of such glycoNPs for anticancer drug methotrexate *via* UV−vis experiments indicated that the presence of β-CD moieties on the AuNP surface enhanced their abilities to load such drug.

Acknowledgment

The authors acknowledge the Andalusian Government (Consejería de Economía, Innovación y Ciencia, Grant FQM6903), the Spanish Ministry of Economy and Competitiveness—ERD Fund (Grant CTQ2013-48380-R), and the Marie Curie ITN program (CYCLON Hit 608407) for financial support.

References

[1] Lee, Y. C.; Lee, R. T. *Acc. Chem. Res.* **1995**, *28*, 321-327.

[2] Chabre, Y. M.; Roy, R. *Adv. Carbohydr. Chem. Biochem.* **2010**, *63*, 165-393.

[3] Dwek, R. A. *Chem. Rev.* **1996**, *96*, 683-720.

[4] Lis, H.; Sharon, N. *Chem. Rev.* **1998**, *98*, 637–674.

[5] Lee, R. T.; Lee, Y. C. *Glycoconjugate J.* **2000**, *17*, 543-551.

[6] Lundquist, J. J.; Toone, E. J. *Chem. Rev.* **2002**, *102*, 555-578.

[7] Mammen, M.; Choi, S.; Whitesides, G. M. *Angew. Chem. Int. Ed.* **1998**, *37*, 2754-2794.

[8] Jiménez Blanco, J. L.; Ortiz Mellet, C.; García Fernández, J. M. *Chem. Soc. Rev.* **2013**, *42*, 4518-4531.

[9] Ortiz Mellet, C.; Defaye, J.; García Fernandez, J. M. *Chem. Eur. J.* **2002**, *8*, 1982-1990.

[10] Lahmann, M. *Top. Curr. Chem.* **2009**, *288*, 17-65.

[11] Vargas-Berenguel, A.; Ortega-Caballero, F.; Casas-Solvas, J. M. *Mini-Rev. Org. Chem.* **2007**, *4*, 1-14.

[12] Peri, F. *Chem. Soc. Rev.* **2013**, *42*, 4543-4556.

[13] Spinelli, N.; Defrancq, E.; Morvan, F. *Chem. Soc. Rev.* **2013**, *42*, 4557-4573.

[14] Hatano, K.; Matsuoka, K.; Terunuma, D. *Chem. Soc. Rev.* **2013**, *42*, 4574-4598.

[15] Galan, M. C.; Dumy, P.; Renaudet, O. *Chem. Soc. Rev.* **2013**, *42*, 4599-4612.

[16] Sansone, F.; Casnati, A. *Chem. Soc. Rev.* **2013**, *42*, 4623-4639.

[17] Chabre, Y. M.; Roy, R. *Chem. Soc. Rev.* **2013**, *42*, 4657-4708.

[18] Martinez, A.; Ortiz Mellet, C.; Garcia Fernandez, J. M. *Chem. Soc. Rev.* **2013**, *42*, 4746-4773.

[19] Weis, W.; Brown, J. H.; Cusack, S.; Paulson, J. C.; Skehel, J. J.; Wiley, D. C. *Nature* **1988**, *333*, 426-431.

[20] Roy, R.; Zanini, D.; Meunier, S.; Romanowska, A. *Chem. Commun.* **1993**, 1869–1872.

[21] Ohta, T.; Miura, N.; Fujitani, N.; Nakajima, F.; Niikura, K.; Sadamoto, R.; Guo, C.-T.; Suzuki, T.; Suzuki, Y.; Monde, K.; Nishimura, S.-I. *Angew. Chem. Int. Ed.* **2003**, *42*, 5186-5189.

[22] Marra, A.; Moni, L.; Pazzi, D.; Corallini, A.; Bridi, D.; Dondoni, A. *Org. Biomol. Chem.* **2008**, *6*, 1396-1409.

[23] Proft, T.; ed.; *Microbial Toxins: Current Research and Future Trends*; Caister Academic Press, **2009**.

[24] Kitov, P. I.; Sadowska, J. M.; Mulvey, G.; Armstrong, G. D.; Ling, H.; Pannu, N. S.; Read, R. J.; Bundle, D. R. *Nature* **2000**, *403*, 669-672.

[25] Mulvey, G. L.; Marcato, P.; Kitov, P. I.; Sadowska, J.; Bundle, D. R.; Armstrong, G. D. *J. Infec. Dis.* **2003**, *187*, 640-649.

[26] Solomon, D.; Kitov, P. I.; Paszkiewicz, E.; Grant, G. A.; Sadowska, J. M.; Bundle, D. R. *Org. Lett.* **2005**, *7*, 2369-4372.

[27] Nishikawa, K.; Matsuoka, K.; Kita, E.; Okabe, N.; Mizuguchi, M.; Hino, K.; Miyazawa, S.; Yamasaki, C.; Aoki, J.; Takashima, S.; Yamakawa, Y.; Nishijima, M.; Terunuma, D.; Kuzuhara, H.; Natori, Y. *Proc. Natl. Acad. Sci. U.S.A.* **2002**, *99*, 7669-7674.

[28] Nishikawa, K.; Matsuoka, K.; Watanabe, M.; Igai, K.; Hino, K.; Hatano, K.; Yamada, A.; Abe, N.; Terunuma, D.; Kuzuhara, H.; Natori, Y. *J. Infect. Dis.* **2005**, *191*, 2097-2105.

[29] Cuatrecasas, P. *Biochemistry* **1973**, *12*, 3547-3558.

[30] Fan, E.; Zhang, Z.; Minke, W. E.; Hou, Z.; Verlinde, C. L. M. J.; Hol, W. G. J. *J.* Am. *Chem. Soc.* **2000**, *122*, 2663-2664.

[31] Merritt, E. A.; Zhang, Z.; Pickens, J. C.; Ahn, M.; Hol, W. G. J.; Fan, E. *J. Am. Chem. Soc*. **2002**, *124*, 8818-8824.

[32] Zhang, Z.; Merritt, E. A.; Ahn, M.; Roach, C.; Hou, Z.; Verlinde, C. L. M. J.; Hol, W. G. J.; Fan, E. *J. Am. Chem. Soc.* **2002**, *124*, 12991-12998.

[33] Zhang, Z.; Pickens, J. C.; Hol, W. G. J.; Fan, E. *Org. Lett.* **2004**, *6*, 1377-1380.

[34] Zhang, A.; Liu, J.; Verlinde, C. L. M. J.; Hol, W. G. J.; Fan, E. *J. Org. Chem.* **2004**, *69*, 7737-7740.

[35] Arosio, D.; Fontanella, M.; Baldini, L.; Mauri, L.; Bernardi, A.; Casnati, A.; Sansone, F.; Ungaro, R. *J. Am. Chem. Soc.* **2005**, *127*, 3660-3661.

[36] Garcia-Hartjes, J.; Bernardi, S.; Weijers, C. A. G. M.; Wennekes, T.; Sansone, F.; Casnati, A.; Zuilhof, H. *Org. Biomol. Chem.* **2013**, *11*, 4340-4349.

[37] Mattarella, M.; Garcia-Hartjes, J.; Wennekes, T.; Zuilhof, H.; Siegel, J. S. *Org. Biomol. Chem.* **2013**, *11*, 4333-4339.

[38] Branson, T. R.; McAllister, T. E.; Garcia-Hartjes, J.; Fascione, M. A.; Ross, J. F.; Warriner, S. L.; Wennekes, T.; Zuilhof, H.; Turnbull, W. B. *Angew. Chem. Int. Ed.* **2014**, *53*, 8323-8327.

[39] Dubber, M.; Sperling, O.; Lindhorst, T. K. *Org. Biomol. Chem.* **2006**, *4*, 3901-3912.

[40] Almant, M.; Moreau, V.; Kovensky, J.; Bouckaert, J.; Gouin, S. G. *Chem. Eur. J.* **2011**, *17*, 10029-10038.

[41] Gouin, S. G.; Wellens, A.; Bouckaert, J.; Kovensky, J. *ChemMedChem* **2009**, *4*, 749-755.

[42] Touaibia, M.; Wellens, A.; Shiao, T. C.; Wang, Q.; Sirois, S.; Bouckaert, J.; Roy, R. *ChemMedChem* **2007**, *2*, 1190-1201.

[43] Bouckaert, J.; Li, Z.; Xavier, C.; Almant, M.; Caveliers, V.; Lahoutte, T.; Weeks, S. D.; Kovensky, J.; Gouin, S. G. *Chem. Eur. J.* **2013**, *19*, 7847-7855.

[44] Nierengarten, I.; Buffet, K.; Holler, M.; Vincent, S. P.; Nierengarten, J.-F. *Tetrahedron Lett.* **2013**, *54*, 2398-2402.

[45] Obritsch, M. D.; Fish, D. N.; MacLaren, R.; Jung, R. *Pharmacotherapy* **2005**, *25*, 1353-1364.

[46] Cecioni, S.; Lalor, R.; Blanchard, B.; Praly, J.-P.; Imberty, A.; Matthews, S. E.; Vidal, S. *Chem. Eur. J.* **2009**, *15*, 13232-13240.

[47] Soomro, Z. H.; Cecioni, S.; Blanchard, H.; Praly, J.-P.; Imberty, A.; Vidal, S.; Matthews, S. E. *Org. Biomol. Chem.* **2011**, *9*, 6587-6597.

[48] Gening, M. L.; Titov, D. V.; Cecioni, S.; Audfray, A.; Gerbst, A. G.; Tsevetkov, Y. E.; Krylov, V. B.; Imberty, A.; Nifantiev, N. E.; Vidal, S. *Chem. Eur. J.* **2013**, *19*, 9272-9285.

[49] Consoli, G. M. L.; Granata, G.; Cafiso, V.; Stefani, S.; Geraci, C. *Tetrahedron Lett.* **2011**, *52*, 5831-5834.

[50] Morvan, F.; Meyer, A.; Jochum, A.; Sabin, C.; Chevolot, Y.; Imberty, A.; Praly, J.-P.; Vasseur, J.-J.; Souteyrand, E.; Vidal, S. *Bioconjugate Chem.* **2007**, *18*, 1637-1643.

[51] Ligeour, C.; Audfray, A.; Gillon, E.; Meyer, A.; Galanos, N.; Vidal, S.; Vasseur, J.-J.; Imberty, A.; Morvan, F. *RSC Advances* **2013**, *3*, 19515-19524.

[52] Cecioni, S.; Faure, S.; Darbost, U.; Bonnamour, I.; Parrot-Lopez, H.; Roy, O.; Taillefumier, C.; Wimmerová, M.; Praly, J.-P.; Imberty, A.; Vidal, S. *Chem. Eur. J.* **2011**, *17*, 2146-2159.

[53] Varga, N.; Sutkeviciute, I.; Ribeiro-Viana, R.; Berzi, A.; Ramdasi, R.; Daghetti, A.; Vettoretti, G.; Amara, A.; Clerici, M.; Rojo, J.; Fieschi, F.; Bernardi, A. *Biomaterials* **2014**, *35*, 4175-4184.

[54] André, S.; Sansone, F.; Kaltner, H.; Casnati, A.; Kopitz, J.; Gabius, H.-J.; Ungaro, R. *ChemBioChem* **2008**, *9*, 1649-1661.

[55] Consoli, G. M. L.; Cunsolo, F.; Geraci, C.; Sgarlata, V. *Org. Lett.* **2004**, *6*, 4163-4166.

[56] André, S.; Grandjean, C.; Gautier, F.-M.; Bernardi, S.; Sansone, F.; Gabius, H.-J.; Ungaro, R. *Chem. Commun.* **2011**, *47*, 6126-6128.

[57] André, S.; Liu, B.; Gabius, H.-J.; Roy, R. *Org. Biomol. Chem.* **2003**, *1*, 3909-3916.

[58] Wang, G.-N.; André, S.; Gabius, H.-J.; Murphy, P. V. *Org. Biomol. Chem.* **2012**, *10*, 6893-6907.

[59] Giguère, D.; Patnam, R.; Bellefleur, M.-A.; St-Pierre, C.; Sato, S.; Roy, R. *Chem. Commun.* **2006**, 2379-2381.

[60] Marotte, K.; Préville, C.; Sabin, C.; Moumé-Pymbock, M.; Imberty, A.; Roy, R. *Org. Biomol. Chem.* **2007**, *5*, 2953-2961.

[61] Giguère, D.; André, S.; Bonin, M.-A.; Bellefleur, M.-A.; Provencal, A.; Cloutier, P.; Pucci, B.; Roy, R.; Gabius, H.-J. *Bioorg. Med. Chem.* **2011**, *19*, 3280-3287.

[62] Astronomo, R. D.; Burton, D. R. *Nat. Rev. Drug Discov.* **2010**, *9*, 308-324.

[63] Hakomori, S. *Adv. Cancer Res.* **1989**, *52*, 257–331.

[64] Lo-Man, R.; Bay, S.; Vichier-Guerre, S.; Dériaud, E.; Cantacuzène, D.; Leclerc, C. *Cancer Res.* **1999**, *59*, 1520-1524.

[65] Lo-Man, R.; Vichier-Guerre, S.; Bay, S.; Dériaud, E.; Cantacuzène, E.; Leclerc, C. *J. Immunol.* **2001**, *166*, 2849-2854.

[66] Ragupathi, G.; Coltart, D. M.; Williams, L. J.; Koide, F.; Kagan, E.; Allen, J.; Harris, C.; Glunz, P. W.; Livingston, P. O.; Danishefsky, S. J. *Proc. Nat. Acad. Sci.* **2002**, *99*, 13699-13704.

[67] Ragupathi, G.; Koide, F.; Livingston, P. O.; Cho, Y. S.; Endo, A.; Wan, Q.; Spassova, M. K.; Keding, S. J.; Allen, J.; Ouerfelli, O.; Wilson, R. M.; Danishefsky, S. J. *J. Am. Chem. Soc.* **2006**, *128*, 2715-2725.

[68] Zhu, J.; Wan, Q.; Lee, D.; Yang, G.; Spassova, M. K.; Ouerfelli, O.; Ragupathi, G.; Damani, P.; Livingston, P. O.; Danishefsky, S. J. *J. Am. Chem. Soc.* **2009**, *131*, 9298-9303.

[69] For a recent account, see: Wilson, R. M.; Danishefsky, S. J. *J. Am. Chem. Soc.* **2013**, *135*, 14462-14472.

[70] Freire, T.; Lo-Man, R.; Piller, F.; Piller, V.; Leclerc, C.; Bay, S. *Glycobiology* **2006**, *16*, 390-401.

[71] Grigalevicius, S.; Chierici, S.; Renaudet, O.; Lo-Man, R.; Dériaud, E.; Leclerc, C.; Dumy, P. *Bioconjugate Chem.* **2005**, *16*, 1149-1159.

[72] Renaudet, O.; BenMohamed, L.; Dasgupta, G.; Bettahi, I.; Dumy, P. *ChemMedChem* **2008**, *3*, 737-741.

[73] Bettahi, I.; Dasgupta, G.; Renaudet, O.; Chentoufi, A. A.; Zhang, X.; Carpenter, D.; Yoon, S.; Dumy, P.; BenMohamed, L. *Cancer Immunol. Immunother.* **2009**, *58*, 187-200.

[74] Fiore, M.; Thomas, B.; Duléry, V.; Dumy, P.; Renaudet, O. *New J. Chem.* **2013**, *37*, 286-289.

[75] Richichi, B.; Thomas, B.; Fiore, M.; Bosco, R.; Qureshi, H.; Nativi, C.; Renaudet, O.; BenMohamed, L. *Angew. Chem. Int. Ed.* **2014**, *53*, 11917-11920.

[76] Geraci, C.; Consoli, G. M. L.; Galante, E.; Bousquet, E.; Pappalardo, M.; Spadaro, A. *Bioconjugate Chem.* **2008**, *19*, 751-758.

[77] Krauss, I. J.; Joyce, J. G.; Finnefrock, A. C.; Song, H. C.; Dudkin, V. Y.; Geng, X.; Warren, J. D.; Chastain, M.; Shiver, J. W.; Danishefsky, S. J. *J. Am. Chem. Soc.* **2007**, *129*, 11042-11044.

[78] Joyce, J. G.; Krauss, I. J.; Song H. C.; Opalka, D. W.; Grimm, K. M.; Nahas, D. D.; Esser, M. T.; Hrin, R.; Feng, M.; Dudkin, V. Y.; Chastain, M.; Shiver, J. W.; Danishefsky, S. J. *Proc. Natl. Acad. Sci. U. S. A.* **2008**, *105*, 15684-15689.

[79] Wang, J.; Li, H.; Zou, G.; Wang, L.-X. *Org. Biomol. Chem.* **2007**, *5*, 1529-1540.

[80] Wang, L.-X.; Ni, J.; Singh, S.; Li, H. *Chem. Biol.* **2004**, *11*, 127-134.

[81] Li, H.; Wang, L.-X. *Org. Biomol. Chem.* **2004**, *2*, 483-488.

[82] Ni, J.; Song, H.; Wang, Y.; Stamatos, N. M.; Wang, L.-X. *Bioconjugate Chem.* **2006**, *17*, 493-500.

[83] Horiya, S.; Bailey, J. K.; Temme, J. S.; Schlippe, Y. V. G.; Krauss, I. J. *J. Am. Chem. Soc.* **2014**, *136*, 5407-5415.

[84] Grandjean, C.; Rommens, C.; Gras-Masse, H.; Melnyk, O. *Angew. Chem. Int. Ed.* **2000**, *39*, 1068-1072.

[85] Grandjean, C.; Angyalosi, G.; Loing, E.; Adriaenssens, E.; Melnyk, O.; Pancré , V.; Auriault, C.; Gras-Masse, H. *ChemBioChem* **2001**, *2*, 747-757.

[86] Adamo, R.; Hu, Q.-Y.; Torosantucci, A.; Crotti, S.; Brogioni, G.; Allan, M.; Chiani, P.; Bromuro, C.; Quinn, D.; Tontini, M.; Berti, F. *Chem. Sci.* **2014**, *5*, 4302-4311.

[87] Aoyama, Y. *Chem. Eur. J.* **2004**, *10*, 588-593.

[88] Avvakumova, S.; Fezzardi, P.; Pandolfi, L.; Colombo, M.; Sansone, F.; Casnati, A.; Prosperi, D. *Chem. Commun.* **2014**, *50*, 11029-11032.

[89] Díaz-Moscoso, A.; Guilloteau, N.; Bienvenu, C.; Méndez-Ardoy, A.; Jiménez Blanco, J. L.; Benito, J. M.; Le Gourriérec, L.; Di Giorgio, C.; Vierling, P.; Defaye, J.; Ortiz Mellet, C.; García Fernández, J. M. *Biomaterials* **2011**, *32*, 7263-7273.

[90] Symens, N.; Méndez-Ardoy, A.; Díaz-Moscoso, A.; Sánchez-Fernández, E.; Remaut, K.; Demeester, J.; García Fernández, J. M.; De Smedt, S. C.; Rejman, J. *Bioconjugate Chem.* **2012**, *23*, 1276-1289.

[91] Aguilar Moncayo, E. M.; Guilloteau, N.; Bienvenu, C.; Jiménez Blanco, J. L.; Di Giorgio, C.; Vierling, P.; Benito, J. M.; Ortiz Mellet, C.; García Fernández, J. M. *New J. Chem.* **2014**, *38*, 5215-5225.

[92] Arima, H.; Yamashita, S.; Mori, Y.; Hayashi, Y.; Motoyama, K.; Hattori, K.; Takeuchi, T.; Jono, H.; Ando, Y.; Hirayama, F.; Uekama, K. *J. Control. Release* **2010**, *146*, 106-117.

[93] Motoyama, K.; Mori, Y.; Yamashita, S.; Hayashi, Y.; Jono, H.; Ando, Y.; Hirayama, F.; Uekama, K.; Arima, H. *J. Incl. Phenom. Macrocycl. Chem.* **2011**, *70*, 333-338.

[94] Baussanne, I.; Law, H.; Defaye, J.; Benito, J. M.; Ortiz Mellet, C.; García Fernández, J. M. *Chem. Commun.* **2000**, 1489-1490.

[95] Benito, J. M.; Gómez-García, M.; Ortiz Mellet, C.; Baussanne, I.; Defaye, J.; García Fernández, J. M. *J. Am. Chem. Soc.* **2004**, *126*, 10355-10363.

[96] de Robertis, L.; Lancelon-Pin, C.; Driguez, H. *Bioorg. Med. Chem. Lett.* **1994**, *4*, 1127-1130.

[97] Lainé, V.; Coste-Sarguet, A.; Gadelle, A.; Defaye, J.; Perly, B.; Djedaïni-Pilard, F. J. *Chem Soc. Perkin. Trans. 2* **1995**, 1479-1487.

[98] Furuike, T.; Aiba, S.; Nishimura, S. I. *Tetrahedron* **2000**, *56*, 9909-9915.

[99] André, S.; Kaltner, H.; Furuike, T.; Nishimura, S.-I.; Gabius, H.-J. *Bioconjugate Chem.* **2004**, *15*, 87-98.

[100] Furuike, T.; Sadamoto, R.; Niikura, K.; Monde, K.; Sakairi, Nishimura, S. I. *Tetrahedron* **2005**, *61*, 1737-1742.

[101] Yasuda, N.; Aoki, N.; Abe, H.; Hattori, K. *Chem. Lett.* **2000**, 706-707.

[102] García-López, J. J.; Hernández-Mateo, F.; Isac-García, J.; Kim, J.; Roy, R.; Santoyo-González, F.; Vargas-Berenguel, A. *J. Org. Chem.* **1998**, *64*, 522-531.

[103] García-López, J. J.; Santoyo-González, F.; Vargas-Berenguel, A.; Giménez-Martínez, J. J. *Chem. Eur. J.* **1999**, *5*, 1775-1784.

[104] Ortega-Caballero, F.; Giménez Martínez, J. J.; García-Fuentes, L.; Ortiz-Salmerón, E.; Santoyo-González, F.; Vargas-Berenguel, A. *J. Org. Chem.* **2001**, *66*, 7786-7795.

[105] Vargas-Berenguel, A.; Ortega-Caballero, F.; Santoyo-González, F.; Giménez-Martínez, J. J.; García-Fuentes, L.; Ortiz-Salmerón, E. *Chem. Eur. J.* **2002**, *8*, 812-827.

[106] Ortiz Mellet, C.; Benito, J. M.; García Fernández, J. M.; Law, H.; Chmurski, K.; Defaye, J.; O'Sullivan, M. L.; Caro, H. N. *Chem. Eur. J.* **1998**, *4*, 2523-2531.

[107] Baussane, I.; Benito, J. M.; Ortiz Mellet, C.; García Fernández, J. M.; Defaye, J. *ChemBiochem* **2001**, *2*, 777-783.

[108] Abe, H.; Kenmoku, A.; Yamaguch, N.; Hattori, K. *J. Inclusion Phenom. Macrocyclic Chem.* **2002**, *44*, 39-47.

[109] Oda, Y.; Yanagisawa, H.; Maruyama, M.; Hattori, K.; Yamanoi, T. *Bioorg. Med. Chem.* **2008**, *16*, 8830-8840.

[110] Bernardes, G. J. L.; Kikkeri, R.; Maglinao, M.; Laurino, P.; Collot, M.; Hong, S. Y.; Lepeniesa, B.; Seeberger, P. H. *Org. Biomol. Chem.* **2010**, *8*, 4987-4996.

[111] Zhang, Q.; Su, L.; Collins, J.; Chen, G.; Wallis, R.; Mitchell, D. A.; Haddleton, D. M.; Becer, C. R. *J. Am. Chem. Soc.* **2014**, *136*, 4325-4332.

[112] Mazzaglia, A.; Forde, D.; Garozzo, D.; Malvagna, P.; Ravoo, B. J.; Darcy, R. *Org. Biomol. Chem.* **2004**, *2*, 957-960.

[113] Mazzaglia, A.; Valerio, A.; Villari, V.; Rencurosi, A.; Lay, L.; Spadaro, S.; Scolarof, L. M.; Micali, N. *New J. Chem.* **2006**, *30*, 1662-1668.

[114] Aykaç, A.; Martos-Maldonado, M. C.; Casas-Solvas, J. M.; Quesada-Soriano, I.; García-Maroto, F.; García-Fuentes, L.; Vargas-Berenguel, A. *Langmuir* **2014**, *30*, 234–242.

Figure legends

Figure 7-1. Influenza virus hemagglutinin (HA) inhibitors based on a cyclopeptide (**1**) and calix[4]arene (**2-4**) showing sialyl groups as vector moieties.

Figure 7-2. B_5 pentamer Shiga-like toxins (Stx-1/2) inhibitors centered on glucose (Starfish **5**, Daisy **6**, and Bait **7**) or carbosilane (SUPER TWIG-12 **8**) cores using globotriaosyl (Gb3) as binding residues.

Figure 7-3. Cholera toxin B pentamer (CTB) inhibitors **9-18** designed on a pentacyclen core displaying five galactose residues.

Figure 7-4. Cholera toxin B pentamer (CTB) inhibitors **19-23** presenting natural ganglioside GM1 and unnatural pseudo-GM2 mimic residues grafted on calix[4]arene, calix[5]arene and corannulene scaffolds.

Figure 7-5. Antiadhesive cluster mannosiedes based on linear β-(1→4)-glucosides, pentaerythitol, β-cyclodextrin and pillar[5]arene cores **24-31** against FimH lectin, present in Type 1 piliated bacteria such as *E. coli.*

Figure 7-6. High affinity ligands for galactose-binding PA-IL (LecA) and fucose-binding PA-IIL (LecB) lectins from *Pseudomonas aeruginosa* (**32-42** and **43-47**,

respectively) based on calix[4]arene, calix[4]resorcarene and pentaerythritol phosphodiester oligomer (PePOs) cores.

Figure 7-7. Fucosylated antiadhesive agents against BambL lectin from *Burkholderia ambifaria* bacteria (**48**-**52**) centered on mannose and pentaerythritol phosphodiester oligomers (PePOs), as well as HIV-1 and Dengue viruses inhibitors (**53** and **54**) bearing a non-natural pseudo-disaccharide DC-SIGN antagonist.

Figure 7-8. High affinity ligands for galactose-binding AB toxin *Viscum album* agglutinin (VVA) and tumor-overexpressed lectins Gal-1, -3, -7, -8 and -9, consisting on the attachment of galactose, lactose, 2'-fucosyllactose and 4-fucosylglucosamine residues on calix[n]arene (n = 4, 6 or 8), pentaerythritol or 1,3,5-benzene cores.

Figure 7-9. Tumour-Associated Carbohydrate Antigens (TACAs) commonly used in synthetic anti-cancer vaccines development.

Figure 7-10. Anti-cancer vaccines based on the appendage of one or several TACAs on branched (**76** and **77**) or lineal (**78**-**81**) oligopeptides, using polivirus type 1 PV oligopeptide or keyhole limpet hemocyanin (KLH) carrier protein, respectively.

Figure 7-11. Anti cancer vaccines containing Tn and Tn-antigen mimetic MIM_Tn clusters grafted on 10-Residues Addressable Functionalized Template (RAFT) (**82**-**85**) and calix[4]arene (**86**) as scaffolds.

Figure 7-12. Carbohydrate-based vaccines against HIV designed as clusters of gp120 glypan ($Man_9GlcNAc_2$) or its structurally simpler D1 tetramannoside arm grafted on different scaffolds such as 14- (**87**) and 10-RAFTs (**88** and **89**), galactose (**90**) and cholic acid (**91**).

Figure 7-13. Mannosylated $HA_{307-319}$ peptidic epitope from Influenza virus hemagglutinin.

Figure 7-14. Synthetic vaccines **93**-**95** against *Candida albicans* based on the attachment of a controlled number of β-(1→3) glucan hexasaccharide moieties to tyrosine or lysine residues of CRM_{197} carrier protein from diphtheria toxin.

Figure 7-15. Artificial glycoviruses based on the supramolecular aggregation of calix[4]resorcarene-scaffolded glycoclusters **96**-**98** as DNA delivery systems. Amphiphilic glycocalix[4]arene **99** and its non-covalently self-assembly on *n*-dodecanyl AuNPs as a potential drug delivery system.

Figure 7-16. Polycationic amphiphilic β-CD-based mannosyl clusters **100**-**102** as pDNA and mRNA nanocarriers targeting macrophage mannose (MMR) and asyaloglycoprotein (ASGPr) receptors.

Figure 7-17. ASGPr-mediated gene delivery system in HepG2 cells using G2-PAMAM dendrimer as core.

Figure 7-18. Primary face monosubstituted β-CD derivatives **104**-**109** and β-CD dimer **110** as mammalian mannose/fucose specific cell surface receptor targeted delivery systems for water insoluble anti-cancer drug docetaxel.

Figure 7-19. β-CD Glycoclusters persubstituted on primary face (**111**-**121** and **123**-**133**).

Figure 7-20. Mono- (**141**-**143**) and divalent (**135**-**140** and **144**) galactosylated β-CD derivatives as DXR delivery systems.

Figure 7-21. Nonavalent galactosylated β-CD conjugate **145** as a HepG2 hepatocyte-targeted delivery system for Rhodamine B and anti-cancer drug DXR.

Figure 7-22. β-CD-based star mannosylated glycopolymers **146**-**148** as DC-SIGN-mediated delivery systems for anti-cancer agent docosahexaenoic acid and anti-HIV

drug Saquinavir, as well as amphiphilic β-CD derivatives **150** and **151** grafted in their secondary faces with galactose residues as nanoparticles- and vesicles-forming nanocarriers.

Figure 7-23. Dually functionalized gold nanoparticle **152** bearing simultenously lactose residues as targeting ligands for Gal-3 lectin and β-CD macrocycles as encapsulating moieties for anti-cancer drug methotrexate (MTX).

Figures

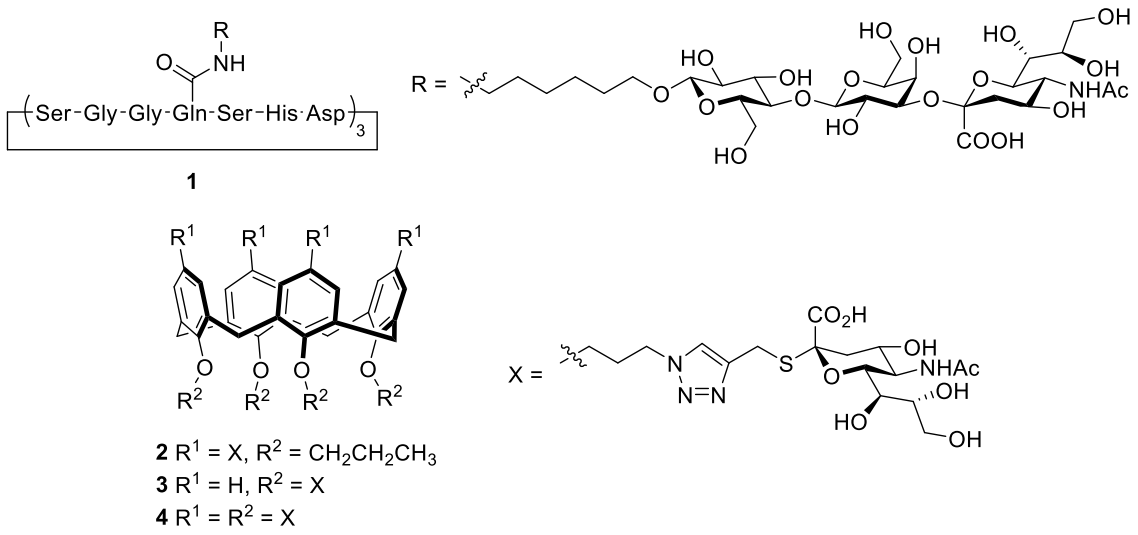

Figure 7-1.

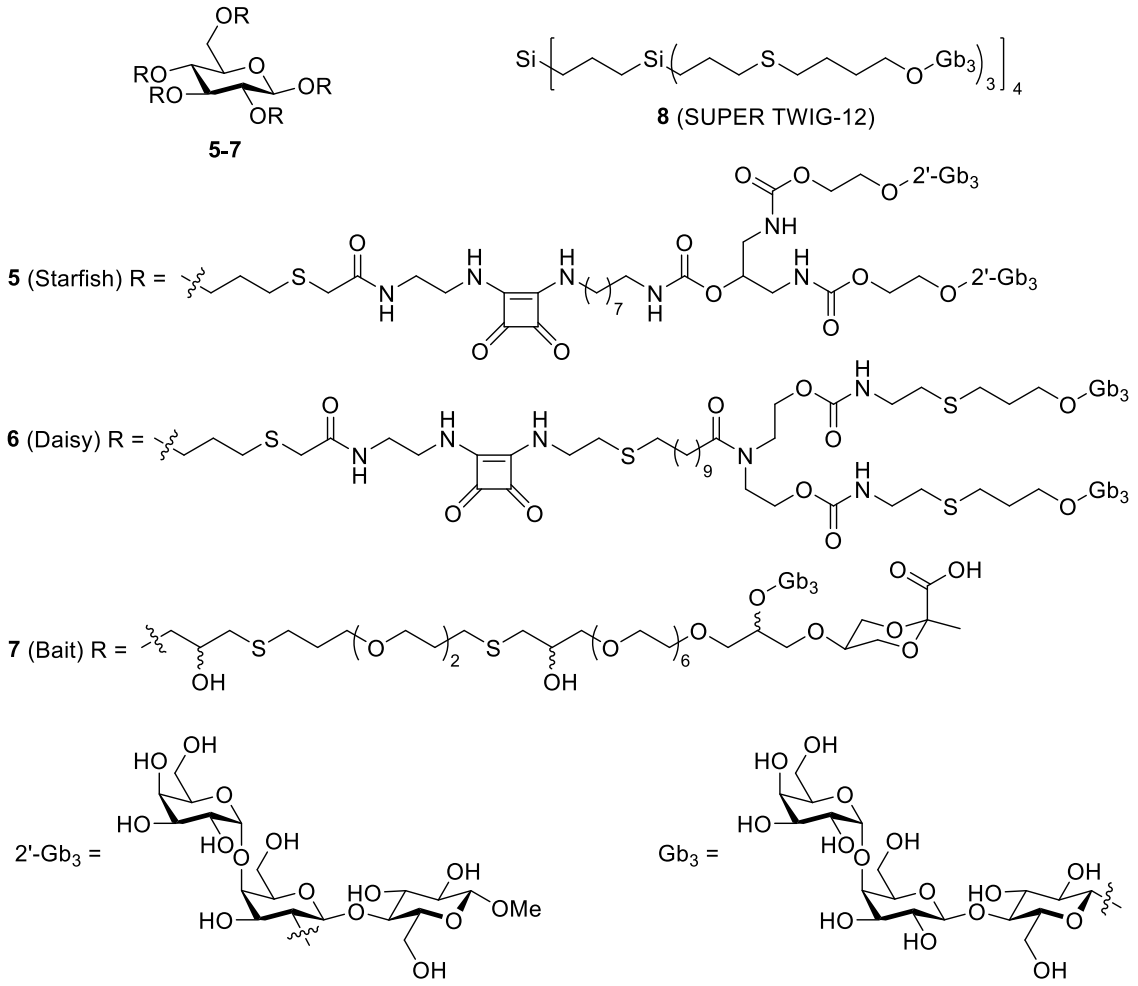

Figure 7-2.

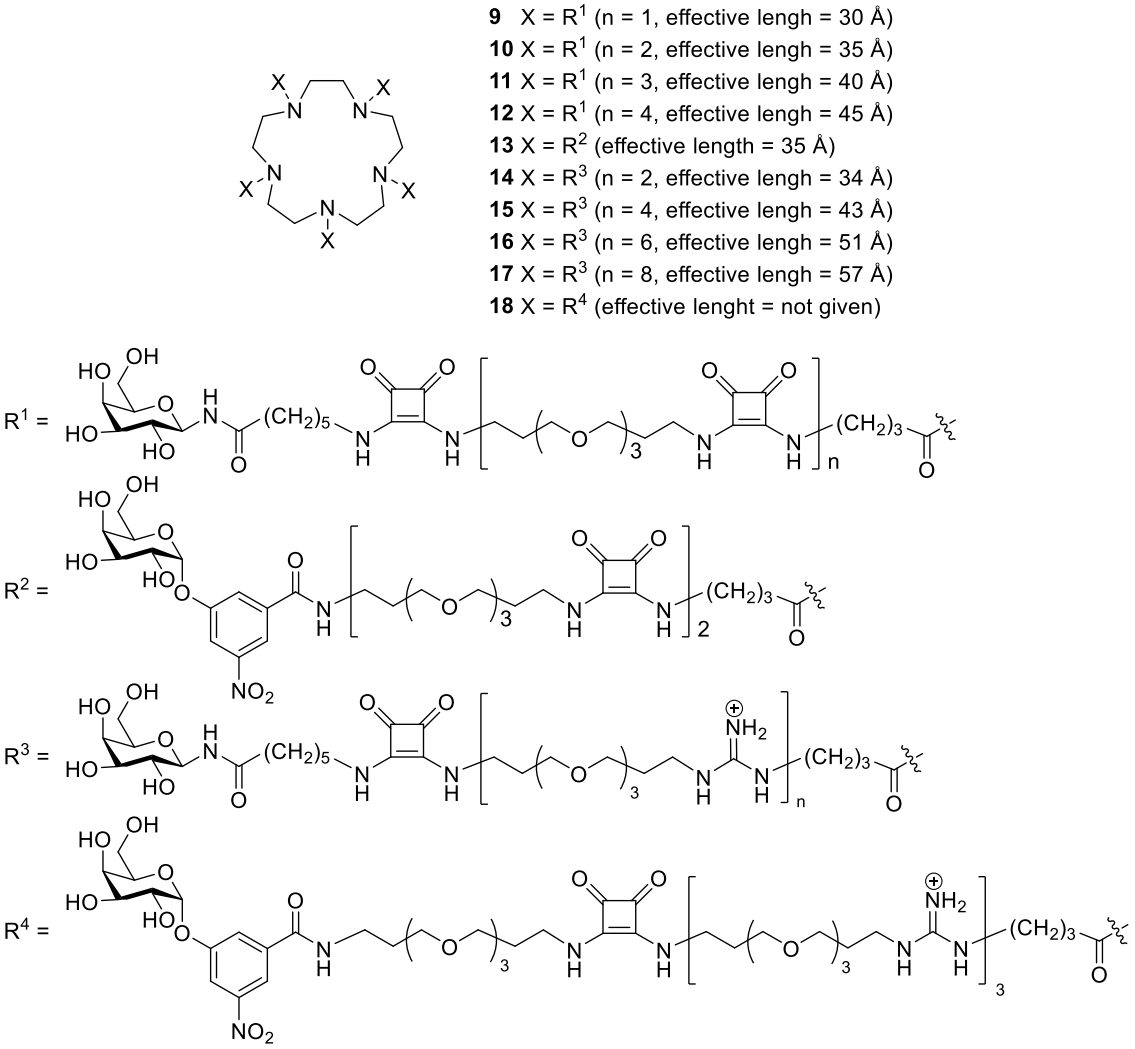
9 X = R1 (n = 1, effective lengh = 30 Å)
10 X = R1 (n = 2, effective lengh = 35 Å)
11 X = R1 (n = 3, effective lengh = 40 Å)
12 X = R1 (n = 4, effective lengh = 45 Å)
13 X = R2 (effective length = 35 Å)
14 X = R3 (n = 2, effective lengh = 34 Å)
15 X = R3 (n = 4, effective lengh = 43 Å)
16 X = R3 (n = 6, effective lengh = 51 Å)
17 X = R3 (n = 8, effective lengh = 57 Å)
18 X = R4 (effective lenght = not given)
R1 =
R2 =
R3 =
R4 =

Figure 7-3.

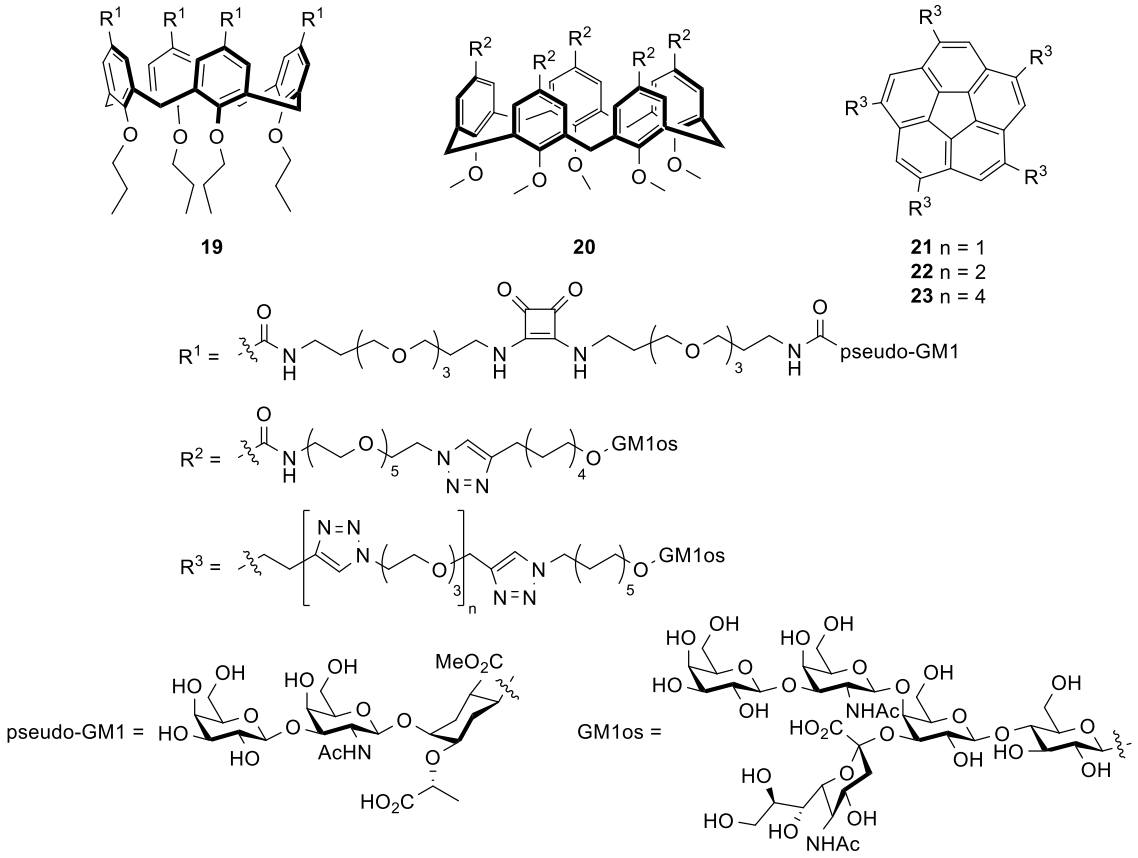
19
20
21 n = 1
22 n = 2
23 n = 4
R1 =
pseudo-GM1
R2 =
GM1os
R3 =
GM1os
pseudo-GM1 =
GM1os =

Figure 7-4.

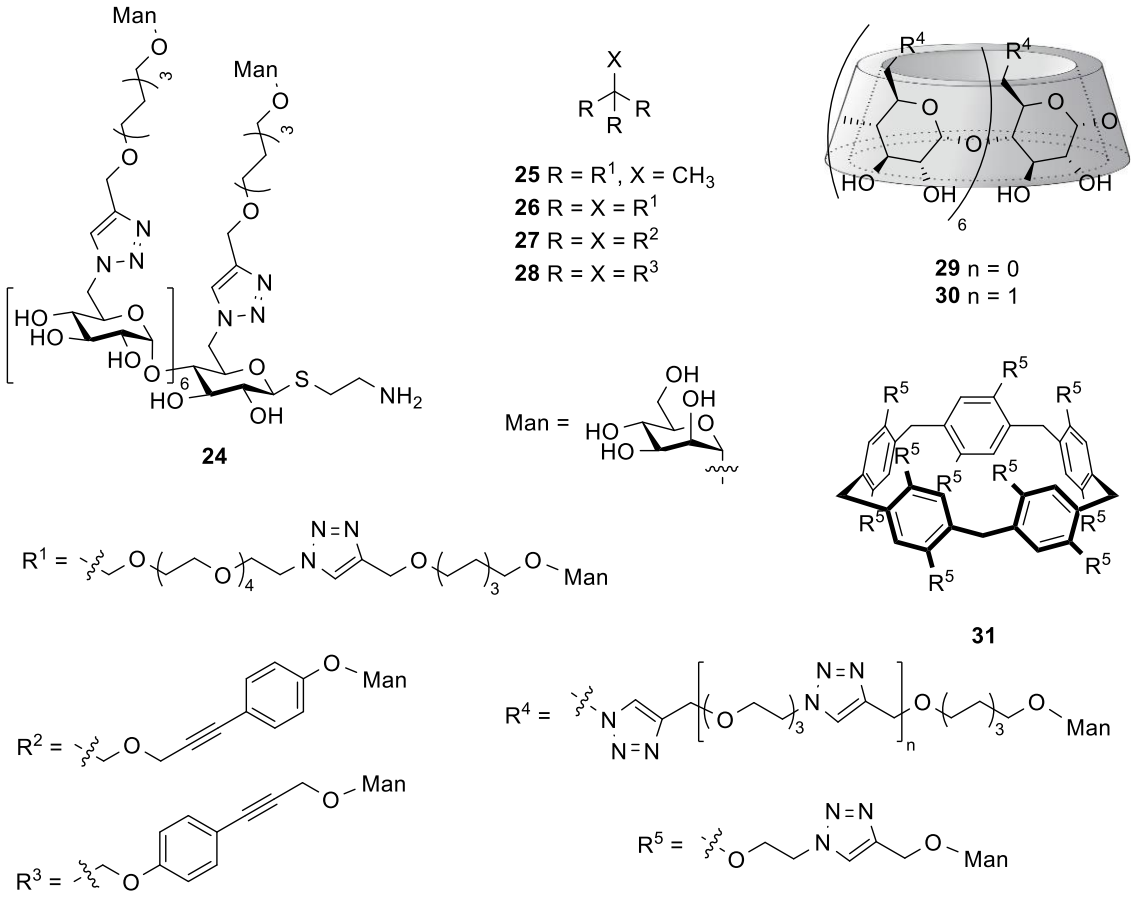
Man
Man
24
25 R = R1, X = CH3
26 R = X = R1
27 R = X = R2
28 R = X = R3
29 n = 0
30 n = 1
Man =
R1 =
R2 =
R3 =
R4 =
R5 =
31

Figure 7-5.

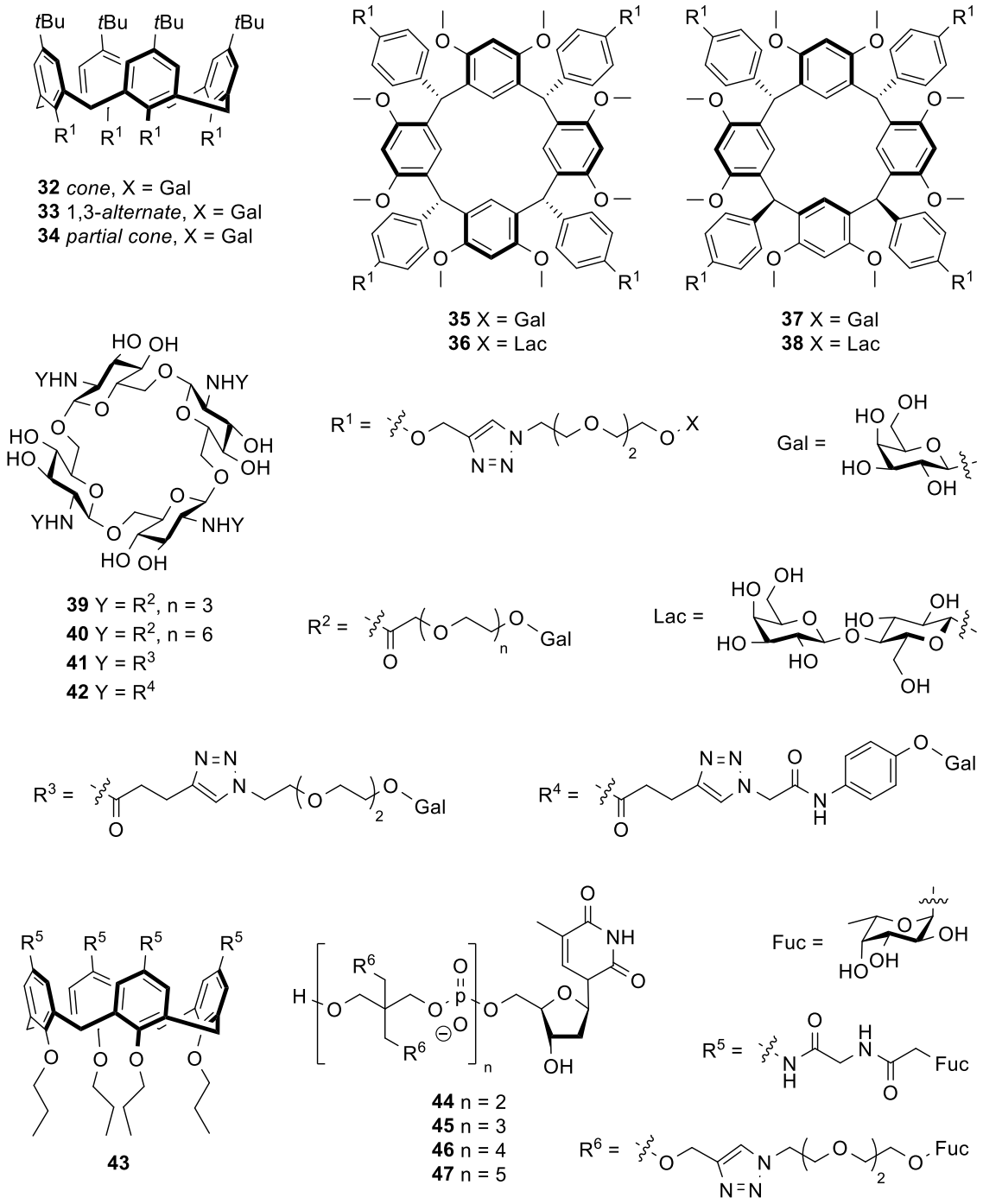
32 *cone*, X = Gal
33 1,3-*alternate*, X = Gal
34 *partial cone*, X = Gal
35 X = Gal
36 X = Lac
37 X = Gal
38 X = Lac
39 Y = R^2, n = 3
40 Y = R^2, n = 6
41 Y = R^3
42 Y = R^4
R^1 =
Gal =
R^2 =
Lac =
R^3 =
R^4 =
43
44 n = 2
45 n = 3
46 n = 4
47 n = 5
Fuc =
R^5 =
R^6 =

Figure 7-6.

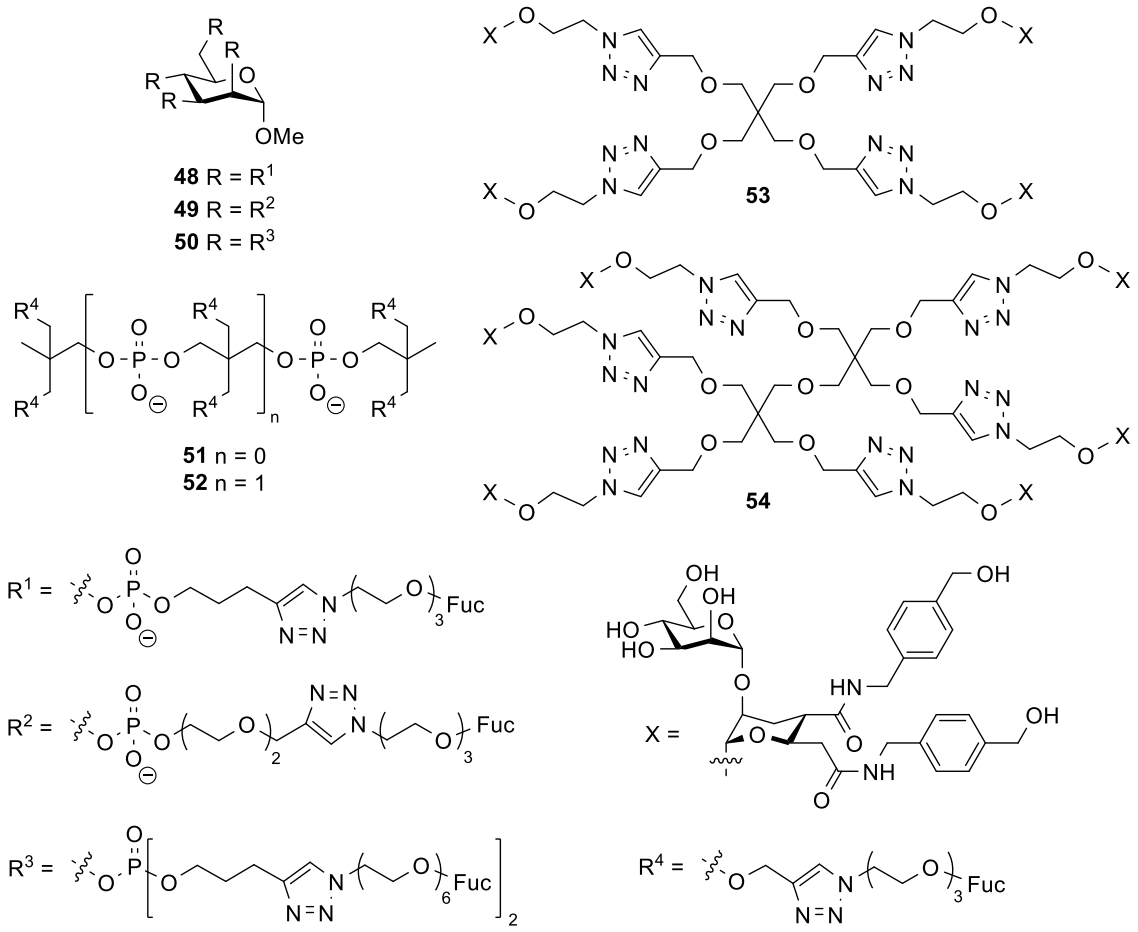

Figure 7-7.

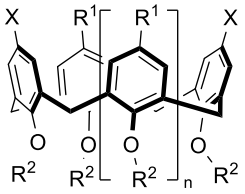

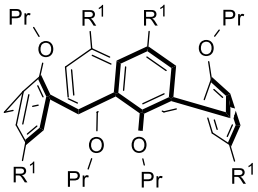

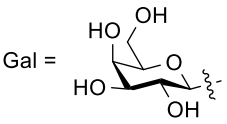

55 R^1 = X = NH(CS)NHGal, R^2 = Pr, n = 1
56 R^1 = X = NH(CS)NHLac, R^2 = Pr, n = 1
57 R^1 = NH(CS)NHGal, X = H, R^2 = Pr, n = 1
58 R^1 = NH(CS)NHLac, X = H, R^2 = Pr, n = 1
59 R^1 = NH(CS)NHGal, X = H, R^2 = Me, n = 1
60 R^1 = NH(CS)NHLac, X = H, R^2 = Me, n = 1
61 R^1 = X = NH(CS)NHGal, R^2 = Me, n = 1
62 R^1 = X = NH(CS)NHGal, R^2 = Me, n = 3
63 R^1 = X = NH(CS)NHGal, R^2 = Me, n = 5
64 R^1 = X = NH(CS)NHLac, R^2 = Me, n = 1
65 R^1 = X = NH(CS)NHLac, R^2 = Me, n = 3
66 R^1 = X = NH(CS)NHLac, R^2 = Me, n = 5

67 R^1 = NH(CS)NHGal
68 R^1 = NH(CS)NHLac

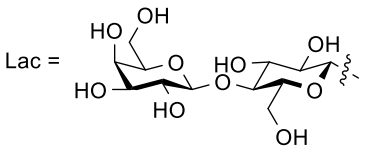

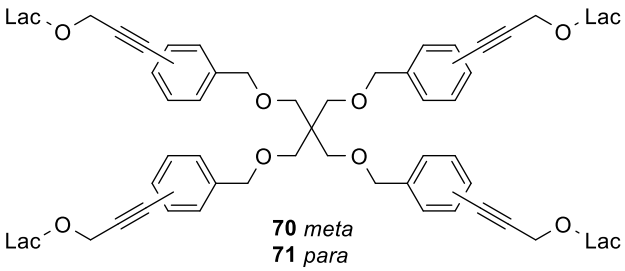

70 *meta*
71 *para*

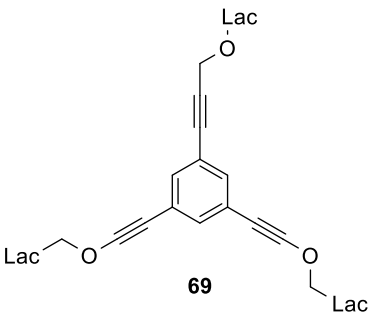

69

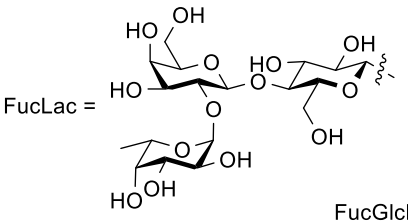

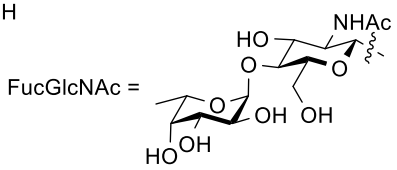

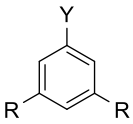

72 R = Y = R^3
73 R = R^4, Y = CH_2NH_2
74 R = Y = R^5, Z = Lac
75 R = Y = R^5, Z = FucGlcNAc

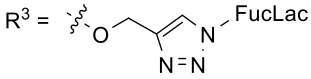

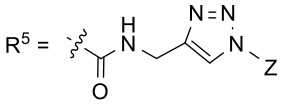

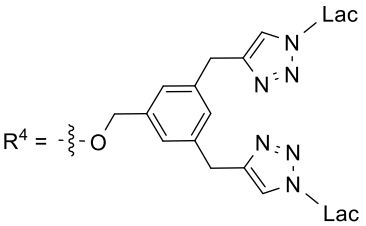

Figure 7-8.

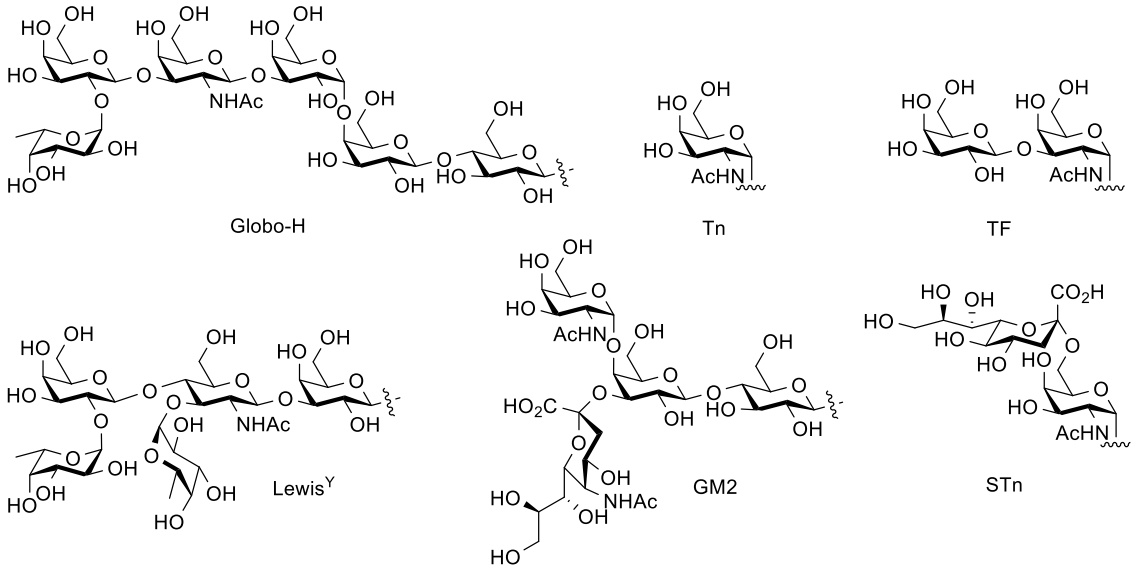

Figure 7-9.

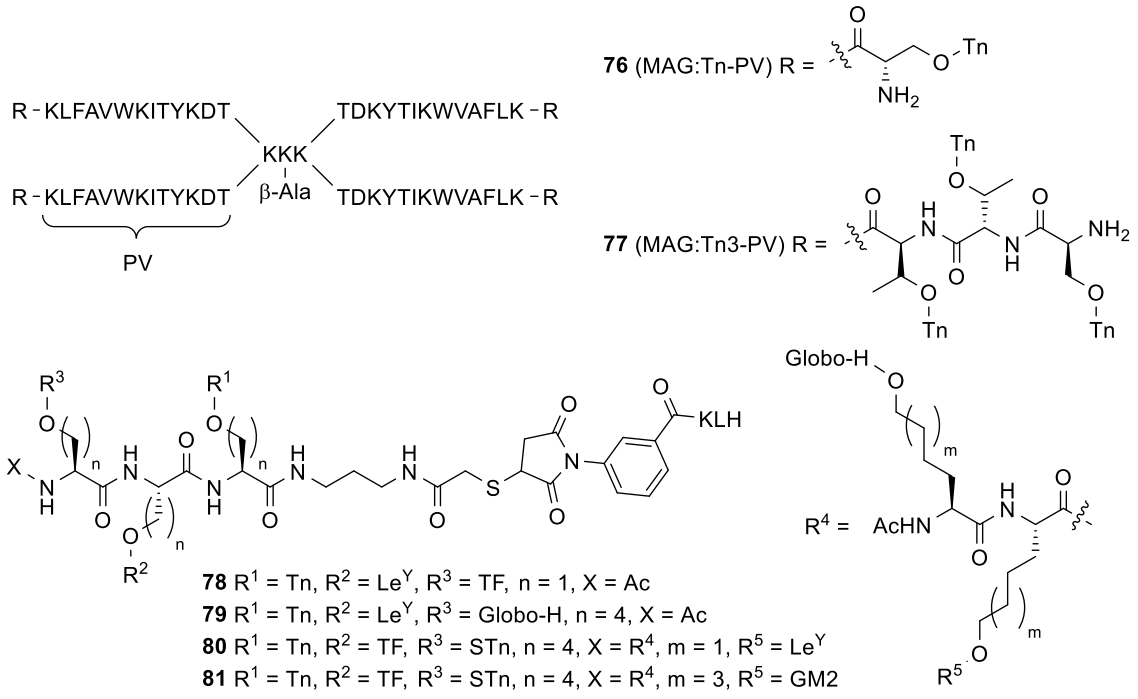

Figure 7-10.

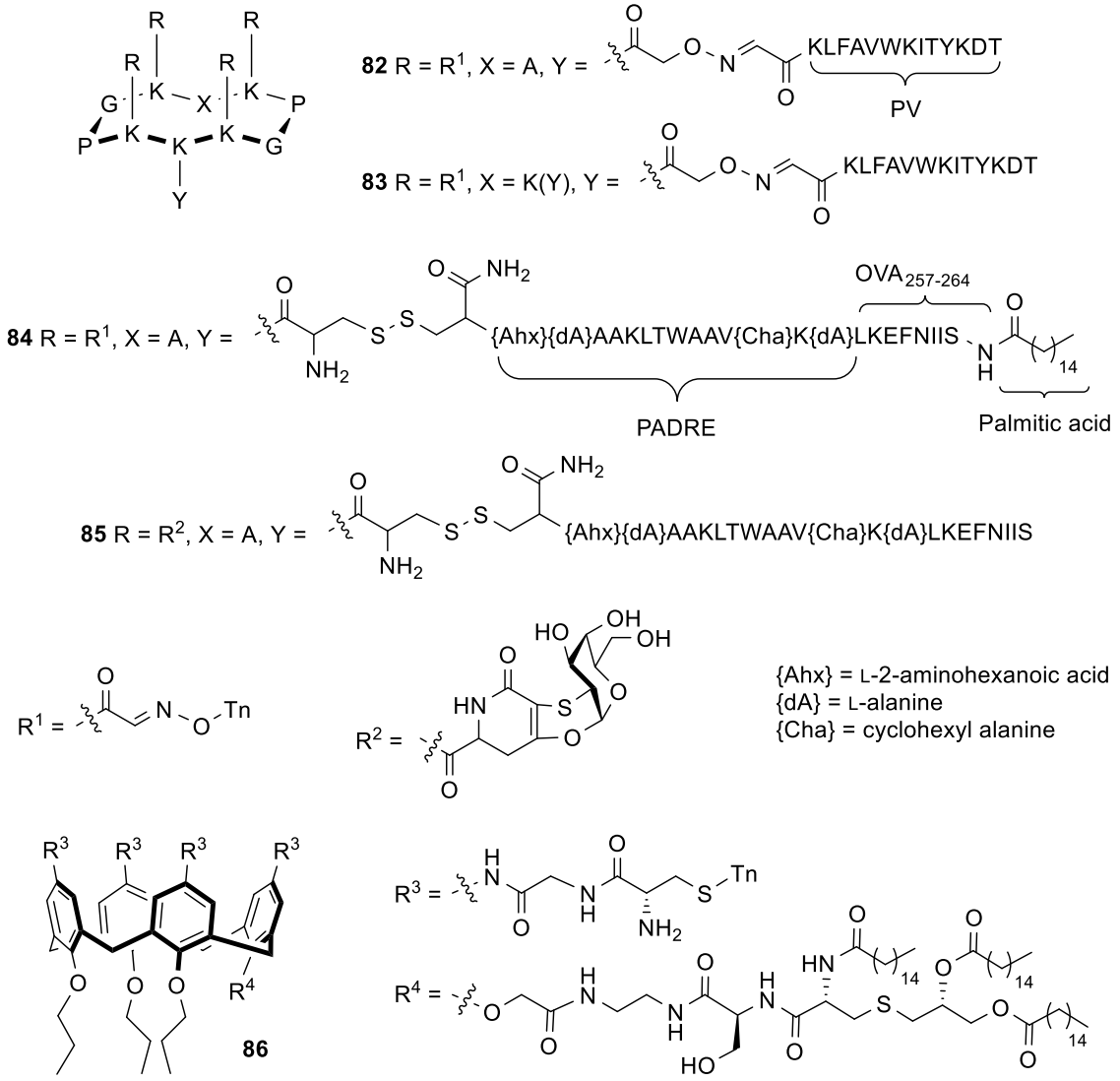
82 R = R1, X = A, Y = KLFAVWKITYKDT
PV
83 R = R1, X = K(Y), Y = KLFAVWKITYKDT
84 R = R1, X = A, Y = {Ahx}{dA}AAKLTWAAV{Cha}K{dA}LKEFNIIS
OVA257-264
PADRE
Palmitic acid
85 R = R2, X = A, Y = {Ahx}{dA}AAKLTWAAV{Cha}K{dA}LKEFNIIS
{Ahx} = L-2-aminohexanoic acid
{dA} = L-alanine
{Cha} = cyclohexyl alanine
86

Figure 7-11.

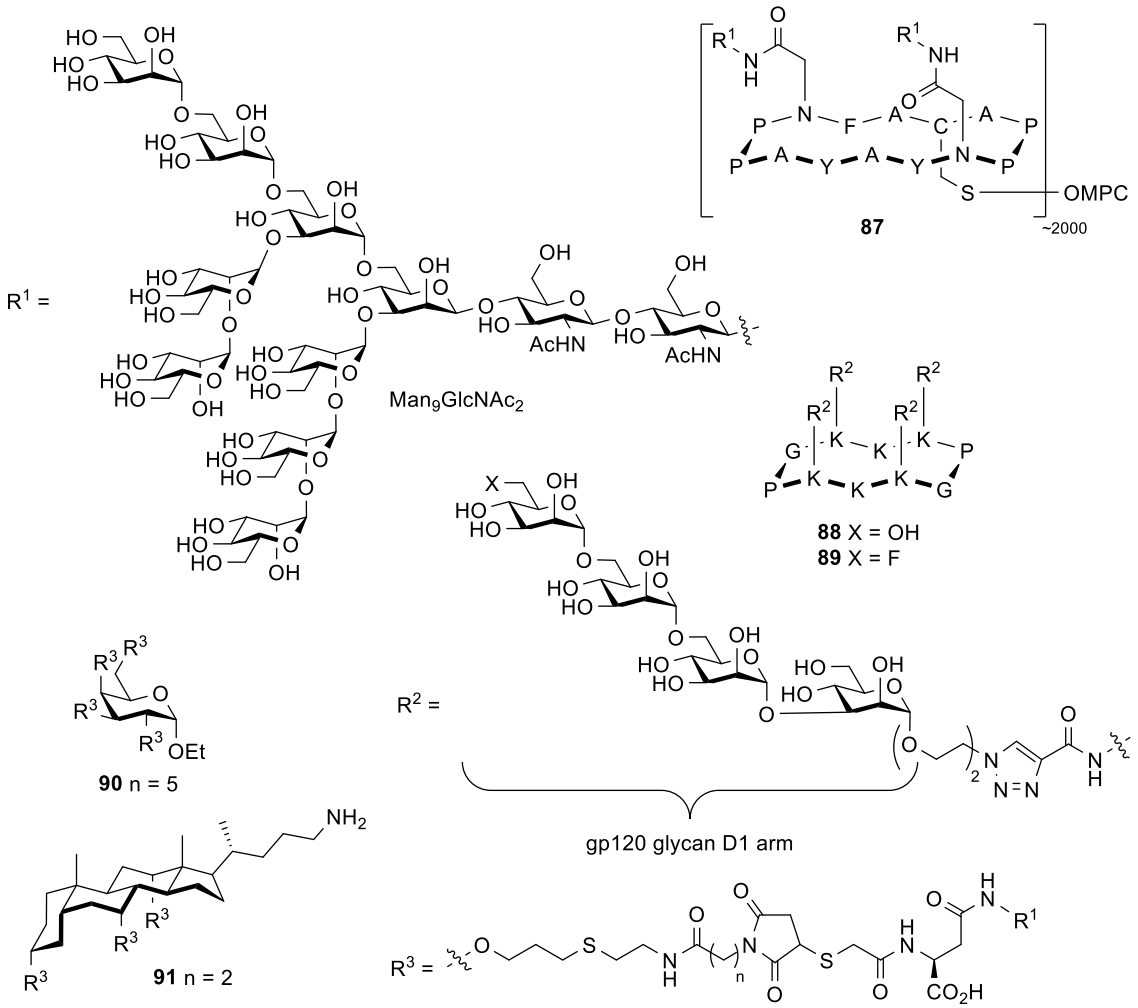
R1 =
Man9GlcNAc2
AcHN
AcHN
87
~2000
OMPC
88 X = OH
89 X = F
90 n = 5
91 n = 2
R2 =
gp120 glycan D1 arm
R3 =
CO2H

Figure 7-12.

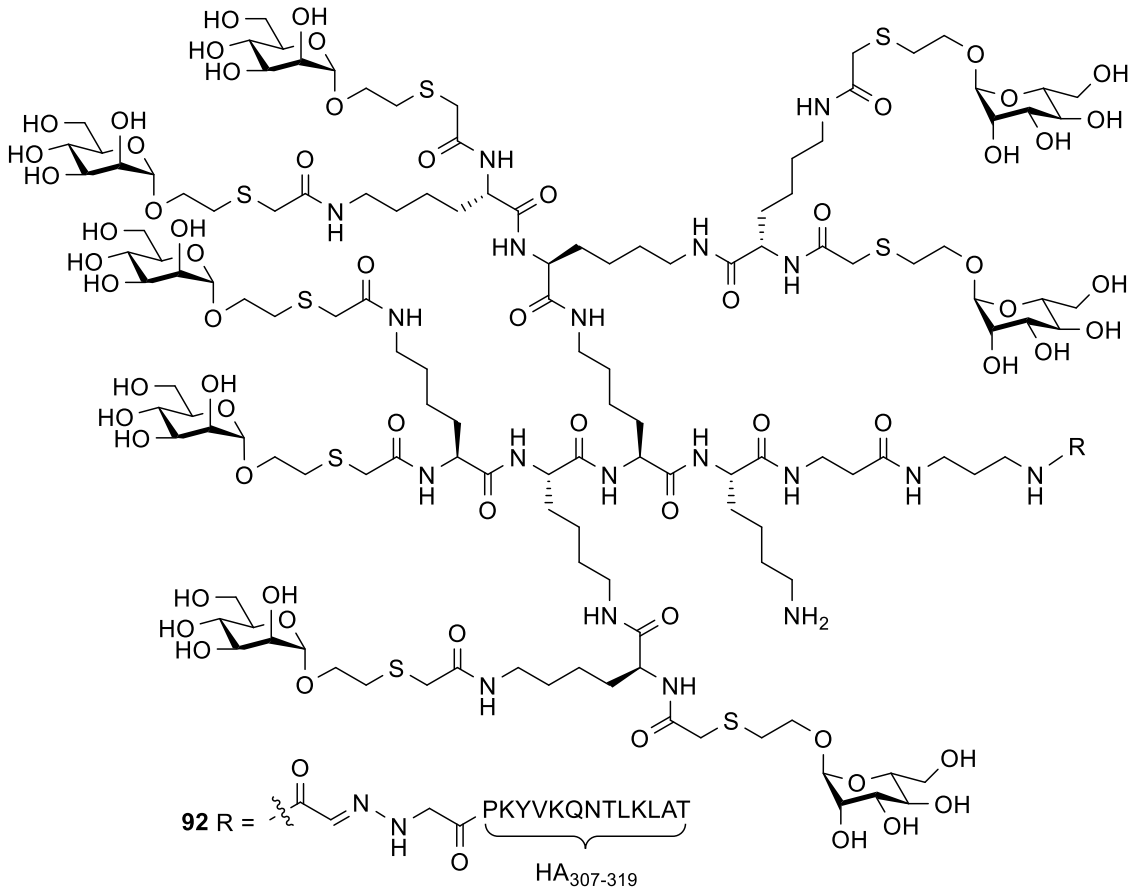

Figure 7-13.

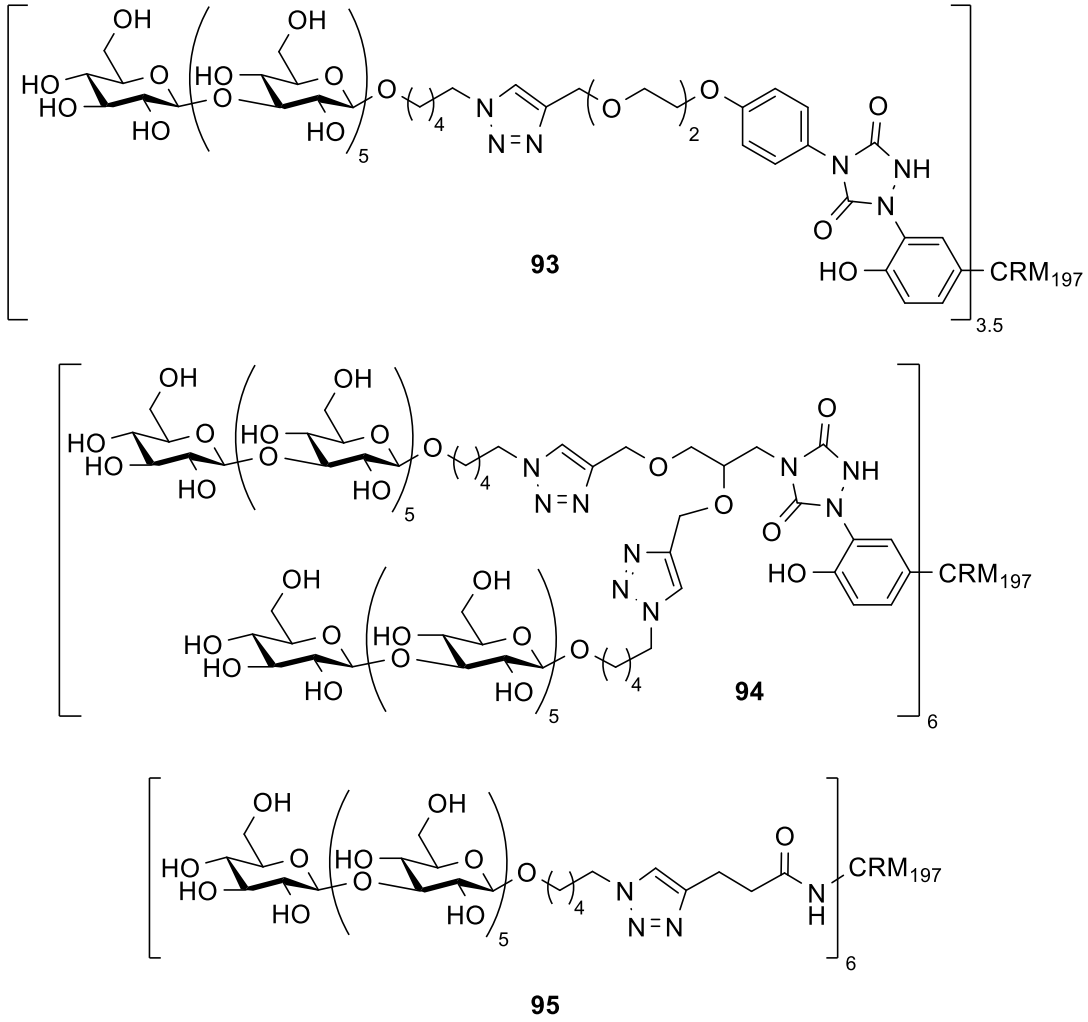

Figure 7-14.

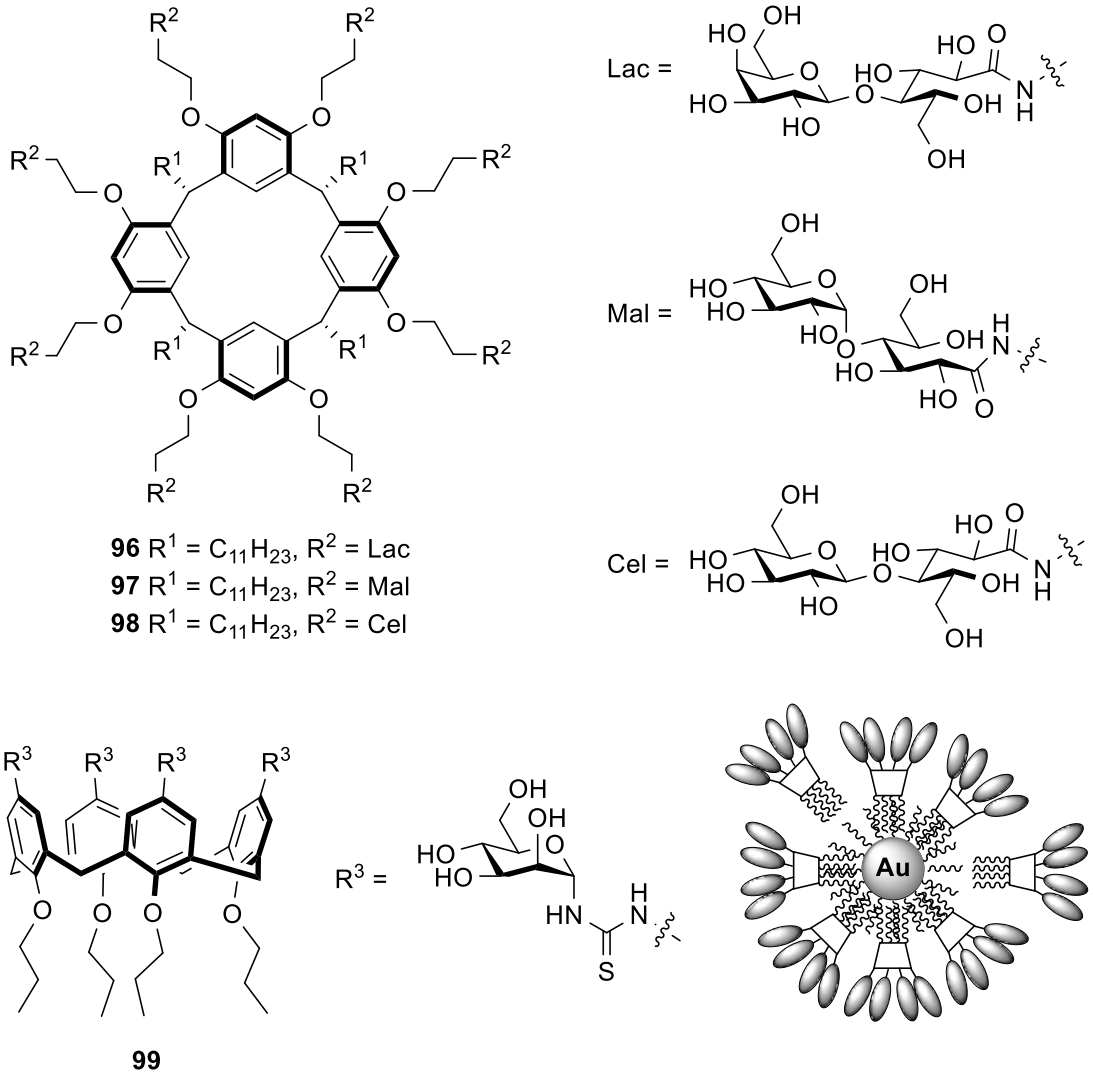
Lac =
Mal =
Cel =
96 $R^1 = C_{11}H_{23}$, R^2 = Lac
97 $R^1 = C_{11}H_{23}$, R^2 = Mal
98 $R^1 = C_{11}H_{23}$, R^2 = Cel
R^3 =
Au
99

Figure 7-15.

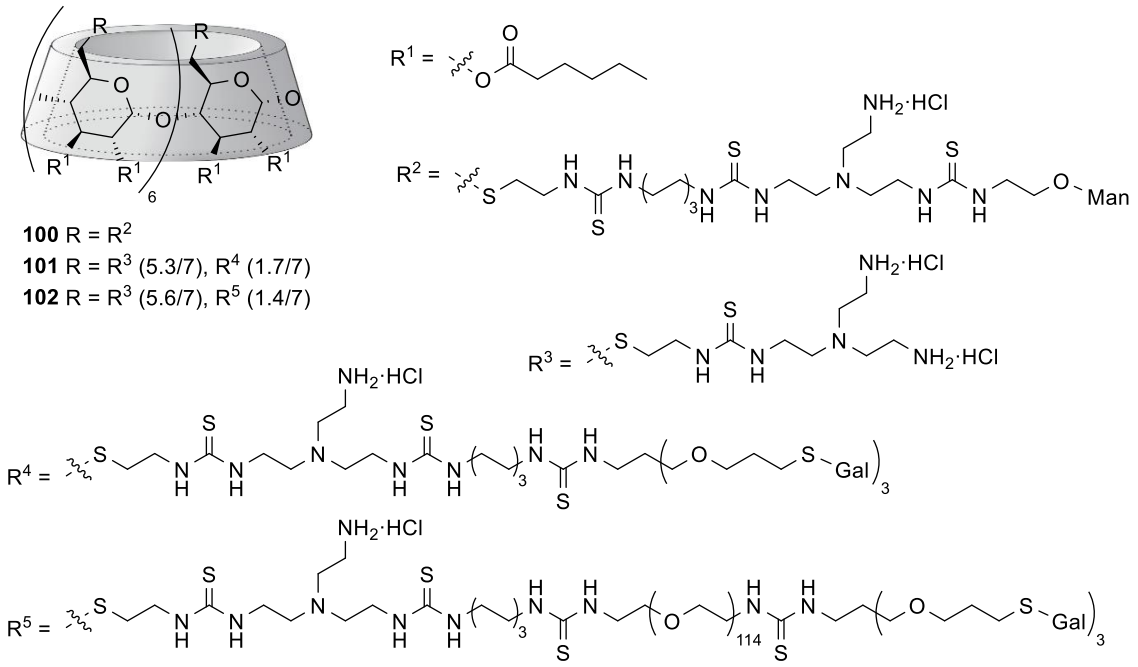

Figure 7-16.

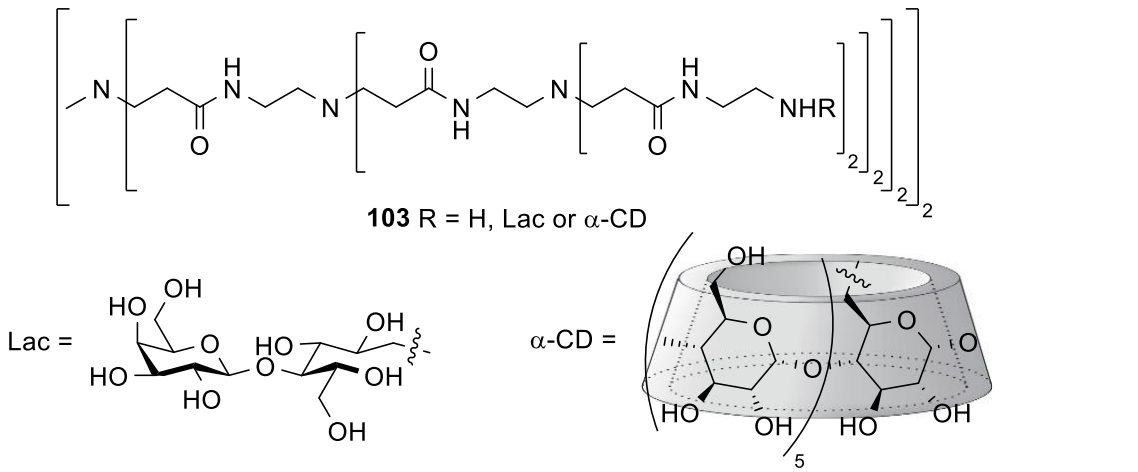

Figure 7-17.

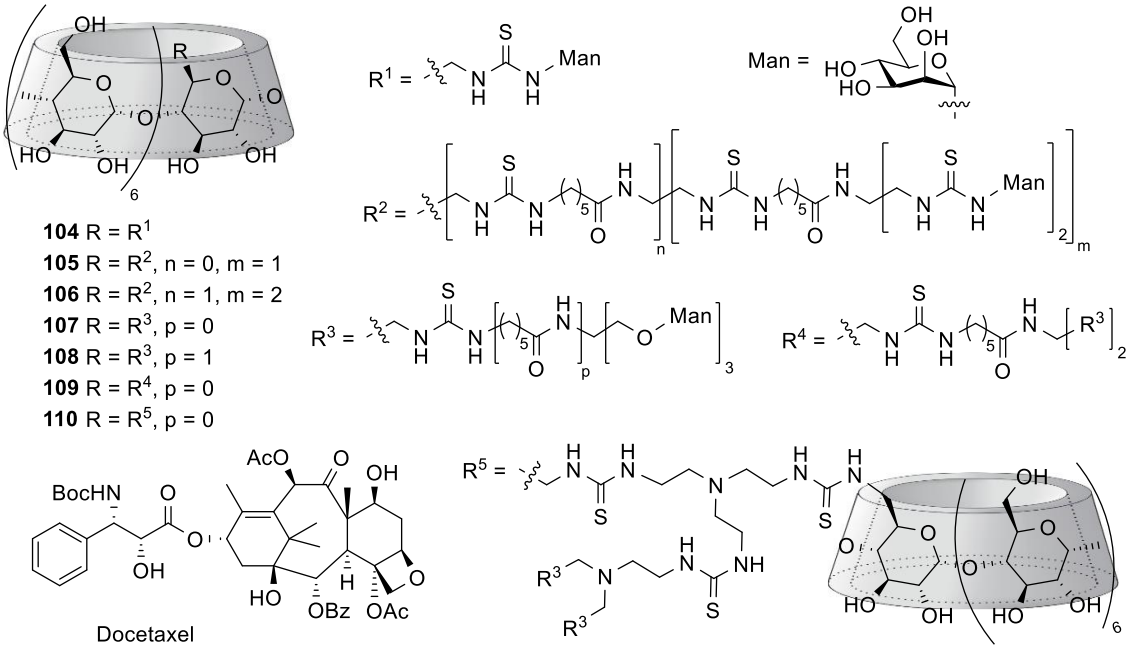
104 R = R1
105 R = R2, n = 0, m = 1
106 R = R2, n = 1, m = 2
107 R = R3, p = 0
108 R = R3, p = 1
109 R = R4, p = 0
110 R = R5, p = 0
Man =
Docetaxel

Figure 7-18.

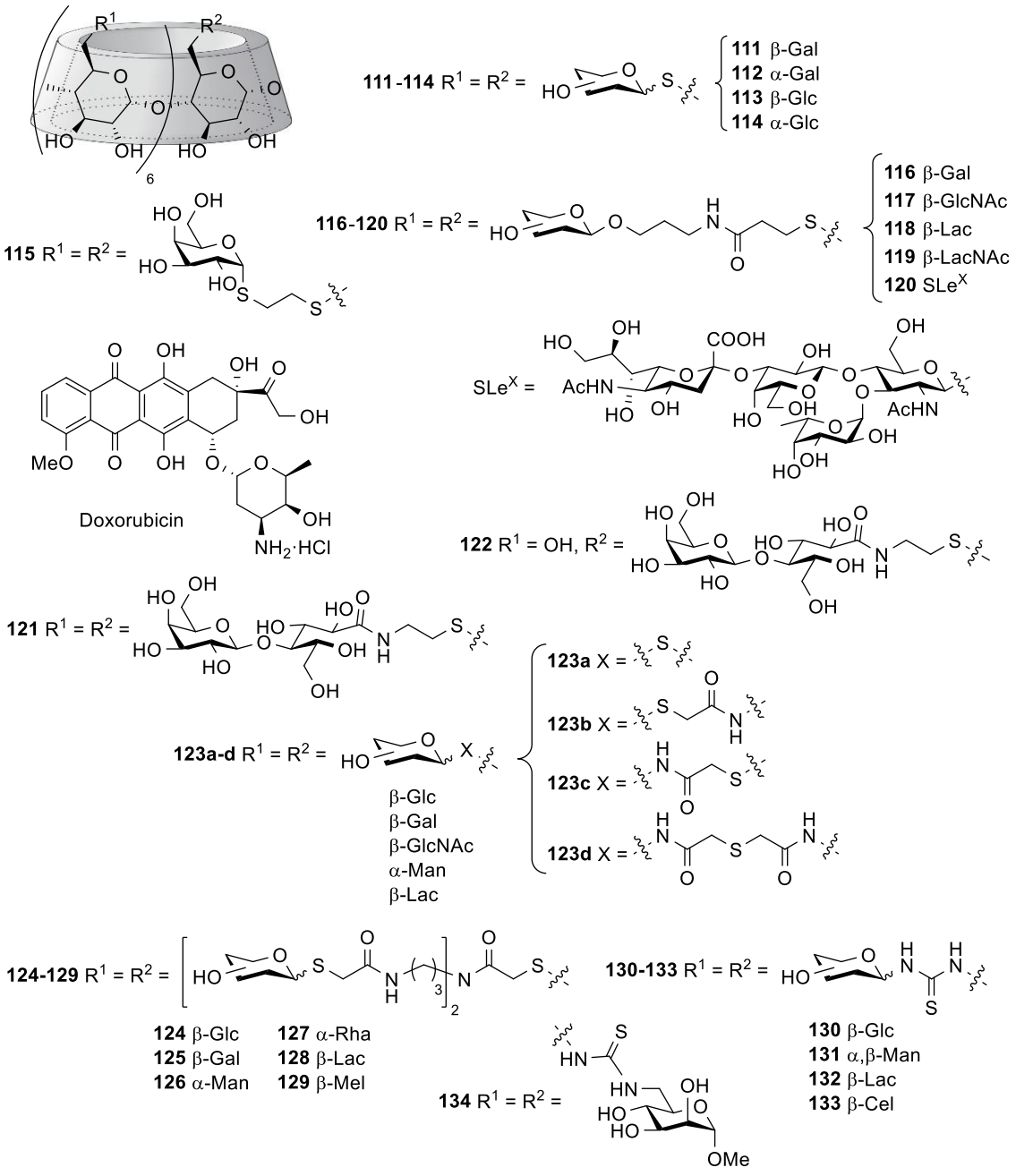
111-114 R1 = R2 =
111 β-Gal
112 α-Gal
113 β-Glc
114 α-Glc
115 R1 = R2 =
116-120 R1 = R2 =
116 β-Gal
117 β-GlcNAc
118 β-Lac
119 β-LacNAc
120 SLeX
SLeX =
Doxorubicin
122 R1 = OH, R2 =
121 R1 = R2 =
123a-d R1 = R2 =
123a X =
123b X =
123c X =
123d X =
β-Glc
β-Gal
β-GlcNAc
α-Man
β-Lac
124-129 R1 = R2 =
124 β-Glc
125 β-Gal
126 α-Man
127 α-Rha
128 β-Lac
129 β-Mel
130-133 R1 = R2 =
130 β-Glc
131 α,β-Man
132 β-Lac
133 β-Cel
134 R1 = R2 =

Figure 7-19.

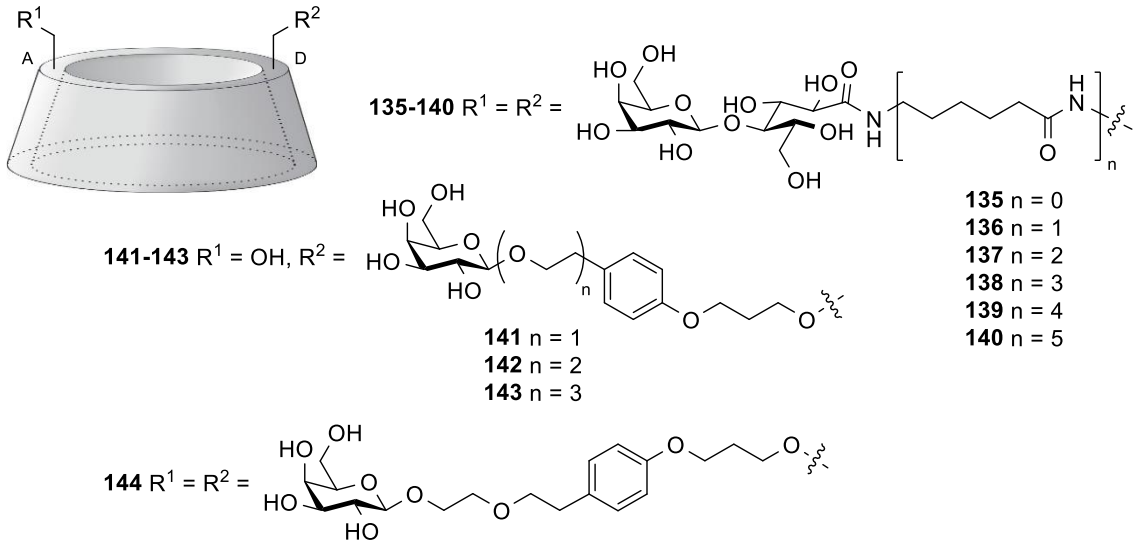

Figure 7-20.

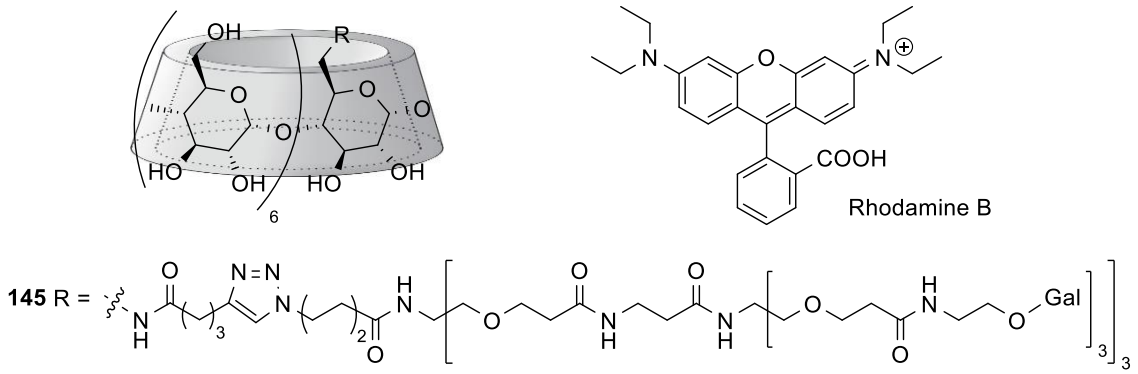

Figure 7-21.

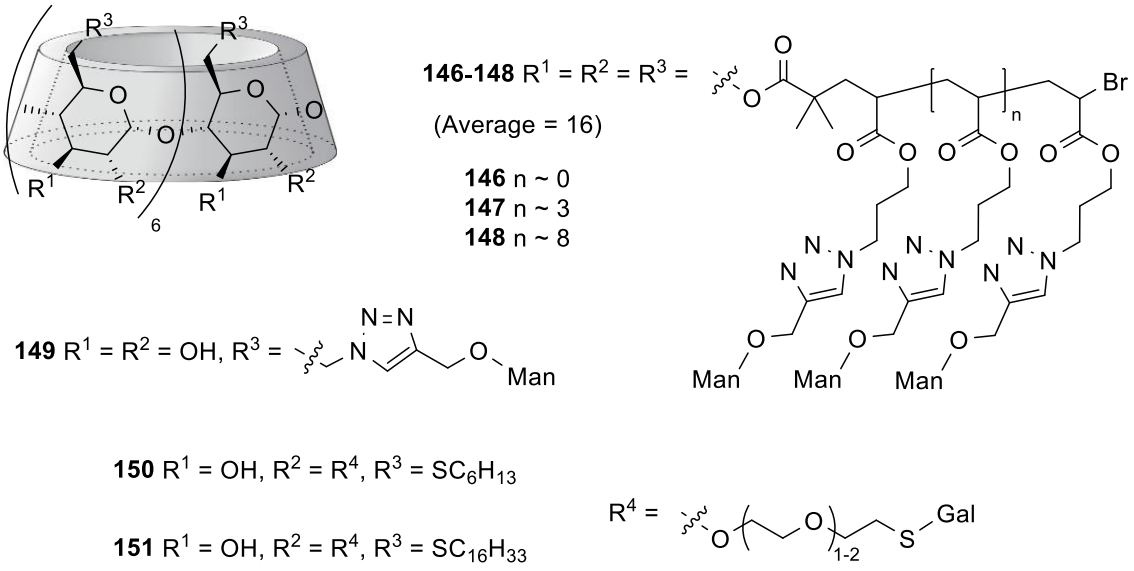

Figure 7-22.

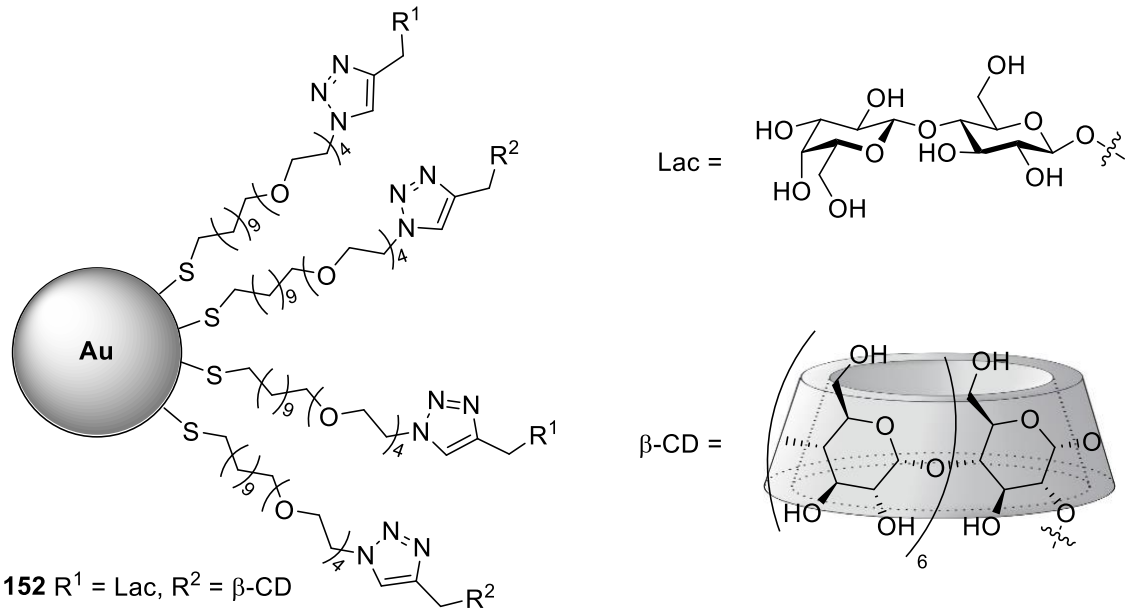

Figure 7-23.